

DISSERTATION

Defining Therapeutic Networks of Deep Brain Stimulation in  
Movement Disorders

Charakterisierung der therapeutischen Netzwerke der Tiefen  
Hirnstimulation bei Bewegungsstörungen

zur Erlangung des akademischen Grades  
Medical Doctor - Doctor of Philosophy (MD/PhD)

vorgelegt der Medizinischen Fakultät  
Charité – Universitätsmedizin Berlin

von  
Bassam Al-Fatly

Datum der Promotion: 29.11.2024



## Table of contents

List of figures.....	iii
List of abbreviations .....	iv
Abstract .....	1
1 Introduction .....	3
1.1 The Human Brain Connectome .....	4
1.2 Movement Disorders as Network Diseases .....	5
1.3 Deep Brain Stimulation Therapy .....	6
1.4 Connectomic Deep Brain Stimulation .....	7
1.5 Aims of the Dissertation .....	9
2 Methods .....	10
2.1 Localizing Deep Brain Stimulation Electrodes in a Common Brain Template .	10
2.1.1 Clinical cohorts .....	10
2.1.2 Clinical Scoring.....	11
2.1.3 Spatial Normalization of Patients' Images to the MNI space.....	12
2.1.4 Reconstructing Deep Brain Stimulation Electrodes.....	12
2.2 Modeling Volume of Stimulation.....	13
2.3 Adult Normative Connectomes .....	13
2.4 Pediatric Functional Normative Connectome .....	14
2.5 Estimating Stimulation-related Connectivity Profiles .....	15
2.6 Building Optimal Connectivity Fingerprints.....	16
2.7 Using Anatomical Lesion Locations to Identify Therapeutic Deep Brain Stimulation Network.....	18
2.7.1 Identifying Cases of Lesions from the Literature .....	18

---

2.7.2	Lesions Tracing and Lesion Network Mapping.....	18
2.7.3	Relevance of the Lesion Network Map to DBS-related Outcome.....	19
3	Results .....	21
3.1	Patients' Demographics.....	21
3.1.1	Essential tremor cohort (Study 1).....	21
3.1.2	Tourette syndrome cohorts (Study 2).....	21
3.1.3	Pediatric dystonia cohort (Study 3).....	22
3.2	Optimal Therapeutic Connectivity in Patients with Essential Tremor.....	22
3.3	Lesion-derived Connectivity Explains DBS-related Tics Improvement.....	26
3.4	An Anti-dystonic Functional Network in Children.....	29
4	Discussion.....	32
4.1	Short summary of results.....	332
4.2	Network Correlates of Therapeutic Effects.....	32
4.3	Somatotopic Organization of the Therapeutic Networks .....	35
4.4	Towards Age-specific Connectomic Analyses .....	35
4.5	Implications for Practice and Future Research.....	36
4.6	Limitations.....	37
5	Conclusions .....	39
	Reference list .....	40
	Statutory Declaration.....	64
	Declaration of your own contribution to the publications.....	65
	Printing copy(s) of the publication(s).....	66
	Curriculum Vitae.....	104
	Publication list .....	105
	Acknowledgments .....	108

---

## List of figures

<b>Figure 1.</b> Connectivity correlates of DBS improvement in ET patients.....	24
<b>Figure 2.</b> Connectomic anti-tremor DBS sweetspot. ....	25
<b>Figure 3.</b> Lesion Network Map of secondary tics disorders.....	27
<b>Figure 4.</b> Connectivity to the LNM of secondary tics correlates with tics-outcome after DBS in TS patients.....	28
<b>Figure 5.</b> Connectomic DBS in pediatric dystonia .....	30

---

## List of abbreviations

<b>CM/Pf</b>	Ceblromedian/parafascicular thalamic nuclei
<b>CTC</b>	cerebello-thalamo-cortical
<b>CT</b>	computed tomography
<b>DBS</b>	deep brain stimulation
<b>BOLD</b>	Blood-oxygen-level-dependent
<b>ET</b>	Essential tremor
<b>dMRI</b>	diffusion magnetic resonance imaging
<b>DTI</b>	diffusion-tensor imaging
<b>fMRI</b>	functional magnetic resonance imaging
<b>FWE</b>	Family-wise error
<b>GPi</b>	internal globus pallidus
<b>LOOCV</b>	Leave-one-out cross-validation
<b>MNI</b>	Montreal Neurological Institute
<b>MRI</b>	magnetic resonance imaging
<b>PD</b>	Parkinson's disease
<b>PSA</b>	Posterior-subthalamic area
<b>STN</b>	subthalamic nucleus
<b>VIM</b>	ventral intermediate nucleus of the thalamus
<b>YGTSS</b>	Yale Global Tic Severity Score
<b>Zi</b>	zona incerta

## Abstract

Deep brain stimulation (DBS) is a therapeutic surgical intervention that is commonly used to treat pharmaco-resistant movement disorders. DBS is highly effective in controlling patient's symptom but its performance could highly depend on multiple factors. The factors can range from surgical planning to clinical programming and patient's related factors like comorbidity, age, sex and disease severity to name a few. Recent studies demonstrated substantial evidence on the relationship between electrode location and DBS outcomes. Although defining beneficial local sites of stimulation could seem compelling on first sight, it does not provide broader insights on the distributed brain networks involved in DBS effects. This dissertation presents results of three publications that have demonstrated therapeutic DBS networks in three movement disorders. Specifically, neuroimaging data from patients with Essential tremor, Tourette syndrome and pediatric dystonia was analyzed to localize DBS electrodes, modeling their stimulation volumes and lastly deriving connectivity fingerprints that correlate with symptoms improvement. These network fingerprints were calculated using normative human connectomes. The results showed similarities between the therapeutic networks and the canonical pathological networks of each disease. Additionally, individual improvement could be predicted in Essential tremor using leave-one out cross-validation. In Tourette syndrome, reduction in tics severity was associated with the strength of connectivity of DBS sites to a lesion network map derived from lesions causative of secondary tics. The use of age-specific pediatric connectome has also demonstrated that the anti-dystonic DBS-network was in agreement with the pathological network of dystonia in cases with pediatric dystonia. Taken together, the results shown here demonstrated the utility of brain connectomics in drawing therapeutic networks. The networks can be targeted by different therapeutic modalities and additionally agreed with the pathological network models of the studied disorders in different ages.

## Zusammenfassung

Die tiefe Hirnstimulation (DBS) ist ein therapeutischer chirurgischer Eingriff, der in der Regel zur Behandlung pharmakoresistenter Bewegungsstörungen eingesetzt wird. Die DBS ist hochwirksam bei der Eindämmung der Patientensymptome, aber ihr Erfolg kann von zahlreichen Faktoren abhängen. Diese Faktoren können von der chirurgischen Planung über die klinische Programmierung bis hin zu patientenbezogenen Faktoren wie Komorbidität, Alter, Geschlecht und Schweregrad der Erkrankung reichen, um nur einige zu nennen. Jüngste Studien haben den Zusammenhang zwischen der Lage der Elektroden und den Ergebnissen der DBS deutlich aufgezeigt. Obwohl die Definition von vorteilhaften lokalen Stimulationsorten auf den ersten Blick überzeugend erscheint, liefert sie keine umfassenderen Erkenntnisse über die verteilten Gehirnetzwerke, die an den Auswirkungen der DBS beteiligt sind. In dieser Dissertation werden die Ergebnisse von drei Publikationen vorgestellt, die therapeutische DBS-Netzwerke bei drei Bewegungsstörungen nachgewiesen haben. Konkret wurden Neuroimaging-Daten von Patienten mit essentiellen Tremor, Tourette-Syndrom und pädiatrischer Dystonie analysiert, um DBS-Elektroden zu lokalisieren, deren Stimulationsvolumen zu modellieren und schließlich Konnektivitäts-Fingerprints abzuleiten, die mit der Verbesserung der Symptome korrelieren. Diese Netzwerk-Fingerabdrücke wurden anhand von normativen menschlichen Konnektomen berechnet. Die Ergebnisse zeigten Ähnlichkeiten zwischen den therapeutischen Netzwerken und den kanonischen pathologischen Netzwerken der jeweiligen Krankheit. Darüber hinaus konnte beim Essentiellen Tremor mittels Kreuzvalidierung (leave-one out) eine individuelle Verbesserung vorhergesagt werden. Beim Tourette-Syndrom wurde eine Verringerung des Schweregrads der Tics mit der Stärke der Konnektivität der DBS-Stellen zu einer Karte des Läsionsnetzwerks in Verbindung gebracht, die von Läsionen abgeleitet wurde, die für sekundäre Tics verantwortlich sind. Die Verwendung altersspezifischer pädiatrischer Konnektive hat auch gezeigt, dass das antidystonische DBS-Netzwerk mit dem pathologischen Netzwerk der Dystonie in Fällen mit pädiatrischer Dystonie übereinstimmte. Insgesamt haben die hier gezeigten Ergebnisse den Nutzen der Konnektomik des Gehirns bei der Zeichnung therapeutischer Netzwerke gezeigt. Die Netzwerke können durch verschiedene therapeutische Modalitäten beeinflusst werden und stimmten zudem mit den pathologischen Netzwerkmodellen der untersuchten Störungen in verschiedenen Altersgruppen überein.



## 1. Introduction

An imperative goal of successful physicians is to treat their patients with efficient therapeutic strategy that can ensure optimal clinical outcomes. In the field of neurology, such strategies can be exemplified by the use of medications to alleviate debilitating symptoms. However, neurological diseases, including the diverse array of movement disorders, are mostly non-static pathologies that can progress over time<sup>1</sup>. With this progress, many pharmacological treatments can lose their efficacy and an alternative therapeutic approach must be used. Deep brain stimulation (DBS) is a common contemporary surgical alternative to medical therapies and has proven effective in treating pharmaco-resistant movement disorders<sup>2</sup>.

The success of DBS therapy is dependent on multiple factors. Some of these factors are relatively modifiable; like anatomical target selection, surgical planning and postoperative clinical programming<sup>3,4</sup>. Others are non-modifiable and mainly patient determined; like age at implantation, comorbidities, severity of preoperative symptoms and disease progression<sup>2</sup>. The interplay between these factors determines the clinical effects of DBS surgery in many movement disorders. This interplay can be modified by optimizing the techniques in hands of clinicians and surgeons. As such, local and remotely distributed anatomical information could help defining better surgical targets and optimal programming settings that ensure side-effects free efficient DBS therapy<sup>5,6</sup>. Inferring such information mandate the use of high-resolution imaging techniques to determine local DBS surgical targets<sup>7</sup>. On the other hand, the advent of the human brain connectome<sup>8</sup> lends the possibility to depict a brain-wide connectivity signature that can summarize DBS efficacy<sup>3</sup>. The latter represents a distributed set of brain regions that are remotely located from stimulation sites but still play pivotal roles in the clinical outcomes of DBS surgery.

In the present dissertation, the aim is to delineate therapeutic networks of selected movement disorders, namely Essential tremor (ET), tics and pediatric dystonia. Data from patients implanted with deep brain stimulation system in different subcortical targets were used and their network fingerprints of effective clinical outcome were traced using normative brain connectomes. To this end, the following sections will discuss the concept of the human brain connectome and how it changed our understanding of the mechanistic underpinning of movement disorders. Additionally, the concept of connectomic deep brain

stimulation and its power to integrate anatomical and clinical information to identify optimal therapeutic networks will be introduced. These networks represent unifying neuroanatomical substrates that can be targeted using different invasive and non-invasive neuro-modulation therapies.

## 1.1 The Human Brain Connectome

The term “*connectome*” was first coined by Olaf Sporns and colleagues in 2005 to denote the connection matrix of the human brain<sup>8</sup>. Simply, a connectome deciphers a wiring diagram that collectively describes every possible connection between the elements of the human brain, how those elements interact and exchange information, and how strong is this connection between them<sup>9</sup>. Importantly, the term “connectome” is not essentially equal to “connectivity”, with the latter has been introduced early on from historical perspective<sup>10,11</sup>. The advances made in the field of radiology did afford the opportunity to non-invasively measure brain activities and delineate white matter axonal pathways in living humans. These advances were exemplified by the introduction of magnetic resonance imaging (MRI)<sup>12</sup> and its versatile applications (diffusion acquisitions<sup>13</sup>, resting-state and task-based functional MRI - fMRI<sup>14</sup>). The latter MRI techniques paved the way towards the introduction of the concept of a brain connectome. A connectome entails parcellating the brain into regions and finding the degree of connectivity between these regions<sup>15</sup>. From this, it is already conceivable that connectivity is a measurement that can be used to quantify the value of connectedness between brain elements, i.e., the “parcels”. These parcels can be single neurons, neuronal assemblies, or a large anatomically or functionally relevant brain regions. Connectivity between these different parcel classes gives rise to the definition of micro-, meso- and macroscale connectomes, respectively<sup>16</sup>. The principle of mathematically calculating connectivity between brain parcels has stemmed from the mathematical “graph theoretical” methods. In graph theory, parcels represent the nodes of the graph while the connectivity between them represents the edges<sup>17</sup>. In neuroscience, the graph theoretical description of the brain connectome is usually summarized in “adjacency” or connectivity matrices<sup>18</sup>. The rows and columns of these matrices feature the brain nodes or parcels, while the values inside the cells quantify the edges or connectivity strength. Needless to say, that only the macroscale level of the connectome can be assessed with MRI<sup>19</sup>.

The first step in building a brain connectome is to acquire MRI data from subjects. If the connectome is created to describe anatomical (“*structural*”) connections between brain regions, a diffusion MRI (dMRI) will be acquired which provides means to estimate axonal pathways within the white matter of the brain<sup>19</sup>. On the other hand, functional MRI (measuring the blood-oxygen-level-dependent - BOLD) will be acquired from the subjects in case the connectome is featuring the “*functional*” connectivity between brain regions<sup>20</sup>. A connectome can be “normative”, meaning that the MRI acquisitions have been performed on normal, healthy subjects, or can be “disease-specific”, which means that the acquisitions belong to specific subjects’ cohort that has been diagnosed with a specific disease condition<sup>21,22</sup>. A connectome is usually stored as an average connectivity matrix of all the subjects who participated in the MRI acquisitions.

## 1.2 Movement Disorders as Network Diseases

The aforementioned concepts of the human brain connectome have changed the perspective with which neurologists and neuroscientists look at brain disorders and functionalities<sup>23</sup>. For instance, the first description of Broca’s expressive aphasia by the French surgeon, Pierre Paul Broca, has exemplified the “localizationist” notion in neurology for almost a century<sup>24</sup>. The localizationist perspective was until a few decades the dominating concept in determining the anatomical underpinnings of neuropsychiatric disorders. The contemporary view has undergone a paradigm-shift as a result of this location-linked perspective. Neuropsychiatric disorders are being currently understood as network diseases or “*circuitopathies*”<sup>25</sup>. In its core, a network disease is simply caused by pathological alteration in specific network nodes and edges. Movement disorders were among the common examples in neurology to be described as disorders of brain networks<sup>2,25</sup>. The main pathological processes in movement disorders occur in the cortico-basal ganglia-thalamo-cortical or cerebello-thalamo-cortical circuits (CTC)<sup>26,27</sup>. Since the basal ganglia comprise deep grey matter nuclei and their related axonal pathways, these elements have been regarded as a home for possible pathological signals communications that mark the electrophysiological changes in movement disorders<sup>28,29</sup>. The basal ganglia and their loops condense information from different regions of the cortex and act as signal filters, integrators, and information processors<sup>30,31</sup>. These deep brain nuclei interact vastly with each other, with the cortex and with the cerebellum to shape human behaviors and movement. Recent, lesion network mapping studies have identified multiple different networks

as neuroimaging correlates of different movement disorders<sup>32–40</sup>. In addition to that, electrophysiological studies have illustrated different physiological hubs conveying the pathological signals from different brain sources in different pathologies<sup>41,42</sup>. Specifically, a plethora of studies has illustrated the network-based pathological mechanism in essential tremor (ET)<sup>43</sup>. Tremor activities and related pathological signals have been recorded using electro- and magnetoencephalography in different nodes of the CTC circuit favoring the importance of network derangement in tremor pathology<sup>43–46</sup>. Furthermore, invasive neurophysiological studies identified tremor cells in the ventral intermediate nucleus (VIM) of the thalamus that is centrally located in the CTC pathway<sup>47–50</sup>. On the other hand, different brain regions have been implicated in the pathophysiology of dystonia spanning the subthalamic nucleus<sup>51</sup>, the striatum<sup>52</sup>, the pallidum<sup>53</sup> and the cerebellum<sup>54</sup>. Additionally, the sensorimotor cortices have gained special attention as a central role player in the mal-plastic pathophysiological process of dystonia<sup>55</sup>. Tourette syndrome (TS), the primary form of tic disorders, has been thoroughly investigated using different neuroimaging and electrophysiological approaches<sup>56,57</sup>. In patients undergoing surgical intervention for TS, invasive neurophysiological recording has pointed towards the presence of tics related activities in the globus pallidus internus (GPi) and the centromedian nucleus of the thalamus<sup>58</sup>. Apart from the basal ganglia, different neuroimaging reports investigated the regions related to tics occurrence (e.g., the primary motor and supplementary motor cortices)<sup>59</sup>, premonitory urges (e.g., the insula)<sup>60</sup> and tic suppression (e.g., frontal cortex)<sup>60</sup>. All these examples imply the essence of defining movement disorders as network diseases. Of note, the three abovementioned disorders are the subjects of the three publications of the present dissertation.

### 1.3 Deep Brain Stimulation Therapy

Neurosurgical interventions have been used since ancient ages as therapeutic approaches to treat brain disorders<sup>61</sup>. Historically, a diseased part of the brain was removed or a lesion was placed in its region to relief the associated symptoms. During the evolution of the neurosurgical approaches, invasive electrical stimulation has started to appear in the scene of therapeutic modulation<sup>62,63</sup>. However, it remained an as an investigative tool to test responses in different surgical targets during lesional surgeries. In 1987 and 1989, Alim Louis Benabid and colleagues have been the first to describe successful clinical control in ET and Parkinsonian tremor patients implanted with chronic high-frequency

electrical stimulation<sup>64,65</sup>. This marked the birth of modern-day DBS surgery. DBS surgery involves surgical targeting of specific subcortical brain structures (grey or white matter) to deliver high-frequency electrical stimulation that can treat specific symptoms<sup>2</sup>. The surgical target selection depends highly on the type of symptoms undergoing therapy. The surgeon implants unilateral or bilateral electrodes that are attached to DBS leads which are connected to an impulse-generator<sup>66</sup>. The impulse generator is usually implanted in a second stage surgery underneath patient's skin (in the chest or abdomen). The impulse generator can be programmed by the clinicians during the postoperative follow-up sessions to determine the most efficacious set of parameters<sup>67</sup>. The whole process necessitates high surgical and clinical precision including, but not limited to, the surgical planning and the postoperative clinical programming.

DBS therapy has been used to treat a multitude of neuropsychiatric disorders like Parkinson's disease<sup>68</sup>, ET<sup>69</sup>, dystonia<sup>70</sup>, TS<sup>71</sup> and obsessive-compulsive disorders<sup>72</sup> to name a few. In ET, thalamic DBS (targeting the VIM nucleus) has proven a striking efficacy to control contralateral upper limb tremor, reaching to 50-80%<sup>73,74</sup>. While different targets have been suggested as candidates for DBS therapy in TS, an average improvement in the Yale Global Tic Severity Scale (YGTSS) was reported to be ~53% in one meta-analysis and across different surgical targets<sup>75</sup>. Different DBS targets have demonstrated similar trend of postoperative tics improvement hinting towards the possibility of modulating a common neural circuitry. In patients with dystonia, the rate of improvement after DBS surgery was highly dependent on the classification and the varying etiologies of the cases being treated<sup>70</sup>. In general, an acceptable reduction in primary generalized dystonia symptoms can be achieved with GPi-DBS, with an improvement of 51% in one prospective, controlled, multicenter study<sup>76</sup>. DBS therapy has become a standard of care, FDA-approved treatment in many medication-resistant brain disorders<sup>77</sup>.

#### **1.4 Connectomic Deep Brain Stimulation**

Since brain disorders are network pathologies as it has been alluded to in the previous sections, the concept of targeting a neural circuit instead of a single brain region has become tempting<sup>78</sup>. Henderson et al. have first proposed the approach of "*surgical connectomics*", where a brain disorder can be treated by retuning the disease-associated part of the human connectome<sup>79</sup>. While Henderson's concept could be seen as primarily tailored for lesional surgeries, it can also be applied in DBS surgeries<sup>3</sup>. Instead of creating

a physical lesion, DBS can produce an informational lesion by perturbing pathological brain signals when placed in specific deep nuclei<sup>80</sup>. The presence of such a “*virtual*” lesion could partly be treated similarly to its physical counterpart when being placed in specific pathological network<sup>81</sup>. The exact mechanism of DBS has been debated since its advent<sup>82</sup>. However, activation or inhibition of the up- and downstream axonal pathways that are in close vicinity to the electrodes could play a major role in the neuromodulatory capability of DBS. Additionally, changes in the firing rate of different neuronal populations residing in the deep brain nuclei have been noticed as a response to the high-frequency stimulation of one of the nuclei<sup>83,84</sup>. Importantly, recent studies have implemented the use of state-of-the-art neuroimaging techniques to investigate the possibility to use brain networks as targets for DBS surgeries<sup>3,85–87</sup>. Diffusion-tensor imaging (DTI) was used in some studies to target axonal pathways in DBS surgeries for ET and depression patients<sup>88–90</sup>. In another study, fMRI has been implemented to delineate the VIM location as a target for DBS in ET patients<sup>91</sup>.

As such, the last decade has seen massive exploratory efforts to elucidate the feasibility to derive the brain networks that are correlated with DBS induced symptomatic improvement in different neuropsychiatric illnesses<sup>87</sup>. The initial work by Horn et al.<sup>86</sup> has nailed the pillars for such a framework and illustrated the possibility to predict symptoms improvement in cohorts of Parkinson’s disease treated with subthalamic DBS. Horn and colleagues introduced a data-driven whole-brain connectomic approach to decipher an optimal therapeutic network using structural and functional normative connectomes. This work has been followed by numerous different studies which exemplified the power of different connectomic DBS approaches tracing different therapeutic network targets for DBS<sup>85,87,92</sup>. Besides, this method could also help in defining targets for non-invasive therapeutic modalities like transcranial magnetic stimulation<sup>93</sup>. Furthermore, different therapeutic networks identified using the connectomic DBS methodology found common neuronal substrates that match neurophysiological evidence in many neurological diseases<sup>86,94–96</sup>. Additionally, evidence from lesion network mapping studies has pointed to the unified distribution of causality-associated neuronal circuits and different therapeutic networks<sup>34,37,38,40</sup>.

## 1.5 Aims of the Dissertation

The main goal of the dissertation is to delineate the topological distribution of the beneficial therapeutic networks in three examples of movement. As such, the aims of the three studies, which culminate into the previously stated overarching aim, can be summarized in the following:

1. Study 1<sup>97</sup>: to estimate the structural and functional brain connectivity correlates of effective thalamic DBS therapy in ET patients. Since tremor can present with different severity scores in different body parts (specifically head and upper limbs tremor), the aim was also to test whether the connectivity fingerprints of tremor improvement in these body parts can align with the canonical somatotopic maps of the motor cortex homuncular strip and the cerebellar body representation. Ultimately, the identification of a connectomic-determined local sweetspot for DBS in ET was sought.
2. Study 2<sup>35</sup>: to test the hypothesis that a neural network identified using focal brain lesions causative of secondary tics can serve as a network target for DBS in TS patients implanted in two different targets (GPi and CM/Pf).
3. Study 3<sup>98</sup>: to implement the usability of functional normative connectomics in pediatric dystonia patients treated with globus pallidus internus (GPi) DBS and trace a network correlate representative of the clinical outcomes.

## 2. Methods

The sections below will discuss in details the methods pertinent to each of the three studies in this dissertation. Briefly, each patient received bilateral DBS electrodes which have been reconstructed and simulated in a common brain template to ease the group-level analyses. The volumes of stimulation surrounding the active contacts were then modeled based on the clinical stimulation parameters. These volumes were then used as seeds to estimate connectivity maps reflecting whole-brain connections. The connectivity maps were then correlated with the clinical improvement to calculate a whole-brain statistical map featuring voxel-wise correlation values as an optimal therapeutic model. Additionally, in one study (study 2), connectivity between the volume of stimulation and a lesion network map derived from causative focal lesions was calculated and subsequently correlated with postoperative clinical improvement<sup>35</sup>. Study 3 demanded the assembly of an age-specific connectome and the use of age-specific template to comply with the cohort age (pediatric)<sup>98</sup>. The methods of building an optimal brain model were also used in study 1 to estimate the somatotopic distribution of the clinical DBS effect projected on the whole-brain connectivity profiles<sup>97</sup>. Side-effects connectivity signatures were additionally estimated whenever appropriate.

### 1.1 Localizing Deep Brain Stimulation Electrodes in a Common Brain Template

#### 2.1.1 Clinical Cohorts

Study 1 included 36 retrospective patients who have been diagnosed with ET that required bilateral deep brain stimulation as an advanced treatment for their tremor symptoms<sup>97</sup>. All patients were surgically operated on in Charité–Universitätsmedizin Berlin for the period between 2001 and 2017. The diagnosis has been carried out according to a thorough clinical examination by movement disorder specialists according to the consensus diagnostic criteria published in<sup>99,100</sup>. Patients were regarded as ET cases and selected if they have upper limb bilateral symmetric postural or kinetic tremor with or without additional head tremor. Cases with *isolated* lower limb, chin, tongue, voice tremor were excluded. Furthermore, neuropathic, orthostatic, dystonic, physiological or psychological tremor were regarded as exclusion criteria.

DBS patients of study 2 included 30 adults, who have been diagnosed with TS and were implanted with a bilateral DBS system in three different anatomical targets from three



clinical centers in Europe<sup>35</sup>. Fifteen patients underwent DBS surgery in Cologne targeting the centromedian-ventro-oralis (n = 12) or the ventroanterior/ventrolateral nucleus of the thalamus (n = 3). The latter patients had their most distal contacts residing in the field of Forel/subthalamic nucleus. This sub-cohort comprised the *thalamic DBS-cohort* of the study. Another set of 15 patients were bilaterally implanted in Maastricht (n = 6) and in Paris (n = 9) targeting the anteromedial part of the Globus Pallidus internus.

In study 3, 20 children and adolescents diagnosed with pharmaco-resistant dystonia who required DBS-surgery to control their symptoms were retrospectively included<sup>98</sup>. This cohort is part of the German Registry on Pediatric DBS (GEPESTIM)<sup>101</sup> and was selected based on meticulous screening of available neuroimaging data. Patients of this cohort were bilaterally implanted with DBS electrodes in 5 German centers targeting the GPi. Reasons for exclusion were bad quality or lack of neuroimaging data, insufficient or absent documentation of DBS parameters and inadequate period of postoperative DBS follow-up.

### 2.1.2 Clinical Scoring

Patients who underwent DBS surgeries in each of the three studies were either assessed using recorded videos preoperatively (or DBS OFF postoperatively) and DBS ON postoperatively or were assessed during a hospital visit (for the pediatric cohort, the patients were assessed by a specialist pediatric neurologist). The type of the clinical score depends on the pathological entity under investigation in each study. That is, for ET patients in study 1, Fahn-Tolosa-Marin tremor scoring (FTM) was used to rate tremor severity in both preoperatively (or DBS OFF) and DBS ON video recordings<sup>102</sup>. The Yale Global Tic Severity Scale (YGTSS) was used to rate tic severity in patients of study 2<sup>103</sup>. Finally, for the pediatric patients in study 3, the Burke-Fahn-Marsden Dystonia Rating Scale (BFMDRS) was used to quantify dystonia severity<sup>104</sup>. Then, percent improvement, as a clinical metric of DBS clinical effects in each cohort, was calculated as follows:

$$\% \text{ improvement} = (DBS \text{ OFF} - DBS \text{ ON}) / DBS \text{ OFF} \times 100\%$$

where DBS OFF means the clinical score of the respective disease before operation or after operation but when the DBS system is turned off for a sufficient time that allows for wash-out of its clinical effects and DBS ON means the clinical score of the respective disease after the operation and while the DBS system is turned on for a sufficient time for the stimulation to take its clinical effects.

### 2.1.3 Spatial Normalization of Patients' Images to the MNI Space

Obtained pre- and postoperative patients' images were submitted to the Lead-DBS software ([www.lead-dbs.org](http://www.lead-dbs.org))<sup>105–107</sup>. Lead-DBS is a multitool neuroimaging suit which is written in MATLAB and primarily used to localize DBS electrodes in native and common brain spaces as well as performing more advanced group-level statistical tasks like local sweetspot and whole-brain network analyses<sup>4</sup>. Preoperative anatomical T1 MRIs were always included in addition to T2, positron density (PD) and fast gray matter acquisition T1 inversion recovery (FGATIR) sequences whenever available. This ensures that the multispectral capability of Lead-DBS normalization algorithms can be exploited to highly optimize the spatial warping to the common brain template (MNI space)<sup>108</sup>. The default settings for images coregistration and normalization algorithms implemented in Lead-DBS were used. First, preoperative MRIs were linearly aligned and coregistered to the postoperative MRIs or CT scans, depending on the availability of the latter using Statistical Parametric Mapping (SPM12; <http://www.fil.ion.ucl.ac.uk/spm/software/spm12/>)<sup>109,110</sup> for MRI-to-MRI coregistration or advanced normalization tools (ANTs; <http://stnava.github.io/ANTs/>)<sup>111</sup> for CT to MRI coregistration. Coregistration entails bias-field correction and intensity normalization of MRIs as preprocessing stages in addition to tone-mapping of postoperative CT. Later, spatial resampling and linear registration of the postoperative modality to the preoperative MRI has been carried out to align the images. Next, non-linear normalization was applied using in Lead-DBS SyN Symmetric Diffeomorphic algorithm of ANTs and a preset of 'effective: low variance + subcortical refinement'<sup>111</sup>. This allows warping of the preoperative MRI to the ICBM 2009b NLIN asymmetric space adult MNI space in case of studies 1 and 2 (<https://nist.mni.mcgill.ca/icbm-152-nonlinear-atlases-2009>). On the contrary, images of the pediatric cases included in study 3 were normalized to the unbiased pediatric MNI template (<https://nist.mni.mcgill.ca/pediatric-atlases-4-5-18-5y>)<sup>112</sup>. For this particular purpose, this specific template was incorporated as a routine for pediatric DBS data processing in Lead-DBS in study 3. As a final step, the warp field estimated for normalizing the preoperative images was then applied on the coregistered postoperative images.

### 2.1.4 Reconstructing Deep Brain Stimulation Electrodes

As mentioned above, each DBS patient in each of the three studies has been implanted bilaterally in a different subcortical target nucleus. After normalizing the postoperative

images, electrode artefacts were automatically identified using Precise and Convenient Electrode Reconstruction for Deep Brain Stimulation (PaCER) algorithm (for CT) and the refined TRAC/CORE algorithm (for MRI) implemented in the Lead-DBS software<sup>106,113</sup>. This automatic process was then critically reviewed and manually corrected if needed. The trajectory of the DBS lead was filled with a 3D mesh of the specific electrode model in each patient and visualized in relationship to the different DBS target nuclei depicted in the DISTAL atlas of Lead-DBS<sup>114</sup>.

## 2.2 Modeling Volume of Stimulation

After localizing the DBS electrodes in the respective MNI space, a further step of stimulation parameters entry was performed in the Lead-group tool of Lead-DBS. This step determines which contacts are being used as active or passive contacts, the type of stimulation (monopolar, directed or interleaved), and the amount of stimulation (volts or milli amperes). All these entries will control the site and shape of the volume of tissue undergoing electrical stimulation from the DBS system. A finite element approach (the SimBio/FieldTrip implemented in Lead-DBS) using tetrahedral mesh in the form of four-compartments (electrode conducting and insulating parts in addition to grey and white matter regions of the stimulated tissue) was utilized to estimate the volume of stimulation<sup>86</sup>. Voxel-wise E-field values inside the volume were then estimated and thresholded using a heuristic level of 0.2 V/mm<sup>115</sup>. The latter thresholded volume was further binarized and saved as a mask image to represent the volume of stimulation which will later be used as seed for whole-brain connectivity estimation.

## 2.3 Adult Normative Connectomes

All the connectivity analyses in this dissertation were performed using “*normative*” connectomes. This means that the raw imaging data from which each connectome was built is stemming from normal healthy subjects. Both functional and structural connectomes or one of them were used depending on the type of the study. Study 1 was concerned with ET patients who were implanted with DBS electrodes in the VIM of the thalamus, hence both functional and structural connectivity correlates of the therapeutic effects were derived. This being said, a functional connectome that is created from data of 1,000 healthy subjects from the Brain Genomics Superstruct Project (<https://dataverse.harvard.edu/dataverse/GSP>) was used<sup>116,117</sup>. The imaging sequences of this connectome

were acquired using a 3T Siemens MRI. The preprocessing of the functional images involved both smoothing with a 6 mm Gaussian kernel and a global BOLD signal regression among other spatial normalization steps that warp the data into the adult MNI space. In addition, to estimate the structural correlate of the DBS effects in study 1, a structural connectome that included high density fibers tracts belonging to diffusion data of 20 normal subjects was used<sup>118</sup>. Single-shot spin-echo planar imaging was selected as the MRI sequence to acquire the diffusion data from these subjects (echo time = 94 ms, matrix size =  $2 \times 2 \times 2 \text{ mm}^3$ , repetition time = 10,000 ms, and each volume contains 69 slices). The preprocessing steps of this connectome involved spatial normalization algorithms of both the anatomical and the diffusion data to the adult MNI space. Additionally, Global fiber-tracking using Gibb's algorithm was implemented in the modeling of the fiber streamlines<sup>119</sup>. The Gibb's-tracking algorithm provides a powerful method to estimate fiber tracts from diffusion imaging without the need to determine seeds and regions of interest (i.e., estimating global brain fibers architecture without a priori defined regions of connection). It is worth mentioning that only the functional normative connectome was used in study 2 since the aim was to find a widely distributed network target that could unify causality with therapy. The functional connectome offers to derive polysynaptic long-range networks<sup>120</sup>. These networks are not essentially constrained by the anatomical boundaries depicted by axonal pathways as it is the case with the structural connectome<sup>121</sup>.

#### **2.4 Pediatric Functional Normative Connectome**

For the specific purpose of study 3, an age-specific pediatric connectome from resting-state fMRI acquisitions of 100 children, which were publicly available from the nyu2 sub-cohort of the Consortium for Reliability and Reproducibility (CoRR; [http://fcon\\_1000.projects.nitrc.org/indi/CoRR/html/nyu\\_2.html](http://fcon_1000.projects.nitrc.org/indi/CoRR/html/nyu_2.html)), was assembled<sup>122</sup>. As the aim was to depict the therapeutic network in pediatric patients treated with GPi-DBS, a structural connectome to delineate the axonal pathway relevant to this therapeutic target was not included. The reason is that the anatomical complexity of the connection of the GPi to and from the cortical regions is still unclear and no tracing studies supported such pathways except for indirect neurophysiological studies<sup>123–125</sup>. Hence, the focus was on polysynaptic connectivity that can be probed by functional connectivity and may not be restricted by anatomical pathways. First, only data of neurotypical children ( $n = 107$ ) from the aforementioned database and downloaded anatomical T1 and resting state fMRI images were selected.

These images were preprocessed using a set of neuroimaging software and tools. First, slice timing of the rs-fMRI time series was corrected followed by spatial realignment and motion correction using *mcflirt* functionality of FMRIB Software Library (FSL v6.0; <https://fsl.fmrib.ox.ac.uk>)<sup>126</sup>. At this stage, subjects with framewise displacement that exceeded 0.5 mm in more than 50% of rs-fMRI volumes were excluded ( $n = 7$ )<sup>127</sup>. This left only data from 100 eligible subjects to be used in the connectome assembly. Next, MATLAB codes from Lead-connectome (<https://www.lead-dbs.org/about/lead-connectome/>) were used to regress out the detrimental motion effects from the rs-fMRI time series. A Gaussian kernel with a 6 mm full width at half maximum was applied to imply spatial smoothing on the data followed by a bandwidth filter to filter out data below 0.01 Hz and above 0.08 Hz to lessen the effects of scanner drift and high-frequency noise fluctuations, respectively. Additionally, SPM “*newsegment*” was used to segment the T1-weighted MRI into grey matter, white matter and cerebrospinal fluid masks which were then linearly aligned to the functional images<sup>109</sup>. This step allowed regressing out the average BOLD signal in these masks and the average global BOLD signal from the functional time series using MATLAB codes in the Lead-Connectome tool<sup>106,128,129</sup>. Finally, normalization of the rs-fMRI to the pediatric MNI space was performed both linearly and non-linearly using FSL FNIRT function. The resultant normalized time series was saved as a matrix of  $285,903 \times 180$  dimension, where  $n = 285,903$  is the number of voxels and  $n = 180$  is the number of rs-fMRI volumes acquired. Matrices from 100 subjects included in the connectome were then used by Lead-Connectome Mapper to estimate seed-based connectivity from the volumes of stimulation. Steps for connectome assembly and example seed-based connectivity profiles are shown in Fig.4A and Fig.4B, respectively.

## 2.5 Estimating Stimulation-related Connectivity Profiles

The ultimate aim of this dissertation is to depict brain networks associated with DBS clinical effects. As such, the connectivity correlate of the DBS electrodes should be calculated based on each patient’s stimulation parameters. The volumes of stimulation were used as seed regions to calculate whole-brain connectivity (functional or structural connectivity depending on the study)<sup>86</sup>. Seed-based connectivity of bilaterally modeled volumes of stimulation was estimated ( $n = 72$  in study 1, since right volumes were non-linearly flipped to the left hemisphere to derive a network correlate using contralateral DBS-related improvement in tremor scores;  $n = 60$  in study 2; and  $n = 40$  in study 3) using the tool Lead-

Connectome Mapper<sup>106</sup>. The tool allows the user to select the type of the connectome and to calculate a seed-based connectivity map (which is called here “*connectivity profile*”) from each seed region using the selected connectomes. For functional connectomes, different types of maps can be extracted which represent the average voxel-wise connectivity values of all the subjects in the connectomes when seeded from the volumes of the stimulation. First, connectivity between the average BOLD signal of the seed (volume of stimulation) were statistically correlated to the BOLD activity of the rest of the brain using a voxel-wise Pearson correlation in each subject of the connectome<sup>86</sup>. Lead-Connectome Mapper then averaged these voxels R-coefficients (the results of the Pearson correlation) using mathematical averaging across the connectome subjects and normalizing of the R-values using Fisher-z transform. These types of connectivity profile maps were used in study 1 and 3 to calculate the optimal therapeutic connectivity fingerprints. In addition, a “*T-map*” containing voxel-wise T-scores as a result of voxel-wise mass-univariate one-sample t-test over the whole subjects’ number in the connectome can also be extracted. This T-map was adopted for calculating the connectivity profiles of lesions and volumes of stimulation in study 2. Analogous to the lesion network mapping method<sup>33</sup>, DBS-related connectivity profiles were calculated similarly based on the T-maps. For structural connectivity (study 1), the resulting connectivity profile maps were representative of the fiber counts that reach each voxel of the brain from the seeds (the volumes of stimulation).

## 2.6 Building Optimal Connectivity Fingerprints

To infer a statistical brain model that can play the role of an optimal correlate of therapeutic benefits from DBS, a method commonly used in DBS connectivity analysis called “*DBS network mapping*” was implemented<sup>107</sup>. The method was first introduced in the work of Horn et al. to predict DBS-related improvement in Parkinson’s disease patients who underwent subthalamic nucleus DBS surgeries in two different clinical centers<sup>86</sup>. In this dissertation, the result of this method will be referred to as the “*R-map*”. The R-map is a whole-brain connectivity model that stores voxel-wise values as a result of Pearson correlation between the percent improvement and the voxel-wise connectivity metric stored in the connectivity profile maps (R-values for functional and fiber counts for structural connectivity analysis). The process was repeated iteratively over each voxel and the resulting R-value was stored in each respective voxel. In order to test whether the R-map

model was able to explain variance in DBS-improvement, a leave-one-out cross validation (LOOCV) in study 1 and permutation testing in study 3 was used. Briefly, the LOOCV entailed leaving one connectivity profile map and improvement score out while calculating the R-map based on the rest maps and improvement score. Then, the left-out connectivity map was spatially correlated with the resulting R-map to calculate spatial similarity indices across connectivity profile maps. These similarity indices were then correlated with the respective improvement of each subject. The R-map model was regarded as optimal if the LOOCV method yielded a significant result ( $p < 0.05$ ). The full number of voxels of each map were used without the need for correcting for multiple-comparison since the aim was to test the validity of the R-map in LOOCV. In study 3, the validity of the R-map was tested using a permutation testing<sup>130</sup>. Here, all the connectivity profile maps and their respective improvement scores were included in the calculation of the R-map without applying LOOCV. A Pearson correlation between the non-permuted improvement scores and the similarity indices was then calculated. This correlation was also repeated using shuffled (1,000x permutations) improvement scores to build a null-distribution. The R-map was accepted as an optimal model in case the non-permuted R value was above the level of chance inferred from the null-distribution ( $p < 0.05$ ). The permutation testing was implemented to avoid violation by small-sample size when performing repeated comparison testing<sup>130</sup>. In study 2, however, the R-map to the ensuing tics-related lesion network map was visually compared as the aim was to investigate whether the lesion network map can serve as a target network for neuromodulation through DBS. Direct connectivity between the volumes of stimulation and the lesion network map were, therefore, calculated and the resulting connectivity metric was correlated to the improvement values in each subject.

It is worth mentioning, that the different connectivity fingerprints (or R-maps) derived in this dissertation depend primarily on the type of percent improvement calculated from the clinical examination. For study 1, the connectivity fingerprint of lateralized upper limbs tremor improvement was investigated, since the upper limbs are the primary body parts affected in ET. This analysis has been performed using both functional and structural connectomes. An R-map for bilateral upper limbs and for head tremor improvements was also separately computed using only the functional connectome. The latter analyses lend the opportunity to investigate the somatotopic topology of the optimal therapeutic fingerprints. For study 2 and 3, only the functional (adult or pediatric) connectomes and global

body improvement in YGTSS and BFMDRS were used, respectively. Lastly, a connectomic sweetspot was calculated in study 1 which represents a location where both the structural and the functional connectivity fingerprints maximally overlap. In order to do so, the structural and functional R-maps were first masked to include on cortical and cerebellar regions. Connectivity was estimated seeding from these regions to the rest of the brain using the respective normative connectomes. The resulting connectivity maps were finally mathematically multiplied and the resulting map was tightly thresholded to include only voxels with high values.

## **2.7 Using Anatomical Lesion Locations to Identify Therapeutic Deep Brain Stimulation-Network**

Study 2 encompassed lesion network mapping and therapeutic confirmation of it. This section will describe the part dealing with lesion network mapping and how its subsequent result was used as a network correlate to explain the therapeutic DBS benefit in separate clinical cohorts.

### *2.7.1 Identifying Cases of Lesions from the Literature*

Cases of focal brain lesions causative of secondary tics were collected based on a systematic online search of PubMed (Medline 1966–2020) and EMBASE (1947–2020) using a combination of free-text, MeSH terms, and truncated words. In general, the search focused on identifying any case with the occurrence of tics or TS and an associated focal brain lesion or radiological findings. Cases were included if they were reported in English language. Additionally, case reports, case series, letters, or observational studies were included if they described new-onset tics attributable to lesions of the CNS. The location of the latter should be shown by a neuroimaging figure (slice) that was further described in writing. Relevant articles were then filtered and read thoroughly to assess their eligibility. Reports of *tic-like* phenomena, drug-induced tics and tics due to peripheral nervous system trauma, typical neurodevelopmental or genetic syndrome were excluded. Additionally, any report of surgical lesion associated tics improvement were also excluded.

### *2.7.2 Lesions Tracing and Lesion Network Mapping*

The location and the distribution of the tics-inducing lesions were determined from the imaging figures provided in each publication included in study 2. Next, the level of the



imaging slice available in these figures was matched with a slice in the adult MNI template. The lesions were then drawn (traced) on the specific slice using the openly available 3D Slicer software (<https://www.slicer.org/>). Basically, all the voxels corresponding to the location and the spatial distribution of a lesion in the 2D slice were assigned a value of 1 and stored as a nifty mask image. These lesion masks were then entered as seed to calculate whole-brain functional connectivity profile using the Lead-Connectome Mapper tool<sup>106</sup>. An average T-map was then extracted (see section 2.5 above). Next, each lesion-associated T-map was thresholded to a T-score  $\geq 7$  following the method in<sup>34</sup>. This arbitrary thresholding represents a significance of  $10^{-6}$  – family-wise error (FWE) corrected for multiple comparison. After thresholding, the surviving voxels were assigned a value of 1 to create a mask image per lesion-connectivity profile and later overlaid across lesions to create the “*lesion network map*”. This map was thresholded to include only voxels that were connected to  $\geq 19/22$  lesions which account for  $\sim 85\%$  of cases (Fig.3). This map represented a sensitivity map which means that the voxels included in it are sensitive to the occurrence of tics induced by the lesions. In a next step, a specificity map, in which voxels are specifically connected to the tics-inducing lesions when compared to other types of lesions, was calculated. To do so, a set of 717 focal lesions from the Harvard Lesion Repository was used<sup>36</sup>. Of note, those lesions did not induce tics but rather have induced other neuropsychiatric symptoms (like Holme’s tremor<sup>37</sup>, parkinsonism<sup>38</sup>, dystonia<sup>34</sup>, hallucinations<sup>33</sup>...etc). Their connectivity T-maps were calculated similarly to the method in lesion network mapping while using the same functional normative connectome. Those T-maps were compared with T-maps of the tics-inducing lesions using a two-sample voxel-wise t-test implemented in FSL Permutation Analysis of Linear Models (PALM; <https://fsl.fmrib.ox.ac.uk/fsl/fslwiki/PALM>). As the name implies, it applies permutation testing on voxel-wise manner to extract voxel significance values using different statistical testing and multiple comparison correction methods. Only voxels that have FWE-corrected p-values of  $< 0.05$  were retained to ensure avoidance of false-positive findings<sup>131</sup>. Lastly, a “*conjunction map*” was extracted from the mathematical multiplication of the sensitivity and the specificity maps which contained common voxels for both maps.

### 2.7.3 Relevance of the Lesion Network Map to DBS-related Outcome

The connectivity strength between the seeds (bilateral volumes of simulation in the DBS cohort of study 2) and the regions of interest was first computed (in the present case the

lesion network sensitivity and specificity maps in addition to the conjunction map). This process was performed by averaging the BOLD signal in all the voxels of the seeds as well as in the regions of interest and then calculating the correlation between them. The resulting connectivity strength was used as a metric to quantify how much each stimulation site in the DBS cohorts was connected to the lesion network maps. The connectivity metrics were later correlated with the corresponding percent improvement in the YGTSS scores to investigate whether the magnitude of connectedness of the volumes of simulation is associated with the clinical benefit resulting from the DBS therapy. Of note, the connectivity values were normalized to a Gaussian distribution using the method described by van Albada et al<sup>132</sup>. Crucially, the method adopted in this section was tailored to investigate how tic-improvement in different patients, who were implanted in different centers and targeting different structures, relate to connectivity to specific and/or sensitive voxels distribution in the lesion network map. Lastly, in analogy to the method described in section 2.6, DBS network mapping was used to extract R-maps from each DBS sub-cohort (thalamic and pallidal) using the percent improvement in the YGTSS, which allowed the computation of an “*agreement map*”<sup>133</sup>. The agreement map was designed to find overlapping voxels between the thalamic and the pallidal connectivity fingerprints and allows to compare the results to those of the lesion network map in a spatial distribution fashion.

## 3. Results

The core findings of this dissertation are reflected in the results of the three publications included in it. The connectivity fingerprints of the three studied movement disorders demonstrated interconnected regions that are relevant to the canonical pathophysiological network of each disease. These fingerprints were derived from different normative connectomes using different clinical metrics to measure DBS outcomes. Additionally, these connectivity fingerprints have shown a tendency to respect the somatotopic organization of brain networks. Lastly, the optimal connectivity fingerprints were computed with the aid of age-specific connectomes and neuroimaging templates.

### 1.1 Patients' Demographics

#### 3.1.1 *Essential tremor cohort (Study 1)*

A total of 36 patients with 72 bilaterally implanted DBS electrodes were included. This constituted 13 female and 19 male ET patients with an average age of  $74.3 \pm 11.9$  years and a mean disease-duration of  $24.33 \pm 4.99$  years until DBS surgery. The patients have been mainly implanted with a Medtronic 3387 electrode model ( $n = 33$ ) in addition to  $n = 2$  with a Boston Scientific Vercise Directed and  $n = 1$  St. Jude ActiveTip (6142-6145) electrode models. The average baseline tremor score was  $33.3 \pm 9.6$  (mean  $\pm$  standard deviation), which was decreased to  $10.9 \pm 5.5$  with the chronic DBS therapy. This accounts for an average percent improvement of  $65.1 \pm 18.4\%$  in total tremor score. The baseline contralateral upper limbs tremor score was  $13.4 \pm 4.3$ . It was reduced to an absolute score of  $4.6 \pm 2.9$  postoperatively (% improvement =  $63.4 \pm 22.9\%$ ). The baseline head tremor score was  $3.8 \pm 2.8$ . It was reported as  $1.0 \pm 1.7$  on postoperative follow-up visits (% improvement =  $80.8 \pm 29.5\%$ ). On average, the time to postoperative follow-up visit was  $12 \pm 9.86$  months.

#### 3.1.2 *Tourette syndrome cohorts (Study 2)*

The cohort of TS comprised three sub-cohorts that have been implanted in three different clinical centers. The Cologne/Germany sub-cohort included 15 Tourette patients who have been implanted with bilateral DBS electrodes in thalamic nuclei. The sub-cohort contained 12 male and 3 female subjects with an average absolute baseline YGTSS of

39.1 ± 8.6 and an average follow-up YGSTS of 23.8 ± 10.5. The percent mean improvement gained from chronic DBS therapy was 39.3 ± 22.4%. The pallidal sub-cohort comprised the Maastricht/Netherlands (n = 6 with 3 female subjects) and the Paris/France (n = 9 with 4 female subjects) patients. The Maastricht/Netherlands sub-cohort had an average YGTSS of 40.5 ± 5.8 at baseline and 12.8 ± 4.1 at follow-up with a calculated average percent improvement of 68.2 ± 8.8%. A baseline YGTSS of 44.2 ± 10.1 was reported for the Paris/France sub-cohort with a postoperative YGSTS 13.0 ± 7.0 at time of follow-up and a resulting percent improvement of 53.6 ± 20.3%.

### 3.1.3 Pediatric dystonia cohort (Study 3)

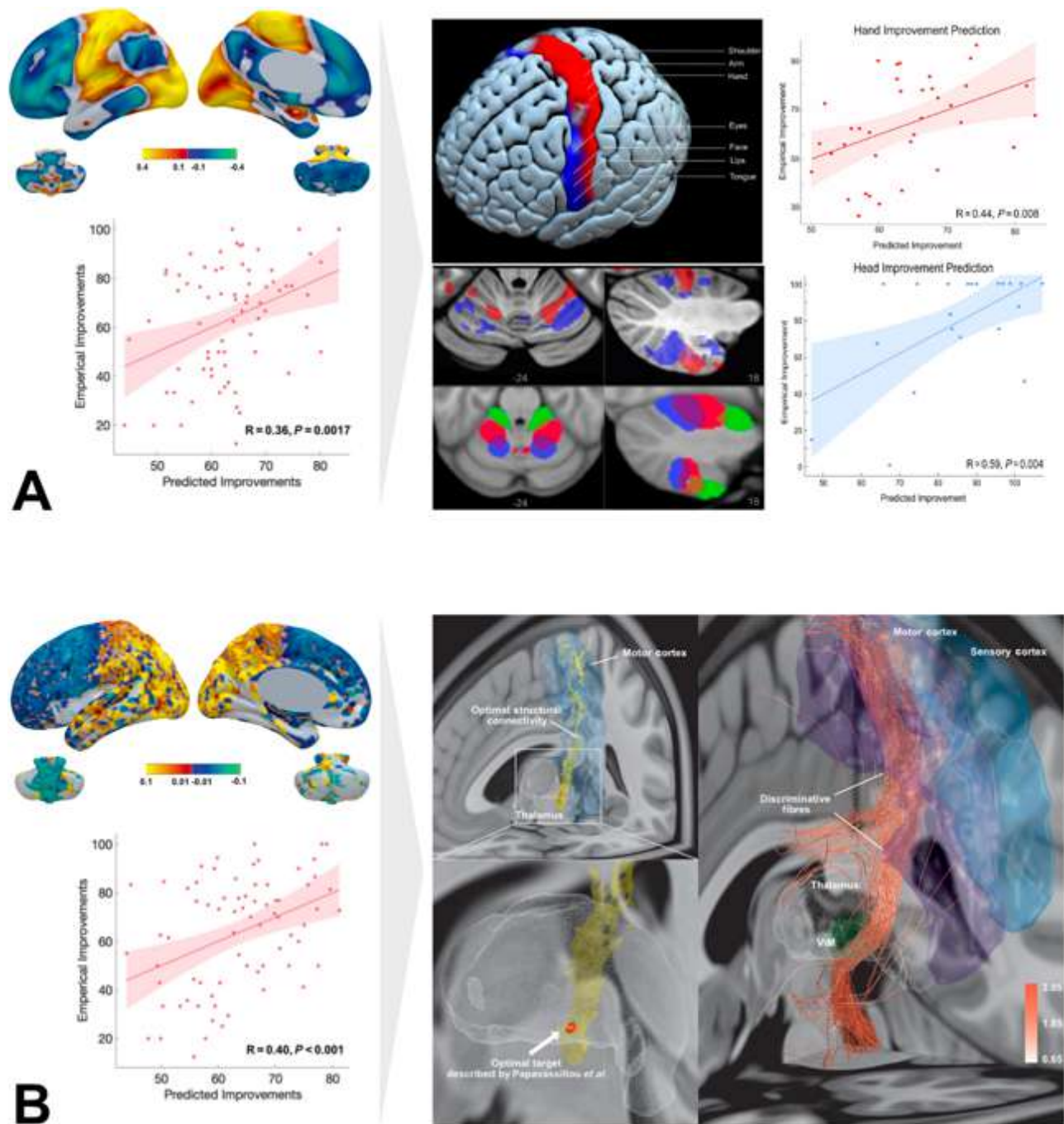
All the retrospective patients included for the pediatric study 3 were part of the GEPESTIM registry. Twenty children were included with an average age at DBS surgery of 11.55 ± 3.91 years. Average patients' age at time of the diagnosis of dystonia was 2.9 ± 3.21 years with an average disease duration of 8.65 ± 5.06 years. The patients were implanted with DBS in five different German clinical centers (Berlin, Lübeck, Düsseldorf, Hannover and Cologne) for the interval between 2008-2020. On average, the baseline BFMDRS was 71.68 ± 26.51 points with a postoperative reduction to an average of 56.43 ± 32.95 points and a percent postoperative improvement of 23.89 ± 30.95%). The classification of dystonia was different across the full cohort. Six patients have been diagnosed with acquired dystonia (with a perinatal brain insult as the main cause) and the other 14 patients were suffering from the idiopathic/inherited types of dystonia (n = 9 idiopathic and n = 5 inherited). In the inherited group, the following gene mutations were identified: DYT-TOR1A (n = 3), GNAO1 (n = 2), DYT-SGCE (n = 1), DYT-PRKRA (n = 1), DYT-ANO3 (n = 1), DYT-KMT2B (n = 1).

## 3.2 Optimal Therapeutic Connectivity in Patients with Essential Tremor

The R-map of study 1 has identified brain regions that are connected to the volume of stimulation and their connectivity positively correlated with tremor improvement. Using a functional connectome, these regions included the primary motor and sensory cortices, the premotor and supplementary motor cortices, the visual cortices and superior and inferior lobules of the cerebellum (Fig. 1A). Structural connectomics highlighted regions that highly overlap with the aforementioned ones. The functional connectivity fingerprint significantly predicted tremor improvement in the contralateral upper limbs in LOOCV (R =

0.36,  $P = 0.0017$ ). Similarly, the structural connectivity fingerprint could also predict contralateral upper limbs tremor improvement (0.40,  $P < 0.001$ ). To investigate their agreement, upper limbs tremor improvement was predicted using cross-modality connectomic fingerprints (i.e., by correlating improvement to the spatial similarity indices of seed-based connectivity of one modality to the R-map of the other modality). The prediction remained valid with ( $R = 0.41$ ,  $P < 0.001$ ) when the structural R-map was used to explain improvement by functional seed-based connectivity, and ( $R = 0.33$ ,  $P = 0.005$ ) when structural seed-based connectivity was explained by the functional R-map. Using bilateral upper limbs tremor scores, the R-map has yielded similar prediction performance. Of note, structural connectivity had also highlighted part of the cerebellothalamocortical pathway when fiber-filtering tool of Lead-DBS was used (Fig.1B).

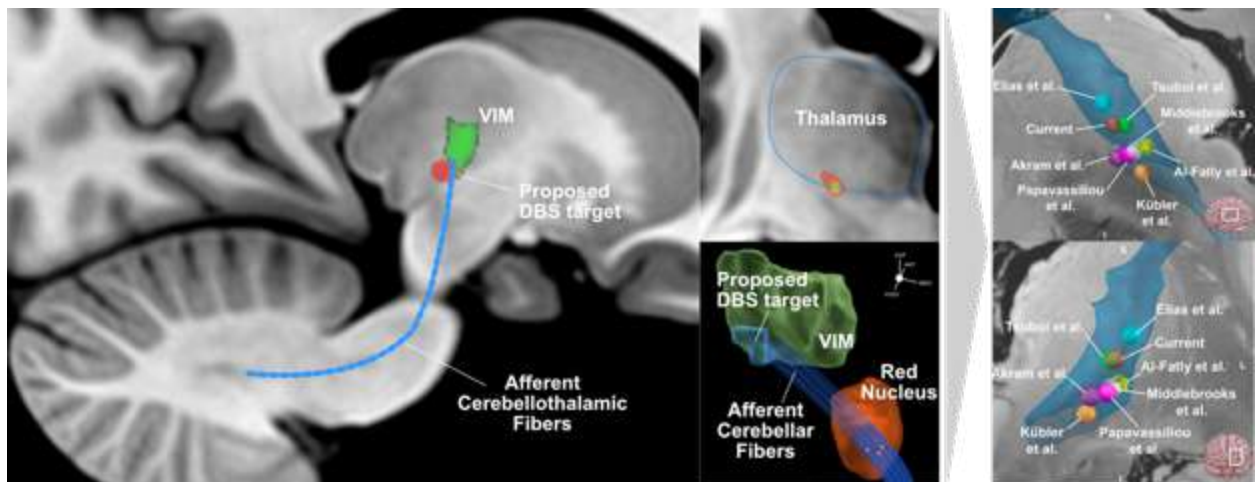
Interestingly, the functional connectivity fingerprint associated with bilateral upper limbs tremor mapped to the hand region of the cortical motor strip and the cerebellum. Furthermore, connectivity fingerprint of head tremor improvement mapped to the tongue regions of the previously mentioned brain areas. Those fingerprints were predictive of respective body-part tremor improvement ( $R = 0.44$ ,  $P = 0.008$  for upper limbs tremor and  $R = 0.59$ ,  $P = 0.004$  for head tremor; Fig. 1A right panel).



**Figure 1: Connectivity correlates of DBS improvement in ET patients. A.** Functional R-map model showing areas with functional connectivity that correlates positively (res-yellow) or negatively (blue-green) with tremor improvement after DBS therapy (left panel). Scatter plot illustrates the leave-one-out cross-validation of the spatial similarities of each stimulation volume to the resulting R-map model and respective DBS outcome ( $R = 0.36$ ,  $P = 0.002$ ). The topology of the R-map aligns with the canonical network implicated in the pathophysiology of tremor. Additionally, using tremor improvement in hand only or head only body regions resulted in a correlative connectivity pattern that distribute to respective

homuncular topology in the motor cortical strip as well as the cerebellum (right panel). **B.** Voxel-wise structural R-map model highlighted regions similar to the functional R-map and could predict DBS outcome in leave-one-out cross-validated correlation ( $R = 0.40$ ,  $P < 0.001$ , left panel). Voxels of highest correlative R-values extended from the motor cortex (blue) to the region of VIM-thalamus and subthalamic area (right panel) and encompass an optimal published DBS target (red sphere). When replicated on fiber streamlines, streamlines predictive of tremor outcome corresponded to a subpart of the cerebello-thalamocortical tract commonly implicated in tremor pathophysiology and therapeutic targeting (streamlines in red-white). Figure adapted from Al-Fatly et al, 2019<sup>97</sup>.

Both connectivity fingerprints (structural and functional) have found a common connectomic sweetspot. By definition, this sweetspot should maximize connectivity from both fingerprints and was located inferoposteriorly to the VIM overlapping with its lower border and with the Zi (MNI coordinates of the center of gravity:  $x = \pm 16$  mm,  $y = -20$  mm,  $z = -2$  mm; Fig.2).



**Figure 2: Connectomic anti-tremor DBS sweetspot.** The sweetspot represents a voxel cluster that maximized functional and structural connectivity associated with the predictive connectomic models. The sweetspot is located mainly in the subthalamic area encroaching on the inferior border of the VIM-thalamus where the majority of the afferent cerebellothalamic fibers enter the cerebellar-receiving thalamic neurons (red, left panel). This sweetspot has been shown to cluster with other recently and previously identified sweetspot of beneficial DBS outcome in ET (right panel). The figure is adapted from Al-Fatly et al<sup>97</sup> (left panel) and Middlebrooks et al<sup>134</sup> (right panel). Names in right panel

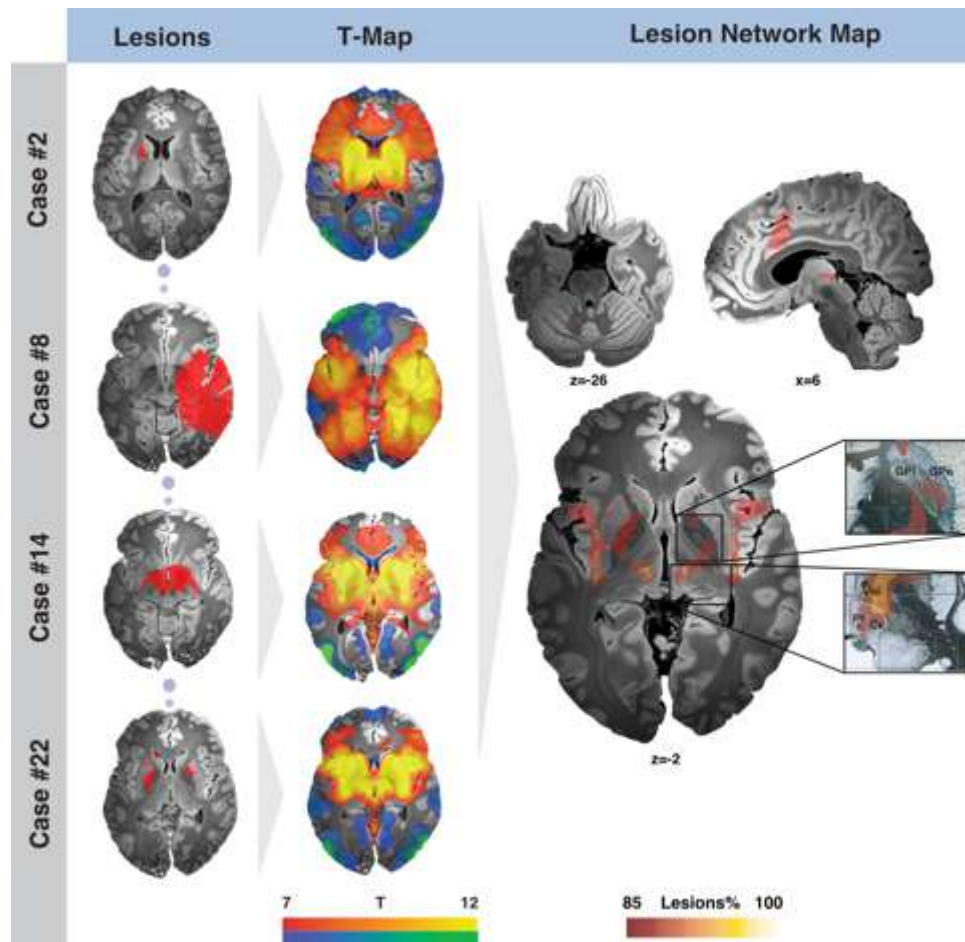
correspond to the respective literature which published the coordinates of beneficial sweetspots.

### **3.3 Lesion-derived Connectivity Explains DBS-related Tics Improvement**

The literature search identified 22 lesion-cases based on the inclusion/exclusion criteria mentioned in the methods section. Lesions distribution elucidated the basal ganglia as a common site in 17 cases. However, basal ganglia locations have expressed a good amount of heterogeneity in addition to involvement of extra-basal ganglia brain sites. The latter included the insula, the parietal and temporal cortices, the brainstem and the thalamus.

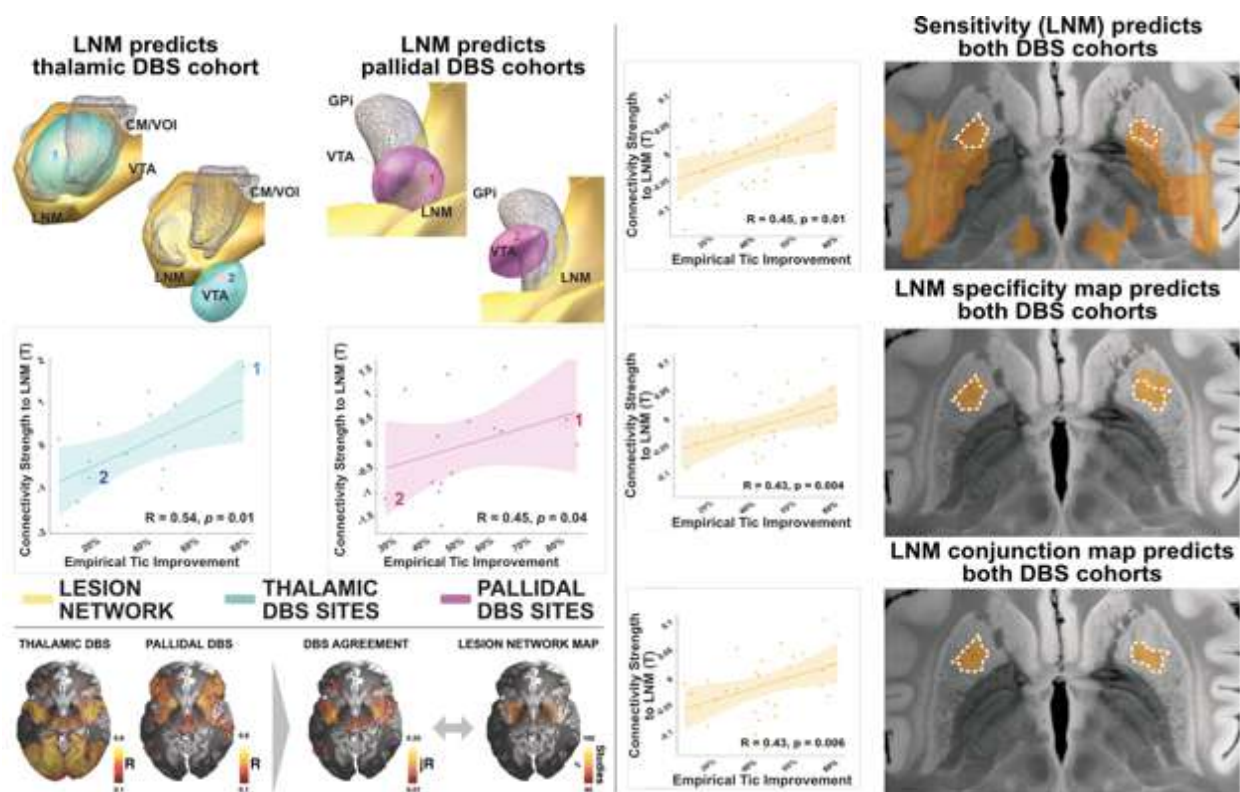
Apart from their heterogenous locations, tics-inducing lesions were connected to a common and unique brain network (Fig. 3). Clusters of voxels located in the striatum, anterior cingulate gyrus, pallidum, thalamus, insula and the cerebellum were connected to ~86% of the lesions (19/22). These clusters were sensitive to tics occurrence. Furthermore, bilateral clusters in the anterior putamen were identified as specific to tics occurrence. These clusters expressed significantly higher functional connectivity to tics-inducing lesions when compared to 717 other lesions associated with other neuropsychiatric presentations.





**Figure 3: Lesion network map of secondary tics disorders.** Lesions were traced on slices of MNI-template (backdrop here is the high-resolution postmortem  $100\mu\text{m}$  7T MRI from<sup>135</sup>) and used as seeds in the 1000 subjects normative connectome. T-maps were extracted and thresholded to  $T > 7$  and subsequently binarized to be overlapped. This results in the lesion network map which later can be thresholded (19/22 ~ 85%) to highlight regions of maximum connectivity to the lesions under study. The topology of the tics-LNM is corresponding to the pathophysiological hubs already known to play major roles in tics generation and phenomena like premonitory urges. The anterior cingulate cortex, insula, cerebellum, thalamus (CM/Pf) and basal ganglia (putamen and GPi/GPe) were highlighted as areas of highest functional connectivity to lesion locations responsible for the development of secondary tics. Of note, the GPi and CM/Pf are two main DBS targets for treatment of TS. Figure is adapted from Ganos and Al-Fatly et al, 2022<sup>35</sup>.

The above-mentioned result of a specific and sensitive network of tics-inducing lesions was intriguing. It has provided the possibility to test the hypothesis that this network could also be targeted by DBS therapy in primary tics disorders. To do so, connectivity from the volumes of stimulation in the thalamic and pallidal DBS cohorts was calculated to each of the sensitivity, specificity and conjunction maps (Fig.4 right panel). The normalized connectivity strength correlated significantly with YGTSS improvement when both pallidal and thalamic sub-cohorts were analyzed (Fig.4 left panel). Indeed, connectivity to the sensitivity map correlated with improvement from DBS in pallidal ( $R = 0.45$ ,  $P = 0.04$ ), thalamic ( $R = 0.54$ ,  $P = 0.01$ ) and both sub-cohorts together ( $R = 0.45$ ,  $P = 0.01$ ). In addition, connectivity to the specificity cluster correlated with improvement when both sub-cohorts analyzed together ( $R = 0.43$ ,  $P = 0.004$ ) and similar result was found when the conjunction cluster was used ( $R = 0.43$ ,  $P = 0.006$ ). Finally, the distribution of the pallidal and thalamic R-maps was merged into an agreement map which maximizes connectivity to both DBS (Fig.4 right panel). The topology of the agreement map aligned with that determined by the lesion network map and further highlighted important nodes in the network (the pallidum, the thalamus, the insula and the putamen).

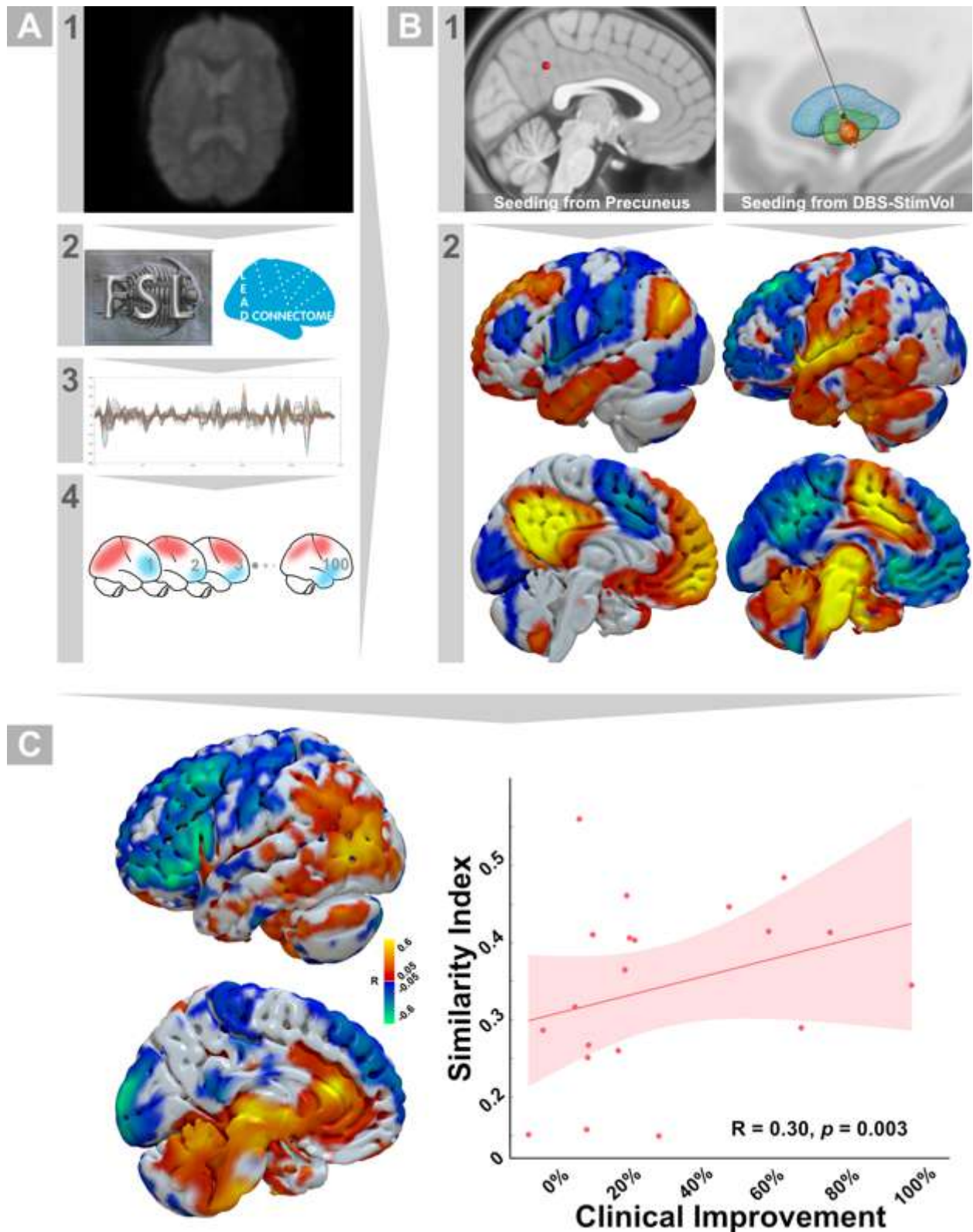


**Figure 4: Connectivity to the LNM of secondary tics correlates with tics-outcome after DBS in TS patients.** Functional connectivity from stimulation volumes in the thalamus (blue) or the pallidum (purple) to the LNM (yellow) correlated with the DBS-induced

YGTSS-outcome in both cohorts separately (left upper panel). The correlation stayed significant when both cohorts accumulated together in the same analyses regardless of the LNM used (sensitive (orange), specific or conjunction maps (white interrupted line), right panel). Spatial topologies of the positive part of pallidal and thalamic R-map models and their agreement map correspond to the same regions highlighted in the sensitive LNM and highly overlap with the cluster identified in the specificity LNM and the conjunction map (left lower panel) hinting toward a common causal and therapeutic network. This figure is adapted from Ganos and Al-Fatly et al <sup>35</sup>.

### **3.4 An Anti-dystonic Functional Network in Children**

In the pediatric dystonia cohort of study 3, a network (R-map) depicting the anti-dystonic effect by correlating BFMDRS improvement to connectivity from DBS volumes of stimulation was estimated (Fig.4). Connectivity to regions like the sensorimotor cortices, frontal cortex, and the posterior cerebellum was negatively correlated with BFMDRS improvement. On the other hand. This means that volumes of stimulation connected to these regions will imply bad clinical outcome after DBS therapy. On the other hand, areas like the parietal cortex, the anterior cingulate cortex, the superior cerebellar regions and the brainstem indicated good clinical outcome when the volumes of stimulation from the DBS electrodes are being connected to them. Generally, similarity between the connectivity profiles seeding from volumes of stimulation to this R-map model was significantly correlated with improvement in BFMDRS using permutation testing ( $R = 0.30$ , permuted  $P = 0.003$ ).



**Figure 5: Connectomic DBS in pediatric dystonia.** A rs-fMRI acquisitions (A1) from 100 neurotypical children were processed using FSL and codes from Lead connectome Matlab pipelines (A2) to extract BOLD time-series (A3). These time-series from each sub-

ject were then stacked into matrices that are ready to be used in Lead-connectome Mapper (A4). **B** Example connectivity profiles from seeds regions (B1) of the precuneus and a representative stimulation volume in the GPi and their corresponding surface topologies (B2). **C** Functional R-map correlates with DBS-improvement of a cohort of 20 children diagnosed with dystonia from the GEPSTIM consortium. P-value represents the significance of permutation used to build the null-distribution. The figure is adapted from Al-Fatly et al, 2023 <sup>98</sup>.

## 4. Discussion

### 4.1 Short Summary of Results

The findings in the present dissertation focus on deriving network fingerprints of the therapeutic effect of DBS. The original publications included in this dissertation could still demonstrate and discuss results that extend beyond the network-perspective, especially studies 2 and 3<sup>35,97,98</sup>. Connectivity patterns of beneficial DBS therapy in three movement disorders (ET – study 1, tics disorder – study 2, and pediatric dystonia – study 3, were shown to be distributed to specific brain topologies. Connectivity from the volumes of stimulation in the respective DBS-cohorts to regions in these networks expressed positive and negative correlations with DBS-related improvement. Improvement in ET severity could be explained by such a data-driven, whole-brain network model. Somatotopic distribution of beneficial connectivity patterns align with the somatotopic representation of the brain<sup>117,136,137</sup>. Additionally, cross-modal connectivity patterns determined a connectomic sweetspot for tremor relief in study 1. Connectivity to regions in the network of tics-inducing lesions correlated with tics reduction in DBS cohorts of different surgical targets. An age-specific connectome was used to derive the connectivity fingerprint when DBS results in children were analyzed. DBS electrodes with connectivity profiles which were approximating this connectivity fingerprint correlated with improvement in dystonia.

### 4.2 Network Correlates of Therapeutic Effects

The principal aim of this dissertation is to identify neural networks that correlate with the clinical outcomes in patients undergoing DBS therapy<sup>138</sup>. These networks have been delineated in three movement disorders: ET, TS, and dystonia in children. First, the three therapeutic networks were in alignment with the canonical disease-specific previously determined pathological networks. ET is usually described as an oscillopathy that affects numerous central neuronal populations connected through the CTC pathway<sup>44,139</sup>. This has been corroborated in the present dissertation by allocating part of the CTC pathway that is relevant to DBS-related tremor improvement<sup>140</sup>. In addition, the sensorimotor, the premotor as well as the thalamus (more specifically the VIM nucleus) have been also regarded as culprits of tremorogenesis<sup>44,141–143</sup>. These regions were among the most positively correlative areas in the functional and structural connectivity fingerprints. Additionally, the motor cerebellum was a key node in the functional R-map. Different pathological,

neurophysiological and neuroimaging studies have all pointed towards the central role of the cerebellar structures in different types of tremors but specifically in ET<sup>144–149</sup>. Strikingly, the visual cortices (primary and associative) were amongst the important nodes in the therapeutic connectivity fingerprints. While this observation could be initially considered as irrelevant, the finding has been demonstrated in different other studies<sup>150–154</sup>. Tuleasca et al. found a relationship between preoperative structural and functional alterations in the visual cortices and postoperative outcome in ET patients after lesional radiosurgery<sup>150–152</sup>. Connectivity of radiosurgical lesions to the visual cortices has been demonstrated to correlate with ET improvement in another recent study<sup>154</sup>. Needless to say, that the visual areas have an essential role in providing the necessary visuospatial inputs to the motor system that could lead to tremor deterioration once pathologically altered<sup>153</sup>. While study 1 endeavored to provide comprehensive tremor-related therapeutic networks leveraging structural and functional brain-wide connectivity, it also afforded a connectomics-derived sweetspot. It is important to emphasize that the method with which this “local” spot has been determined is different from the many available methods for sweetspot analyses<sup>155</sup>. The spot maximized the convergence of the structural and functional anti-tremor therapeutic fingerprints localized to the posterior subthalamic region (PSA); an important surgical target in treating ET<sup>156–159</sup>. The PSA is a complex hub of loose neuronal populations nested inside densely aligned fiber tracts<sup>160</sup>. With its extension between the internal capsule laterally, and the VIM and the sensory thalamic nuclei superiorly, the connectomic sweetspot displayed spatial similarity to a cluster of good clinical efficacy of thalamotomy lesions described in a recent study by Boutet et al.<sup>161</sup>. Additionally, Middlebrooks et al have shown that the center of gravity of the sweetspot with many other spots calculated in different studies had an interesting alignment along the path of the CTC pathway<sup>134</sup>. Interestingly, the same cohort of study 1 has been used in two other studies identifying similar regions based on pure neuroimaging markers or sweetspot analysis for multicenter retrospective assessment of DBS outcomes in ET<sup>162,163</sup>.

Lesion network mapping has been recently used as a powerful tool to derive pathologically and therapeutically relevant brain networks<sup>36</sup>. These networks harbor the necessary neuroanatomical substrates that define the nodes and hubs underpinning the mechanism of specific disease state<sup>37,38,53</sup>. In study 2, rare tics-inciting focal lesions were located in specific brain sites that were interconnected by a common and specific functional neural

network<sup>35</sup>. The network involved areas that were previously identified as essential in tics generation. Specifically, areas in the cortico-basal-ganglia-thalamo-cortical circuit, like the putamen, the pallidum, the thalamus (CM/Pf nuclei), the insular cortex and the anterior cingulate cortex are all well-known nodes in tics pathology<sup>56</sup>. Bohlhalter et al. have found with the aid of fMRI that the onset of tic necessitates recruitment of regions similar to the ones identified in the present dissertation<sup>164</sup>. Of note, activation of the insula and the anterior cingulate cortex have also been associated with premonitory urges, vocalizations and tic occurrence<sup>165–167</sup>. Moreover, pathological studies have highlighted the different structural changes in the basal ganglia regions in tics patients<sup>168,169</sup>. Needless to say, that the GPi and CM/Pf nuclei were already used as anatomical targets for lesional (and later DBS) surgeries by Hassler and Dieckman to treat patients suffering from tics, and they are parts of the network as has been alluded to before<sup>170</sup>. The fact that the lesion network map identified could serve as a target for guiding DBS therapy has been already demonstrated in study 2<sup>35</sup>. Reduction in patients' tics correlated with the degree of connectivity of their stimulation sites to the lesion network map. Furthermore, the patients have been implanted in different centers involving different surgeons, as well as using two different anatomical targets (GPi and CM/Pf). Importantly, the agreement map implemented in study 2 to find the convergence between therapeutic maps of both surgical targets has a similar distribution of the lesion network map. Taken together, these findings extend the observations in a previous study using structural connectivity to explain DBS induced tics improvement which did not use lesions information to extract relevant brain networks<sup>171</sup>.

Lastly, the DBS-network described in the pediatric dystonia cohort (study 3) displayed specific patterns that partially coincide with the network of Horn et al.<sup>92,98</sup>. Importantly, Horn et al. have used adult normative connectomes and neuroimaging tools to estimate the therapeutic connectivity fingerprints on contrary to the methods of study 3 in this dissertation. Regions like the sensorimotor cortex and cerebellum have expressed negative correlation between their connectivity to DBS and improvement in dystonia<sup>92</sup>. This finding has been described in a previous lesion network mapping study, which also identified negative connectivity to a well-characterized pallidal DBS cohort<sup>53</sup>. The sensory cortex is central for the pathological processes involved in dystonia<sup>172</sup>. Multiple neurophysiological and imaging studies have shown its key role in such a context<sup>55,173,174</sup>. The cerebellum, on the other hand, has been considered a target for neuromodulatory techniques as an attempt to treat dystonic symptoms<sup>175–177</sup>. Connectivity from the DBS electrodes to the



anterior cingulate cortex was associated with good clinical outcome as the identified network has shown. Its primary role in developing dystonia is unknown<sup>178</sup>. However, primates studies have proved its relevance to motor function<sup>179</sup>.

### 4.3 Somatotopic Organization of the Therapeutic Networks

The finding of a specific somatotopic distribution of the therapeutic network is intriguing. First, this distribution was totally based on a data-driven approach. Second, reduction in upper limbs and head tremor mapped to the hand and tongue areas of the human M1 homunculus and motor cerebellum, respectively. Third, these connectivity patterns predicted the respective tremor improvements in their corresponding body parts. A salient feature of ET symptomatology is the predominant tremor of the upper limbs<sup>180</sup>. The head is regarded as the second most body part affected by tremor that can be an outcome issue in patients treated with DBS<sup>180,181</sup>. This finding signifies the importance of tailoring DBS therapy according to the predominance of the body part affected by disabling tremor symptomatology<sup>182</sup>. Of note, one study has already demonstrated the utility of somatotopic DBS targeting in dystonic patients<sup>183</sup>. Additionally, two studies have considered somatotopy in magnetic resonance-guided focused ultrasound subthalamotomy for Parkinson's disease and thalamotomy for ET. Notably, the last two studies were published after study 1 of the present dissertation<sup>184,185</sup>.

### 4.4 Towards Age-specific Connectomic Analyses

Understanding brain disorders as network disease is a relatively modern outlook in the field of neuropsychiatry that has been accepted as a contemporary stream in many scientific literatures<sup>3,36,87</sup>. Analytical methods used to infer networks are usually based on group-level estimation<sup>4,36,118</sup>. This requires aggregation of subjects' (usually normative) data in a common brain coordinate system and the use of numerous brain atlases and assembled connectomes<sup>4,108,114,118</sup>. However, an important aspect of the method is to match the possible effects of age of the subjects on possible functional and anatomical variances<sup>186,187</sup>. Since the brain templates and connectomes are usually normative, they should reflect as much as possible the expected developmental brain stage of the study cohort. The template and connectome used in study 3 is a good example of such an age-specific neuroimaging tool<sup>98</sup>. Most of the available neuroimaging tools that could serve

the purpose of group-analyses have data which belong to adult subjects<sup>6,105,118</sup>. Study 3 provided a dataset that is accessible by the scientific community and helps DBS neuroimaging analyses of pediatric patients. The pediatric normative connectome assembled in study 3 parallels the developmental changes in brain connectivity, especially those relevant to the basal ganglia and the motor system<sup>188,189</sup>.

#### **4.5 Implications for Practice and Future Research**

Many implications can be inferred from the findings reported in the present dissertation that are relevant to research or clinical practice. Crucially, the findings discussed here are clinically relevant for possible future refinement of surgical targeting and planning, guiding DBS programming, and finding new targets across different modalities of therapeutic approaches. The concept of delineating networks that encompass different interconnected brain regions instead of one local region is insightful. Such networks could unify different surgical targets that have been previously used and can help explain why some targets are more powerful in controlling specific neuropsychiatric symptoms than others. Additionally, the therapeutic connectivity fingerprints identified in the current dissertation could afford accessible cortical regions that could be modulated by non-invasive stimulation techniques. The somatotopic organization of the therapeutic network of ET (study 1) lends the possibility of personalizing DBS treatment based on the most affected body parts. Indeed, personalizing DBS therapy should profit from symptoms and body parts specific DBS networks. Additionally, the identified upper limbs and head tremor networks in study 1 could call for finding patient's specific somatotopic distribution in order to tailor the DBS therapy (e.g., scanning the patient while performing hand or tongue movement or imagery task under fMRI). Deriving therapeutic networks by harnessing clues for causalities (like focal brain lesions as in study 3) could open a new avenue in the field of neurology. Previous studies have found a good amount of overlap between causative and DBS therapeutic networks. These findings call for further confirmative and systematic investigations in different neuropsychiatric disorders. Actually, one study that has been published after study 2 confirmed the overlap between different therapeutic networks and a network associated with depression induced by stroke lesions. Lastly, children with disabling TS and medication-refractory Epilepsy are being increasingly treated with DBS. Imaging-analyses of the aforementioned example cases could then benefit from the pediatric neuroimaging resource introduced in study 3 (including the template and its accompanying

subcortical atlas in addition to the normative connectome). Besides, the latter connectome could also be used in research areas outside the realm of DBS (e.g., lesion and atrophy network mapping in children with Epilepsy or Autism to give a few examples).

#### 4.6 Limitations

The three studies included in this dissertation have some limitations. Some of them are general to the nature of the group-level connectivity analysis and the others are specific to each study. In general, using normative connectomes could be seen as a limitation on first sight. Since the imaging data in these connectomes stem from normal subjects, seed-based connectivity using them as surrogate dataset does not necessarily reflect the disease states of DBS patients. Furthermore, the measurement of seed-based connectivity relies on mathematical averaging across all the subjects in the connectome. This in turn means that the connectivity measures do not actually represent patient-specific connectivity. Specifically, lesions in study 2 could not express a connectivity pattern similar to the one simulated in a healthy brain if compared to patient-specific connectivity pattern. However, such connectomes have widely been used in stroke, transcranial magnetic stimulation, lesion network mapping, atrophy network mapping and many DBS studies. Additionally, imaging datasets for such connectomes were acquired using state-of-the-art MRI scanners and have better signal-to-noise ratio when compared to data acquired with clinical scanners. Furthermore, acquiring such high-quality data in patients and children with movement disorders could be a hard task because of a higher chance of movement artefacts. Another general limitation is related to the modeling of the stimulation volumes surrounding DBS electrodes. The model used in the studies of this dissertation is a simplified solution in comparison to more sophisticated models. However, the stimulation volumes were used as seeds to derive connectivity pattern in functional and structural connectomes, which have a resolution of  $\sim 2 \text{ mm}^3$ . Imprecisions incurred from such a model could be very subtle for such a coarse resolution though. Another yet important limitation is the use of retrospective DBS cases in all three studies (which also applies for the retrospective nature of literature-based tics lesions). This calls for well-designed multicenter prospective studies to be carried out in order to further prove the validity of the connectivity fingerprints identified here. Nonetheless, the therapeutic connectivity patterns showed in this dissertation could be used to formulate hypotheses for designing future studies.

Other limitations are specific for each of the studies and will be discussed according to the chronological appearance of each publication. Study 1 used VIM-DBS patients who were diagnosed with ET. This category of tremor cannot generalize the connectivity fingerprint identified to other tremor types like Holmes tremor, parkinsonian tremor, dystonic tremor or multiple sclerosis associated tremor. While the connectivity of both tics-inducing lesions and tics-treating DBS sites largely overlaps in study 2, the method cannot directly explain how DBS can correct the disruption induced by the lesions on this network level. DBS could retune the pathological oscillations in this network as it has been shown in Parkinson's disease and dystonia and, as such, this notion could be speculatively adopted as a partial explanation of why both therapeutic and pathological networks overlap. The small sample size is another limitation in the pediatric DBS cohort used in study 3. Besides, patients belonged to different class of dystonia which could add to the heterogeneity of the cohort. However, a notable fact is that dystonia is a rare movement disorder especially in pediatric populations. Yet, the source of heterogeneity in this cohort could be mainly related to the presence of acquired dystonia cases. Exclusion of these cases did not largely change the connectivity fingerprint neither its significance as a correlative model to explain DBS improvement. Needless to say, some cases had some genetic mutations that can lead to expression of further neurological symptoms like epilepsy in GNAO1 mutation. In this regard, the connectivity fingerprint did not include severity scores that can measure such additional manifestations and should only be interpreted as representative of improvement dystonic symptoms. The BFMDRS used as a clinical metric of dystonic severity in this study. This scoring system cannot account for complex hyperkinetic movement disorders which usually co-express with dystonia like ballism and choreoathetosis, in addition to non-motor manifestations. As such, the connectivity fingerprint presented in study 3 cannot be regarded as fully representative of all functional domains that can be presented in all the patients.

## 5. Conclusions

Within the framework of this dissertation, the therapeutic networks of DBS in three movement disorders (ET, tics and childhood dystonia) were identified. These networks align with the canonical pathological networks already identified in each disease respectively. Furthermore, this finding corroborates the notion that the mechanism of action of DBS could partly be explained by its ability to neuromodulate these networks. Clinicians can use these networks to refine DBS therapy of their patients. Furthermore, the effective DBS networks can be traced using lesions responsible for secondary neurological symptoms that are similar to the primary disease manifestations under DBS treatment. The concept of DBS networks can be applied in pediatric as well as adult clinical populations. Finally, the therapeutic networks can translate into brain-wide distributed targets that can be harnessed by different invasive and non-invasive neuromodulatory techniques to treat different neuropsychiatric disorders. In summary, this dissertation shed light on the translational power of unified brain networks in explaining the pathological underpinnings and the therapeutic mechanisms of brain disorders in different stages of the human lifespan.

## Reference list

1. Adali, T., & Ortega, A. (2018). Applications of Graph Theory. *Proceedings of the IEEE*, 106(5), 784–786. <https://doi.org/10.1109/JPROC.2018.2820300>
2. Al-Fatly, B. (2018). Coherence: A Unifying Mechanism of Deep Brain Stimulation. *Journal of Neurophysiology*, jn.00563.2018. <https://doi.org/10.1152/jn.00563.2018>
3. Al-Fatly, B., Ewert, S., Kübler, D., Kroneberg, D., Horn, A., & Kühn, A. A. (2019). Connectivity profile of thalamic deep brain stimulation to effectively treat essential tremor. *Brain*, 142(10), 3086–3098. <https://doi.org/10.1093/BRAIN/AWZ236>
4. Al-Fatly, B., Giesler, S. J., Oxenford, S., Li, N., Dembek, T. A., Achtzehn, J., Krause, P., Visser-Vandewalle, V., Krauss, J. K., Runge, J., Tadic, V., Bäumer, T., Schnitzler, A., Vesper, J., Wirths, J., Timmermann, L., Kühn, A. A., & Koy, A. (2023). Neuroimaging-based analysis of DBS outcomes in pediatric dystonia: Insights from the GEPESTIM registry. *NeuroImage: Clinical*, 39, 103449. <https://doi.org/10.1016/J.NICL.2023.103449>
5. Alshimemeri, S., Vargas-Méndez, D., Chen, R., Lipsman, N., Schwartz, M. L., Lozano, A. M., & Fasano, A. (2022). Functional tremor developing after successful MRI-guided focused ultrasound thalamotomy for essential tremor. *Journal of Neurology, Neurosurgery & Psychiatry*, 93(6), 625–627. <https://doi.org/10.1136/JNNP-2021-327524>
6. Anderson, J. S., Dhatt, H. S., Ferguson, M. A., Lopez-Larson, M., Schrock, L. E., House, P. A., & Yurgelun-Todd, D. (2011). Functional Connectivity Targeting for Deep Brain Stimulation in Essential Tremor. *AJNR: American Journal of Neuroradiology*, 32(10), 1963. <https://doi.org/10.3174/AJNR.A2638>
7. Archer, D. B., Coombes, S. A., Chu, W. T., Chung, J. W., Burciu, R. G., Okun, M. S., Wagle Shukla, A., & Vaillancourt, D. E. (2018). A widespread visually-sensitive functional network relates to symptoms in essential tremor. *Brain: A Journal of Neurology*, 141(2), 472–485. <https://doi.org/10.1093/BRAIN/AWX338>
8. Åström, M., Diczfalusy, E., Martens, H., & Wårdell, K. (2015). Relationship between neural activation and electric field distribution during deep brain stimulation. *IEEE Transactions on Bio-Medical Engineering*, 62(2), 664–672. <https://doi.org/10.1109/TBME.2014.2363494>

9. Avants, B. B., Epstein, C. L., Grossman, M., & Gee, J. C. (2008). Symmetric Diffeomorphic Image Registration with Cross-Correlation: Evaluating Automated Labeling of Elderly and Neurodegenerative Brain. *Medical Image Analysis*, *12*(1), 26. <https://doi.org/10.1016/J.MEDIA.2007.06.004>
10. Baldermann, J. C., Melzer, C., Zapf, A., Kohl, S., Timmermann, L., Tittgemeyer, M., Huys, D., Visser-Vandewalle, V., Kühn, A. A., Horn, A., & Kuhn, J. (2019). Connectivity Profile Predictive of Effective Deep Brain Stimulation in Obsessive-Compulsive Disorder. *Biological Psychiatry*, *85*(9), 735–743. <https://doi.org/10.1016/J.BIOPSYCH.2018.12.019>
11. Baldermann, J. C., Schüller, T., Huys, D., Becker, I., Timmermann, L., Jessen, F., Visser-Vandewalle, V., & Kuhn, J. (2016a). Deep Brain Stimulation for Tourette-Syndrome: A Systematic Review and Meta-Analysis. *Brain Stimulation*, *9*(2), 296–304. <https://doi.org/10.1016/J.BRS.2015.11.005>
12. Baldermann, J. C., Schüller, T., Huys, D., Becker, I., Timmermann, L., Jessen, F., Visser-Vandewalle, V., & Kuhn, J. (2016b). Deep Brain Stimulation for Tourette-Syndrome: A Systematic Review and Meta-Analysis. *Brain Stimulation*, *9*(2), 296–304. <https://doi.org/10.1016/J.BRS.2015.11.005>
13. Barbe, M. T., Reker, P., Hamacher, S., Franklin, J., Kraus, D., Dembek, T. A., Becker, J., Steffen, J. K., Allert, N., Wirths, J., Dafsari, H. S., Voges, J., Fink, G. R., Visser-Vandewalle, V., & Timmermann, L. (2018). DBS of the PSA and the VIM in essential tremor: A randomized, double-blind, crossover trial. *Neurology*, *91*(6), e543–e550. <https://doi.org/10.1212/WNL.0000000000005956>
14. Basha, D., Dostrovsky, J. O., Lopez Rios, A. L., Hodaie, M., Lozano, A. M., & Hutchison, W. D. (2014). Beta oscillatory neurons in the motor thalamus of movement disorder and pain patients. *Experimental Neurology*, *261*, 782–790. <https://doi.org/10.1016/J.EXPNEUROL.2014.08.024>
15. Bassett, D. S., & Sporns, O. (2017). Network neuroscience. *Nature Neuroscience*, *20*(3), 353. <https://doi.org/10.1038/NN.4502>
16. Bellato, A., Norman, L., Idrees, I., Ogawa, C. Y., Waitt, A., Zuccolo, P. F., Tye, C., Radua, J., Groom, M. J., & Shephard, E. (2021). A systematic review and meta-analysis of altered electrophysiological markers of performance monitoring in Obsessive-Compulsive Disorder (OCD), Gilles de la Tourette Syndrome (GTS), At-

- tention-Deficit/Hyperactivity disorder (ADHD) and Autism. *Neuroscience and Biobehavioral Reviews*, 131, 964–987. <https://doi.org/10.1016/J.NEUBIO-REV.2021.10.018>
17. Benabid, A. L., Pollak, P., Hoffmann, D., Gervason, C., Hommel, M., Perret, J. E., de Rougemont, J., & Gao, D. M. (1991). Long-term suppression of tremor by chronic stimulation of the ventral intermediate thalamic nucleus. *The Lancet*, 337(8738), 403–406. [https://doi.org/10.1016/0140-6736\(91\)91175-T](https://doi.org/10.1016/0140-6736(91)91175-T)
18. Benabid, A. L., Pollak, P., Louveau, A., Henry, S., & De Rougemont, J. (1987). Combined (thalamotomy and stimulation) stereotactic surgery of the VIM thalamic nucleus for bilateral Parkinson disease. *Applied Neurophysiology*, 50(1–6), 344–346. <https://doi.org/10.1159/000100803>
19. Bhatia, K. P., Bain, P., Bajaj, N., Elble, R. J., Hallett, M., Louis, E. D., Raethjen, J., Stamelou, M., Testa, C. M., & Deuschl, G. (2018). Consensus Statement on the classification of tremors. from the task force on tremor of the International Parkinson and Movement Disorder Society. *Movement Disorders : Official Journal of the Movement Disorder Society*, 33(1), 75–87. <https://doi.org/10.1002/MDS.27121>
20. Boes, A. D., Prasad, S., Liu, H., Liu, Q., Pascual-Leone, A., Caviness, V. S., & Fox, M. D. (2015). Network localization of neurological symptoms from focal brain lesions. *Brain*, 138(10), 3061. <https://doi.org/10.1093/BRAIN/AWV228>
21. Bohlhalter, S., Goldfine, A., Matteson, S., Garraux, G., Hanakawa, T., Kansaku, K., Wurzman, R., & Hallett, M. (2006). Neural correlates of tic generation in Tourette syndrome: an event-related functional MRI study. *Brain : A Journal of Neurology*, 129(Pt 8), 2029–2037. <https://doi.org/10.1093/BRAIN/AWL050>
22. Boutet, A., Ranjan, M., Zhong, J., Germann, J., Xu, D., Schwartz, M. L., Lipsman, N., Hynynen, K., Devenyi, G. A., Chakravarty, M., Hlasny, E., Llinas, M., Lozano, C. S., Elias, G. J. B., Chan, J., Coblentz, A., Fasano, A., Kucharczyk, W., Hodaie, M., & Lozano, A. M. (2018). Focused ultrasound thalamotomy location determines clinical benefits in patients with essential tremor. *Brain : A Journal of Neurology*, 141(12), 3405–3414. <https://doi.org/10.1093/BRAIN/AWY278>
23. Brinda, A. M., Slopesma, J. P., Butler, R. D., Ikramuddin, S., Beall, T., Guo, W., Chu, C., Patriat, R., Braun, H., Goftari, M., Palnitkar, T., Aman, J., Schrock, L., Cooper, S. E., Matsumoto, J., Vitek, J. L., Harel, N., & Johnson, M. D. (2023). Lateral cerebellothalamic tract activation underlies DBS therapy for Essential



- Tremor. *Brain Stimulation*, 16(2), 445–455.  
<https://doi.org/10.1016/J.BRS.2023.02.002>
24. Brodkey, J. A., Tasker, R. R., Hamani, C., McAndrews, M. P., Dostrovsky, J. O., & Lozano, A. M. (2004). Tremor cells in the human thalamus: differences among neurological disorders. *Journal of Neurosurgery*, 101(1), 43–47.  
<https://doi.org/10.3171/JNS.2004.101.1.0043>
25. Buckner, R. L., Krienen, F. M., Castellanos, A., Diaz, J. C., & Thomas Yeo, B. T. (2011). The organization of the human cerebellum estimated by intrinsic functional connectivity. *Journal of Neurophysiology*, 106(5), 2322–2345.  
<https://doi.org/10.1152/JN.00339.2011>
26. Bullmore, E., & Sporns, O. (2009). Complex brain networks: graph theoretical analysis of structural and functional systems. *Nature Reviews Neuroscience* 2009 10:3, 10(3), 186–198. <https://doi.org/10.1038/nrn2575>
27. Burke, R. E., Fahn, S., Marsden, C. D., Bressman, S. B., Moskowitz, C., & Friedman, J. (1985). Validity and reliability of a rating scale for the primary torsion dystonias. *Neurology*, 35(1), 73–73. <https://doi.org/10.1212/WNL.35.1.73>
28. Butterworth, S., Francis, S., Kelly, E., McGlone, F., Bowtell, R., & Sawle, G. V. (2003). Abnormal cortical sensory activation in dystonia: an fMRI study. *Movement Disorders: Official Journal of the Movement Disorder Society*, 18(6), 673–682.  
<https://doi.org/10.1002/MDS.10416>
29. Caballero-Gaudes, C., & Reynolds, R. C. (2017). Methods for cleaning the BOLD fMRI signal. *NeuroImage*, 154, 128–149. <https://doi.org/10.1016/J.NEUROIMAGE.2016.12.018>
30. Chen, K. H. S., & Chen, R. (2020). Principles of Electrophysiological Assessments for Movement Disorders. *Journal of Movement Disorders*, 13(1), 27.  
<https://doi.org/10.14802/JMD.19064>
31. Coenen, V. A., Allert, N., & Mädler, B. (2011). A role of diffusion tensor imaging fiber tracking in deep brain stimulation surgery: DBS of the dentato-rubro-thalamic tract (drt) for the treatment of therapy-refractory tremor. *Acta Neurochirurgica*, 153(8), 1579–1585. <https://doi.org/10.1007/S00701-011-1036-Z>
32. Coenen, V. A., Sajonz, B., Reiser, M., Bostroem, J., Bewernick, B., Urbach, H., Jenkner, C., Reinacher, P. C., Schlaepfer, T. E., & Mädler, B. (2018). Tractography-assisted deep brain stimulation of the superolateral branch of the medial

- forebrain bundle (sIMFB DBS) in major depression. *NeuroImage. Clinical*, 20, 580–593. <https://doi.org/10.1016/J.NICL.2018.08.020>
33. Coenen, V. A., Varkuti, B., Parpaley, Y., Skodda, S., Prokop, T., Urbach, H., Li, M., & Reinacher, P. C. (2017). Postoperative neuroimaging analysis of DRT deep brain stimulation revision surgery for complicated essential tremor. *Acta Neurochirurgica*, 159(5), 779–787. <https://doi.org/10.1007/S00701-017-3134-Z>
34. Cohen, A. L., Mulder, B. P. F., Prohl, A. K., Soussand, L., Davis, P., Kroeck, M. R., McManus, P., Gholipour, A., Scherrer, B., Bebin, E. M., Wu, J. Y., Northrup, H., Krueger, D. A., Sahin, M., Warfield, S. K., Fox, M. D., & Peters, J. M. (2021). Tuber locations associated with infantile spasms map to a common brain network. *Annals of Neurology*, 89(4), 726. <https://doi.org/10.1002/ANA.26015>
35. Colebatch, J. G., Frackowiak, R. S. J., Brooks, D. J., Colebatch, J. G., Findley, L. J., & Marsden, C. M. (1990). Preliminary report: activation of the cerebellum in essential tremor. *Lancet (London, England)*, 336(8722), 1028–1030. [https://doi.org/10.1016/0140-6736\(90\)92489-5](https://doi.org/10.1016/0140-6736(90)92489-5)
36. Corp, D. T., Joutsa, J., Darby, R. R., Delnooz, C. C. S., Van De Warrenburg, B. P. C., Cooke, D., Prudente, C. N., Ren, J., Reich, M. M., Batla, A., Bhatia, K. P., Jinnah, H. A., Liu, H., & Fox, M. D. (2019). Network localization of cervical dystonia based on causal brain lesions. *Brain*, 142(6), 1660. <https://doi.org/10.1093/BRAIN/AWZ112>
37. Craddock, R. C., Jbabdi, S., Yan, C. G., Vogelstein, J. T., Castellanos, F. X., Di Martino, A., Kelly, C., Heberlein, K., Colcombe, S., & Milham, M. P. (2013). Imaging human connectomes at the macroscale. *Nature Methods*, 10(6), 524. <https://doi.org/10.1038/NMETH.2482>
38. Czarnecki, K., Jones, D. T., Burnett, M. S., Mullan, B., & Matsumoto, J. Y. (2011). SPECT perfusion patterns distinguish psychogenic from essential tremor. *Parkinsonism & Related Disorders*, 17(5), 328–332. <https://doi.org/10.1016/J.PARKRELDIS.2011.01.012>
39. Della Flora, E., Perera, C. L., Cameron, A. L., & Maddern, G. J. (2010). Deep brain stimulation for essential tremor: a systematic review. *Movement Disorders : Official Journal of the Movement Disorder Society*, 25(11), 1550–1559. <https://doi.org/10.1002/MDS.23195>

40. DeLong, M. R., & Wichmann, T. (2007). Circuits and Circuit Disorders of the Basal Ganglia. *Archives of Neurology*, *64*(1), 20–24. <https://doi.org/10.1001/ARCHNEUR.64.1.20>
41. Dembek, T. A., Baldermann, J. C., Petry-Schmelzer, J.-N., Jergas, H., Treuer, H., Visser-Vandewalle, V., Dafsari, H. S., & Barbe, M. T. (2022). Sweetspot Mapping in Deep Brain Stimulation: Strengths and Limitations of Current Approaches. *Neuromodulation: Journal of the International Neuromodulation Society*, *25*(6), 877–887. <https://doi.org/10.1111/ner.13356>
42. Deuschl, G., Bain, P., Brin, M., Agid, Y., Benabid, L., Benecke, R., Berardelli, A., Brooks, D. J., Elble, R., Fahn, S., Findley, L. J., Hallett, M., Jankovic, J., Koller, W. C., Krack, P., Lang, A. E., Lees, A., Lucking, C. H., Marsden, C. D., ... Toloso, E. (1998a). Consensus Statement of the Movement Disorder Society on Tremor. *Movement Disorders*, *13*(S3), 2–23. <https://doi.org/10.1002/MDS.870131303>
43. Deuschl, G., Bain, P., Brin, M., Agid, Y., Benabid, L., Benecke, R., Berardelli, A., Brooks, D. J., Elble, R., Fahn, S., Findley, L. J., Hallett, M., Jankovic, J., Koller, W. C., Krack, P., Lang, A. E., Lees, A., Lucking, C. H., Marsden, C. D., ... Toloso, E. (1998b). Consensus statement of the Movement Disorder Society on Tremor. Ad Hoc Scientific Committee. *Movement Disorders: Official Journal of the Movement Disorder Society*, *13* Suppl 3(SUPPL. 3), 2–23. <https://doi.org/10.1002/MDS.870131303>
44. Eninger, L., & Eninger, L. (1896). Vorlesungen über den Bau der nervösen Centralorgane des Menschen und der Thiere. Für Ärzte und Studirende. In *Vorlesungen über den Bau der nervösen Centralorgane des Menschen und der Thiere. Für Ärzte und Studirende*. F.C.W. Vogel. <https://doi.org/10.5962/bhl.title.1850>
45. Edlow, B. L., Mareyam, A., Horn, A., Polimeni, J. R., Witzel, T., Tisdall, M. D., Augustinack, J. C., Stockmann, J. P., Diamond, B. R., Stevens, A., Tirrell, L. S., Folkerth, R. D., Wald, L. L., Fischl, B., & van der Kouwe, A. (2019). 7 Tesla MRI of the ex vivo human brain at 100 micron resolution. *Scientific Data*, *6*(1). <https://doi.org/10.1038/S41597-019-0254-8>
46. Eklund, A., Nichols, T. E., & Knutsson, H. (2016). Cluster failure: Why fMRI inferences for spatial extent have inflated false-positive rates. *Proceedings of the National Academy of Sciences of the United States of America*, *113*(28), 7900–7905. [https://doi.org/10.1073/PNAS.1602413113/SUPPL\\_FILE/PNAS.1602413113.SAPP.PDF](https://doi.org/10.1073/PNAS.1602413113/SUPPL_FILE/PNAS.1602413113.SAPP.PDF)

47. Ewert, S., Horn, A., Finkel, F., Li, N., Kühn, A. A., & Herrington, T. M. (2019). Optimization and comparative evaluation of nonlinear deformation algorithms for atlas-based segmentation of DBS target nuclei. *NeuroImage*, *184*, 586–598. <https://doi.org/10.1016/J.NEUROIMAGE.2018.09.061>
48. Ewert, S., Plettig, P., Li, N., Chakravarty, M. M., Collins, D. L., Herrington, T. M., Kühn, A. A., & Horn, A. (2018). Toward defining deep brain stimulation targets in MNI space: A subcortical atlas based on multimodal MRI, histology and structural connectivity. *NeuroImage*, *170*, 271–282. <https://doi.org/10.1016/J.NEUROIMAGE.2017.05.015>
49. Fahn S, Tolosa E, & Concepcion M. (1993). Clinical rating scale for tremor In: Jankovic J, Tolosa E, editors. *Parkinson's Disease and Movement Disorders*. Baltimore, MD: Williams and Wilkins, 271–280.
50. Fang, W., Lv, F., Luo, T., Cheng, O., Liao, W., Sheng, K., Wang, X., Wu, F., Hu, Y., Luo, J., Yang, Q. X., & Zhang, H. (2013). Abnormal regional homogeneity in patients with essential tremor revealed by resting-state functional MRI. *PloS One*, *8*(7). <https://doi.org/10.1371/JOURNAL.PONE.0069199>
51. Foerster, O. (1921). Zur analyse und pathophysiologie der striären bewegungsstörungen - Mit 173 Textabbildungen. *Zeitschrift Für Die Gesamte Neurologie Und Psychiatrie*, *73*(1), 1–169. <https://doi.org/10.1007/BF02895293/METRICS>
52. Fonov, V., Evans, A. C., Botteron, K., Almli, C. R., McKinstry, R. C., & Collins, D. L. (2011). Unbiased Average Age-Appropriate Atlases for Pediatric Studies. *NeuroImage*, *54*(1), 313. <https://doi.org/10.1016/J.NEUROIMAGE.2010.07.033>
53. Fox, M. D. (2018). Mapping Symptoms to Brain Networks with the Human Connectome. *New England Journal of Medicine*, *379*(23), 2237–2245. [https://doi.org/10.1056/NEJMRA1706158/SUPPL\\_FILE/NEJMRA1706158\\_DISCLOSURES.PDF](https://doi.org/10.1056/NEJMRA1706158/SUPPL_FILE/NEJMRA1706158_DISCLOSURES.PDF)
54. Fox, M. D., Buckner, R. L., Liu, H., Mallar Chakravarty, M., Lozano, A. M., & Pascual-Leone, A. (2014). Resting-state networks link invasive and noninvasive brain stimulation across diverse psychiatric and neurological diseases. *Proceedings of the National Academy of Sciences of the United States of America*, *111*(41), E4367–E4375. [https://doi.org/10.1073/PNAS.1405003111/SUPPL\\_FILE/PNAS.201405003SI.PDF](https://doi.org/10.1073/PNAS.1405003111/SUPPL_FILE/PNAS.201405003SI.PDF)

55. Fox, M. D., Zhang, D., Snyder, A. Z., & Raichle, M. E. (2009). The global signal and observed anticorrelated resting state brain networks. *Journal of Neurophysiology*, *101*(6), 3270–3283. <https://doi.org/10.1152/JN.90777.2008/ASSET/IMAGES/LARGE/Z9K0060994950007.JPEG>
56. Friston, K. J., Holmes, A. P., Worsley, K. J., Poline, J. -P., Frith, C. D., & Frackowiak, R. S. J. (1994). Statistical parametric maps in functional imaging: A general linear approach. *Human Brain Mapping*, *2*(4), 189–210. <https://doi.org/10.1002/HBM.460020402>
57. Fytagoridis, A., & Blomstedt, P. (2010). Complications and side effects of deep brain stimulation in the posterior subthalamic area. *Stereotactic and Functional Neurosurgery*, *88*(2), 88–93. <https://doi.org/10.1159/000271824>
58. Ganos, C., Al-Fatly, B., Fischer, J.-F., Baldermann, J.-C., Hennen, C., Visser-Vandewalle, V., Neudorfer, C., Martino, D., Li, J., Bouwens, T., Ackermanns, L., Leentjens, A. F. G., Pyatigorskaya, N., Worbe, Y., Fox, M. D., Kühn, A. A., & Horn, A. (2022). A neural network for tics: insights from causal brain lesions and deep brain stimulation. *Brain*, *145*(12), 4385–4397. <https://doi.org/10.1093/brain/awac009>
59. Gardner, J. (2013). A history of deep brain stimulation: Technological innovation and the role of clinical assessment tools. *Social Studies of Science*, *43*(5), 707. <https://doi.org/10.1177/0306312713483678>
60. Gogtay, N., Giedd, J. N., Lusk, L., Hayashi, K. M., Greenstein, D., Vaituzis, A. C., Nugent, T. F., Herman, D. H., Clasen, L. S., Toga, A. W., Rapoport, J. L., & Thompson, P. M. (2004). Dynamic mapping of human cortical development during childhood through early adulthood. *Proceedings of the National Academy of Sciences of the United States of America*, *101*(21), 8174–8179. [https://doi.org/10.1073/PNAS.0402680101/SUPPL\\_FILE/02680MOVIE4.MPG](https://doi.org/10.1073/PNAS.0402680101/SUPPL_FILE/02680MOVIE4.MPG)
61. Grandjean, J., Zerbi, V., Balsters, J. H., Wenderoth, N., & Rudin, M. (2017). Structural Basis of Large-Scale Functional Connectivity in the Mouse. *The Journal of Neuroscience*, *37*(34), 8092. <https://doi.org/10.1523/JNEUROSCI.0438-17.2017>
62. Grill, W. M., Snyder, A. N., & Miocinovic, S. (2004). Deep brain stimulation creates an informational lesion of the stimulated nucleus. *Neuroreport*, *15*(7), 1137–1140. <https://doi.org/10.1097/00001756-200405190-00011>
63. Hallett, M. (1998). The Neurophysiology of Dystonia. *Archives of Neurology*, *55*(5), 601–603. <https://doi.org/10.1001/ARCHNEUR.55.5.601>

64. Hampson, M., Tokoglu, F., King, R. A., Constable, R. T., & Leckman, J. F. (2009). Brain Areas Co-activating with Motor Cortex during Chronic Motor Tics and Intentional Movements. *Biological Psychiatry*, *65*(7), 594. <https://doi.org/10.1016/J.BIOPSYCH.2008.11.012>
65. Hassler R, & Dieckmann G. (1970). [Stereotaxic treatment of tics and inarticulate cries or coprolalia considered as motor obsessional phenomena in Gilles de la Tourette's disease]. *Rev Neurol (Paris)*, *123*, 89–100.
66. Hellwig, B., Häußler, S., Schelter, B., Lauk, M., Guschlbauer, B., Timmer, J., & Lücking, C. H. (2001). Tremor-correlated cortical activity in essential tremor. *Lancet*, *357*(9255), 519–523. [https://doi.org/10.1016/S0140-6736\(00\)04044-7](https://doi.org/10.1016/S0140-6736(00)04044-7)
67. Helmich, R. C., Toni, I., Deuschl, G., & Bloem, B. R. (2013). The pathophysiology of essential tremor and Parkinson's tremor. *Current Neurology and Neuroscience Reports*, *13*(9). <https://doi.org/10.1007/S11910-013-0378-8>
68. Henderson, J. M. (2012). "Connectomic surgery": Diffusion tensor imaging (DTI) tractography as a targeting modality for surgical modulation of neural networks. *Frontiers in Integrative Neuroscience*, *6*(APRIL), 24414. <https://doi.org/10.3389/FNINT.2012.00015/BIBTEX>
69. Herrington, T. M., Cheng, J. J., & Eskandar, E. N. (2016). Neurobiology of Deep Brain Stimulation: Mechanisms of deep brain stimulation. *Journal of Neurophysiology*, *115*(1), 19. <https://doi.org/10.1152/JN.00281.2015>
70. Herzog, J., Fietzek, U., Hamel, W., Morsnowski, A., Steigerwald, F., Schrader, B., Weinert, D., Pfister, G., Müller, D., Mehdorn, H. M., Deuschl, G., & Volkmann, J. (2004). Most effective stimulation site in subthalamic deep brain stimulation for Parkinson's disease. *Movement Disorders: Official Journal of the Movement Disorder Society*, *19*(9), 1050–1054. <https://doi.org/10.1002/MDS.20056>
71. Hollunder, B., Ganos, C., & Horn, A. (2021). Deep Brain Stimulation: From Sweet Spots to Sweet Networks? *Biological Psychiatry: Cognitive Neuroscience and Neuroimaging*, *6*(10), 939–941. <https://doi.org/10.1016/j.bpsc.2021.06.002>
72. Hollunder, B., Rajamani, N., Siddiqi, S. H., Finke, C., Kühn, A. A., Mayberg, H. S., Fox, M. D., Neudorfer, C., & Horn, A. (2022). Toward personalized medicine in connectomic deep brain stimulation. *Progress in Neurobiology*, *210*. <https://doi.org/10.1016/J.PNEUROBIO.2021.102211>
73. Holmes, A. J., Hollinshead, M. O., O'Keefe, T. M., Petrov, V. I., Fariello, G. R., Wald, L. L., Fischl, B., Rosen, B. R., Mair, R. W., Roffman, J. L., Smoller, J. W., &

- Buckner, R. L. (2015). Brain Genomics Superstruct Project initial data release with structural, functional, and behavioral measures. *Scientific Data* 2015 2:1, 2(1), 1–16. <https://doi.org/10.1038/sdata.2015.31>
74. Holtbernd, F., & Shah, N. J. (2021). Imaging the Pathophysiology of Essential Tremor—A Systematic Review. *Frontiers in Neurology*, 12, 680254. <https://doi.org/10.3389/FNEUR.2021.680254/BIBTEX>
75. Horn, A. (2019). The impact of modern-day neuroimaging on the field of deep brain stimulation. *Current Opinion in Neurology*, 32(4), 511–520. <https://doi.org/10.1097/WCO.0000000000000679>
76. Horn, A. (2022). Predicting treatment response based on DBS connectivity. *Connectomic Deep Brain Stimulation*, 375–404. <https://doi.org/10.1016/B978-0-12-821861-7.00015-4>
77. Horn, A., Al-Fatly, B., Neumann, W.-J., & Neudorfer, C. (2022). Connectomic DBS: An introduction. *Connectomic Deep Brain Stimulation*, 3–23. <https://doi.org/10.1016/B978-0-12-821861-7.00020-8>
78. Horn, A., & Blankenburg, F. (2016). Toward a standardized structural-functional group connectome in MNI space. *NeuroImage*, 124(Pt A), 310–322. <https://doi.org/10.1016/J.NEUROIMAGE.2015.08.048>
79. Horn, A., & Fox, M. D. (2020). Opportunities of connectomic neuromodulation. *NeuroImage*, 221, 117180. <https://doi.org/10.1016/J.NEUROIMAGE.2020.117180>
80. Horn, A., & Kühn, A. A. (2015). Lead-DBS: a toolbox for deep brain stimulation electrode localizations and visualizations. *NeuroImage*, 107, 127–135. <https://doi.org/10.1016/J.NEUROIMAGE.2014.12.002>
81. Horn, A., Li, N., Dembek, T. A., Kappel, A., Boulay, C., Ewert, S., Tietze, A., Husch, A., Perera, T., Neumann, W. J., Reiser, M., Si, H., Oostenveld, R., Rorden, C., Yeh, F. C., Fang, Q., Herrington, T. M., Vorwerk, J., & Kühn, A. A. (2019). Lead-DBS v2: Towards a comprehensive pipeline for deep brain stimulation imaging. *NeuroImage*, 184, 293–316. <https://doi.org/10.1016/J.NEUROIMAGE.2018.08.068>
82. Horn, A., Reich, M. M., Ewert, S., Li, N., Al-Fatly, B., Lange, F., Roothans, J., Oxenford, S., Horn, I., Paschen, S., Runge, J., Wodarg, F., Witt, K., Nickl, R. C., Wittstock, M., Schneider, G.-H., Mahlknecht, P., Poewe, W., Eisner, W., ... Kühn, A. A. (2022). Optimal deep brain stimulation sites and networks for cervical vs.

- generalized dystonia. *Proceedings of the National Academy of Sciences*, 119(14). <https://doi.org/10.1073/PNAS.2114985119>
83. Horn, A., Reich, M., Vorwerk, J., Li, N., Wenzel, G., Fang, Q., Schmitz-Hübsch, T., Nickl, R., Kupsch, A., Volkmann, J., Kühn, A. A., & Fox, M. D. (2017). Connectivity Predicts deep brain stimulation outcome in Parkinson disease. *Annals of Neurology*, 82(1), 67–78. <https://doi.org/10.1002/ANA.24974>
84. Hoskovicová, M., Ulmanová, O., Šprdlík, O., Sieger, T., Nováková, J., Jech, R., & Růžička, E. (2013). Disorders of balance and gait in essential tremor are associated with midline tremor and age. *Cerebellum (London, England)*, 12(1), 27–34. <https://doi.org/10.1007/S12311-012-0384-4>
85. Husch, A., V. Petersen, M., Gemmar, P., Goncalves, J., & Hertel, F. (2018). PaCER - A fully automated method for electrode trajectory and contact reconstruction in deep brain stimulation. *NeuroImage: Clinical*, 17, 80–89. <https://doi.org/10.1016/J.NICL.2017.10.004>
86. Jackson, S. R., Loayza, J., Crichton, M., Sigurdsson, H. P., Dyke, K., & Jackson, G. M. (2020). The role of the insula in the generation of motor tics and the experience of the premonitory urge-to-tic in Tourette syndrome. *Cortex; a Journal Devoted to the Study of the Nervous System and Behavior*, 126, 119–133. <https://doi.org/10.1016/J.CORTEX.2019.12.021>
87. Jenkins, I. H., Bain, P. G., Colebatch, J. G., Thompson, P. D., Findley, L. J., Frackowiak, R. S. J., Marsden, C. D., & Brooks, D. J. (1993). A positron emission tomography study of essential tremor: evidence for overactivity of cerebellar connections. *Annals of Neurology*, 34(1), 82–90. <https://doi.org/10.1002/ANA.410340115>
88. Jenkinson, M., Beckmann, C. F., Behrens, T. E. J., Woolrich, M. W., & Smith, S. M. (2012). FSL. *NeuroImage*, 62(2), 782–790. <https://doi.org/10.1016/J.NEUROIMAGE.2011.09.015>
89. Johnson, K. A., Cagle, J. N., Lopes, J. L., Wong, J. K., Okun, M. S., Gunduz, A., Shukla, A. W., Hilliard, J. D., Foote, K. D., & de Hemptinne, C. (2023). Globus pallidus internus deep brain stimulation evokes resonant neural activity in Parkinson's disease. *Brain Communications*, 5(2). <https://doi.org/10.1093/BRAIN-COMMS/FCAD025>
90. Johnson, K. A., Duffley, G., Anderson, D. N., Ostrem, J. L., Welter, M. L., Baldermann, J. C., Kuhn, J., Huys, D., Visser-Vandewalle, V., Foltynie, T., Zrinzo, L.,



- Hariz, M., Leentjens, A. F. G., Mogilner, A. Y., Pourfar, M. H., Almeida, L., Gunduz, A., Foote, K. D., Okun, M. S., & Butson, C. R. (2020). Structural connectivity predicts clinical outcomes of deep brain stimulation for Tourette syndrome. *Brain : A Journal of Neurology*, *143*(8), 2607–2623. <https://doi.org/10.1093/BRAIN/AWAA188>
91. Joutsa, J., Corp, D. T., & Fox, M. D. (2022). Lesion network mapping for symptom localization: Recent developments and future directions. *Current Opinion in Neurology*, *35*(4), 453–459. <https://doi.org/10.1097/WCO.0000000000001085>
92. Joutsa, J., Horn, A., Hsu, J., & Fox, M. D. (2018). Localizing parkinsonism based on focal brain lesions. *Brain*, *141*(8), 2445–2456. <https://doi.org/10.1093/brain/awy161>
93. Joutsa, J., Shih, L. C., & Fox, M. D. (2019). Mapping holmes tremor circuit using the human brain connectome. *Annals of Neurology*, *86*(6). <https://doi.org/10.1002/ana.25618>
94. Kaji, R., Bhatia, K., & Graybiel, A. M. (2018). Review: Pathogenesis of dystonia: is it of cerebellar or basal ganglia origin? *Journal of Neurology, Neurosurgery, and Psychiatry*, *89*(5), 488. <https://doi.org/10.1136/JNNP-2017-316250>
95. Kalanithi, P. S. A., Zheng, W., Kataoka, Y., DiFiglia, M., Grantz, H., Saper, C. B., Schwartz, M. L., Leckman, J. F., & Vaccarino, F. M. (2005). Altered parvalbumin-positive neuron distribution in basal ganglia of individuals with Tourette syndrome. *Proceedings of the National Academy of Sciences of the United States of America*, *102*(37), 13307–13312. <https://doi.org/10.1073/PNAS.0502624102>
96. Kataoka, Y., Kalanithi, P. S. A., Grantz, H., Schwartz, M. L., Saper, C., Leckman, J. F., & Vaccarino, F. M. (2010). Decreased number of parvalbumin and cholinergic interneurons in the striatum of individuals with Tourette syndrome. *The Journal of Comparative Neurology*, *518*(3), 277–291. <https://doi.org/10.1002/CNE.22206>
97. Koch, G., Porcacchia, P., Ponzio, V., Carrillo, F., Cáceres-Redondo, M. T., Brusa, L., Desiato, M. T., Arciprete, F., Di Lorenzo, F., Pisani, A., Caltagirone, C., Palomar, F. J., & Mir, P. (2014). Effects of two weeks of cerebellar theta burst stimulation in cervical dystonia patients. *Brain Stimulation*, *7*(4), 564–572. <https://doi.org/10.1016/J.BRS.2014.05.002>

98. Koeglsperger, T., Palleis, C., Hell, F., Mehrkens, J. H., & Bötzel, K. (2019). Deep brain stimulation programming for movement disorders: Current concepts and evidence-based strategies. *Frontiers in Neurology*, *10*(MAY), 442748. <https://doi.org/10.3389/FNEUR.2019.00410/BIBTEX>
99. Kojovic, M., Pareés, I., Kassavetis, P., Palomar, F. J., Mir, P., Teo, J. T., Cordivari, C., Rothwell, J. C., Bhatia, K. P., & Edwards, M. J. (2013). Secondary and primary dystonia: pathophysiological differences. *Brain : A Journal of Neurology*, *136*(Pt 7), 2038–2049. <https://doi.org/10.1093/BRAIN/AWT150>
100. Koller, W. C., Lyons, K. E., Wilkinson, S. B., Troster, A. I., & Pahwa, R. (2001). Long-term safety and efficacy of unilateral deep brain stimulation of the thalamus in essential tremor. *Movement Disorders : Official Journal of the Movement Disorder Society*, *16*(3), 464–468. <https://doi.org/10.1002/MDS.1089>
101. Koy, A., Weinsheimer, M., Pauls, K. A. M., Kühn, A. A., Krause, P., Huebl, J., Schneider, G.-H., Deuschl, G., Erasmi, R., Falk, D., Krauss, J. K., Lütjens, G., Schnitzler, A., Wojtecki, L., Vesper, J., Korinthenberg, R., Coenen, V. A., Visser-Vandewalle, V., Hellmich, M., & Timmermann, L. (2017). German registry of paediatric deep brain stimulation in patients with childhood-onset dystonia (GEPESTIM). *European Journal of Paediatric Neurology*, *21*(1), 136–146. <https://doi.org/10.1016/j.ejpn.2016.05.023>
102. Krack, P., Volkmann, J., Tinkhauser, G., & Deuschl, G. (2019). Deep Brain Stimulation in Movement Disorders: From Experimental Surgery to Evidence-Based Therapy. *Movement Disorders*, *34*(12), 1795–1810. <https://doi.org/10.1002/MDS.27860>
103. Krauss, J. K., Lipsman, N., Aziz, T., Boutet, A., Brown, P., Chang, J. W., Davidson, B., Grill, W. M., Hariz, M. I., Horn, A., Schulder, M., Mammis, A., Tass, P. A., Volkmann, J., & Lozano, A. M. (2020). Technology of deep brain stimulation: current status and future directions. *Nature Reviews Neurology* 2020 17:2, *17*(2), 75–87. <https://doi.org/10.1038/s41582-020-00426-z>
104. Kübler, D., Kroneberg, D., Al-Fatly, B., Schneider, G. H., Ewert, S., van Riesen, C., Gruber, D., Ebersbach, G., & Kühn, A. A. (2021). Determining an efficient deep brain stimulation target in essential tremor - Cohort study and review of the literature. *Parkinsonism & Related Disorders*, *89*, 54–62. <https://doi.org/10.1016/J.PARKRELDIS.2021.06.019>

105. Lanciego, J. L., Luquin, N., & Obeso, J. A. (2012). Functional Neuroanatomy of the Basal Ganglia. *Cold Spring Harbor Perspectives in Medicine*, 2(12). <https://doi.org/10.1101/CSHPERSPECT.A009621>
106. Le Bihan, D., & Lima, M. (2015). Diffusion Magnetic Resonance Imaging: What Water Tells Us about Biological Tissues. *PLoS Biology*, 13(7). <https://doi.org/10.1371/JOURNAL.PBIO.1002203>
107. LECKMAN, J. F., RIDDLE, M. A., HARDIN, M. T., ORT, S. I., SWARTZ, K. L., STEVENSON, J., & COHEN, D. J. (1989). The Yale Global Tic Severity Scale: Initial Testing of a Clinician-Rated Scale of Tic Severity. *Journal of the American Academy of Child and Adolescent Psychiatry*, 28(4), 566–573. <https://doi.org/10.1097/00004583-198907000-00015>
108. Lee, D. A. (1981). Paul Broca and the history of aphasia. *Neurology*, 31(5), 600–600. <https://doi.org/10.1212/WNL.31.5.600>
109. Lenroot, R. K., & Giedd, J. N. (2006). Brain development in children and adolescents: insights from anatomical magnetic resonance imaging. *Neuroscience and Biobehavioral Reviews*, 30(6), 718–729. <https://doi.org/10.1016/J.NEUBIO-REV.2006.06.001>
110. Lévy, J. P., Nguyen, T. A. K., Lachenmayer, L., Debove, I., Tinkhauser, G., Petermann, K., Amil, A. S., Michelis, J., Schüpbach, M., Nowacki, A., & Pollo, C. (2020). Structure-function relationship of the posterior subthalamic area with directional deep brain stimulation for essential tremor. *NeuroImage: Clinical*, 28. <https://doi.org/10.1016/J.NICL.2020.102486>
111. Li, N., Baldermann, J. C., Kibleur, A., Treu, S., Akram, H., Elias, G. J. B., Boutet, A., Lozano, A. M., Al-Fatly, B., Strange, B., Barcia, J. A., Zrinzo, L., Joyce, E., Chabardes, S., Visser-Vandewalle, V., Polosan, M., Kuhn, J., Kühn, A. A., & Horn, A. (2020). A unified connectomic target for deep brain stimulation in obsessive-compulsive disorder. *Nature Communications* 2020 11:1, 11(1), 1–12. <https://doi.org/10.1038/s41467-020-16734-3>
112. Li, N., Hollunder, B., Baldermann, J. C., Kibleur, A., Treu, S., Akram, H., Al-Fatly, B., Strange, B. A., Barcia, J. A., Zrinzo, L., Joyce, E. M., Chabardes, S., Visser-Vandewalle, V., Polosan, M., Kuhn, J., Kühn, A. A., & Horn, A. (2021). A Unified Functional Network Target for Deep Brain Stimulation in Obsessive-Compulsive Disorder. *Biological Psychiatry*, 90(10), 701–713. <https://doi.org/10.1016/J.BIOPSYCH.2021.04.006>

113. Limousin, P., & Foltynie, T. (2019). Long-term outcomes of deep brain stimulation in Parkinson disease. *Nature Reviews Neurology* 2019 15:4, 15(4), 234–242. <https://doi.org/10.1038/s41582-019-0145-9>
114. Logothetis, N. K. (2003). The Underpinnings of the BOLD Functional Magnetic Resonance Imaging Signal. *The Journal of Neuroscience*, 23(10), 3963. <https://doi.org/10.1523/JNEUROSCI.23-10-03963.2003>
115. Loh, A., Boutet, A., Germann, J., Al-Fatly, B., Elias, G. J. B., Neudorfer, C., Krotz, J., Wong, E. H. Y., Parmar, R., Gramer, R., Paff, M., Horn, A., Chen, J. J., Azevedo, P., Fasano, A., Munhoz, R. P., Hodaie, M., Kalia, S. K., Kucharczyk, W., & Lozano, A. M. (2022). A Functional Connectome of Parkinson's Disease Patients Prior to Deep Brain Stimulation: A Tool for Disease-Specific Connectivity Analyses. *Frontiers in Neuroscience*, 16, 804125. <https://doi.org/10.3389/FNINS.2022.804125>
116. Løkkegaard, A., Herz, D. M., Haagen, B. N., Lorentzen, A. K., Eickhoff, S. B., & Siebner, H. R. (2016). Altered sensorimotor activation patterns in idiopathic dystonia—an activation likelihood estimation meta-analysis of functional brain imaging studies. *Human Brain Mapping*, 37(2), 547–557. <https://doi.org/10.1002/HBM.23050>
117. Lozano, A. M., & Lipsman, N. (2013). Probing and regulating dysfunctional circuits using deep brain stimulation. *Neuron*, 77(3), 406–424. <https://doi.org/10.1016/J.NEURON.2013.01.020>
118. Lozano, A. M., Lipsman, N., Bergman, H., Brown, P., Chabardes, S., Chang, J. W., Matthews, K., McIntyre, C. C., Schlaepfer, T. E., Schulder, M., Temel, Y., Volkman, J., & Krauss, J. K. (2019a). Deep brain stimulation: current challenges and future directions. *Nature Reviews Neurology* 2019 15:3, 15(3), 148–160. <https://doi.org/10.1038/s41582-018-0128-2>
119. Lozano, A. M., Lipsman, N., Bergman, H., Brown, P., Chabardes, S., Chang, J. W., Matthews, K., McIntyre, C. C., Schlaepfer, T. E., Schulder, M., Temel, Y., Volkman, J., & Krauss, J. K. (2019b). Deep brain stimulation: current challenges and future directions. *Nature Reviews Neurology*, 15(3), 148. <https://doi.org/10.1038/S41582-018-0128-2>
120. Luft, F., Sharifi, S., Mugge, W., Schouten, A. C., Bour, L. J., Van Rootselaar, A. F., Veltink, P. H., & Heida, T. (2020). Distinct cortical activity patterns in Parkinson's

- disease and essential tremor during a bimanual tapping task. *Journal of NeuroEngineering and Rehabilitation*, 17(1), 1–10. <https://doi.org/10.1186/S12984-020-00670-W/TABLES/3>
121. Macchia, R. J., Termine, J. E., & Buchen, C. D. (2007). Raymond V. Damadian, M.D.: magnetic resonance imaging and the controversy of the 2003 Nobel Prize in Physiology or Medicine. *The Journal of Urology*, 178(3 Pt 1), 783–785. <https://doi.org/10.1016/J.JURO.2007.05.019>
122. Marsden, J. F., Ashby, P., Limousin-Dowsey, P., Rothwell, J. C., & Brown, P. (2000). Coherence between cerebellar thalamus, cortex and muscle in man: cerebellar thalamus interactions. *Brain: A Journal of Neurology*, 123 ( Pt 7)(7), 1459–1470. <https://doi.org/10.1093/BRAIN/123.7.1459>
123. Martino, D., Ganos, C., & Worbe, Y. (2018). Neuroimaging Applications in Tourette's Syndrome. *International Review of Neurobiology*, 143, 65–108. <https://doi.org/10.1016/BS.IRN.2018.09.008>
124. McAuley, J. H., & Marsden, C. D. (2000). Physiological and pathological tremors and rhythmic central motor control. *Brain: A Journal of Neurology*, 123 ( Pt 8)(8), 1545–1567. <https://doi.org/10.1093/BRAIN/123.8.1545>
125. McCairn, K. W., Nagai, Y., Hori, Y., Ninomiya, T., Kikuchi, E., Lee, J. Y., Suhara, T., Iriki, A., Minamimoto, T., Takada, M., Isoda, M., & Matsumoto, M. (2016). A Primary Role for Nucleus Accumbens and Related Limbic Network in Vocal Tics. *Neuron*, 89(2), 300–307. <https://doi.org/10.1016/J.NEURON.2015.12.025>
126. Middlebrooks, E. H., Okromelidze, L., Wong, J. K., Eisinger, R. S., Burns, M. R., Jain, A., Lin, H. P., Yu, J., Opri, E., Horn, A., Goede, L. L., Foote, K. D., Okun, M. S., Quiñones-Hinojosa, A., Uitti, R. J., Grewal, S. S., & Tsuboi, T. (2021). Connectivity correlates to predict essential tremor deep brain stimulation outcome: Evidence for a common treatment pathway. *NeuroImage: Clinical*, 32, 102846. <https://doi.org/10.1016/J.NICL.2021.102846>
127. Middlebrooks, E. H., Popple, R. A., Greco, E., Okromelidze, L., Walker, H. C., Lakhani, D. A., Anderson, A. R., Thomas, E. M., Deshpande, H. D., McCullough, B. A., Stover, N. P., Sung, V. W., Nicholas, A. P., Standaert, D. G., Yacoubian, T., Dean, M. N., Roper, J. A., Grewal, S. S., Holland, M. T., ... Bredel, M. (2023). Connectomic Basis for Tremor Control in Stereotactic Radiosurgical Thalamotomy. *American Journal of Neuroradiology*, 44(2), 157–164. <https://doi.org/10.3174/AJNR.A7778>

128. Milosevic, L., Kalia, S. K., Hodaie, M., Lozano, A. M., Popovic, M. R., & Hutchison, W. D. (2018). Physiological mechanisms of thalamic ventral intermediate nucleus stimulation for tremor suppression. *Brain*, 141(7), 2142–2155. <https://doi.org/10.1093/BRAIN/AWY139>
129. Mueller, K., Jech, R., Hoskovicová, M., Ulmanová, O., Urgošík, D., Vymazal, J., & Růžička, E. (2017). General and selective brain connectivity alterations in essential tremor: A resting state fMRI study. *NeuroImage. Clinical*, 16, 468–476. <https://doi.org/10.1016/J.NICL.2017.06.004>
130. Murthy, M., Cheng, Y. Y., Holton, J. L., & Bettencourt, C. (2021). Neurodegenerative movement disorders: An epigenetics perspective and promise for the future. *Neuropathology and Applied Neurobiology*, 47(7), 897–909. <https://doi.org/10.1111/NAN.12757>
131. Neudorfer, C., Butenko, K., Oxenford, S., Rajamani, N., Achtzehn, J., Goede, L., Hollunder, B., Ríos, A. S., Hart, L., Tasserie, J., Fernando, K. B., Nguyen, T. A. K., Al-Fatly, B., Vissani, M., Fox, M., Richardson, R. M., van Rienen, U., Kühn, A. A., Husch, A. D., ... Horn, A. (2023). Lead-DBS v3.0: Mapping deep brain stimulation effects to local anatomy and global networks. *NeuroImage*, 268. <https://doi.org/10.1016/J.NEUROIMAGE.2023.119862>
132. Neudorfer, C., Kroneberg, D., Al-Fatly, B., Goede, L., Kübler, D., Faust, K., van Rienen, U., Tietze, A., Picht, T., Herrington, T. M., Middlebrooks, E. H., Kühn, A., Schneider, G. H., & Horn, A. (2022a). Personalizing Deep Brain Stimulation Using Advanced Imaging Sequences. *Annals of Neurology*, 91(5), 613–628. <https://doi.org/10.1002/ANA.26326>
133. Neudorfer, C., Kroneberg, D., Al-Fatly, B., Goede, L., Kübler, D., Faust, K., van Rienen, U., Tietze, A., Picht, T., Herrington, T. M., Middlebrooks, E. H., Kühn, A., Schneider, G. H., & Horn, A. (2022b). Personalizing Deep Brain Stimulation Using Advanced Imaging Sequences. *Annals of Neurology*, 91(5), 613–628. <https://doi.org/10.1002/ANA.26326>
134. Neumann, W. J., Horn, A., Ewert, S., Huebl, J., Brücke, C., Slentz, C., Schneider, G. H., & Kühn, A. A. (2017). A localized pallidal physiomaerker in cervical dystonia. *Annals of Neurology*, 82(6), 912–924. <https://doi.org/10.1002/ANA.25095>
135. Neumann, W. J., Horn, A., & Kühn, A. A. (2023). Insights and opportunities for deep brain stimulation as a brain circuit intervention. *Trends in Neurosciences*, 46(6). <https://doi.org/10.1016/J.TINS.2023.03.009>

136. Neumann, W. J., Huebl, J., Brücke, C., Lofredi, R., Horn, A., Saryyeva, A., Müller-Vahl, K., Krauss, J. K., & Kühn, A. A. (2018). Pallidal and thalamic neural oscillatory patterns in tourette's syndrome. *Annals of Neurology*, 84(4), 505–514. <https://doi.org/10.1002/ANA.25311>
137. Neuner, I., Werner, C. J., Arrubla, J., Stöcker, T., Ehlen, C., Wegener, H. P., Schneider, F., & Jon Shah, N. (2014). Imaging the where and when of tic generation and resting state networks in adult Tourette patients. *Frontiers in Human Neuroscience*, 8(MAY). <https://doi.org/10.3389/FNHUM.2014.00362/PDF>
138. Ni, Z., Kim, S. J., Phielipp, N., Ghosh, S., Udupa, K., Gunraj, C. A., Saha, U., Hodaie, M., Kalia, S. K., Lozano, A. M., Lee, D. J., Moro, E., Fasano, A., Hallett, M., Lang, A. E., & Chen, R. (2018). Pallidal deep brain stimulation modulates cortical excitability and plasticity. *Annals of Neurology*, 83(2), 352–362. <https://doi.org/10.1002/ANA.25156>
139. Padmanabhan, J. L., Cooke, D., Joutsa, J., Siddiqi, S. H., Ferguson, M., Darby, R. R., Soussand, L., Horn, A., Kim, N. Y., Voss, J. L., Naidech, A. M., Brodtmann, A., Egorova, N., Gozzi, S., Phan, T. G., Corbetta, M., Grafman, J., & Fox, M. D. (2019). A Human Depression Circuit Derived From Focal Brain Lesions. *Biological Psychiatry*, 86(10). <https://doi.org/10.1016/j.biopsych.2019.07.023>
140. Pahwa, R., Lyons, K. E., Wilkinson, S. B., Simpson, R. K., Ondo, W. G., Tarsy, D., Norregaard, T., Hubble, J. P., Smith, D. A., Hauser, R. A., & Jankovic, J. (2006). Long-term evaluation of deep brain stimulation of the thalamus. *Journal of Neurosurgery*, 104(4), 506–512. <https://doi.org/10.3171/JNS.2006.104.4.506>
141. Paus, T. (2001). Primate anterior cingulate cortex: Where motor control, drive and cognition interface. *Nature Reviews Neuroscience* 2001 2:6, 2(6), 417–424. <https://doi.org/10.1038/35077500>
142. Pedrosa, D. J., Reck, C., Florin, E., Pauls, K. A. M., Maarouf, M., Wojtecki, L., Dafsari, H. S., Sturm, V., Schnitzler, A., Fink, G. R., & Timmermann, L. (2012). Essential tremor and tremor in Parkinson's disease are associated with distinct "tremor clusters" in the ventral thalamus. *Experimental Neurology*, 237(2), 435–443. <https://doi.org/10.1016/J.EXPNEUROL.2012.07.002>
143. Penfield, W., & Boldrey, E. (1937). SOMATIC MOTOR AND SENSORY REPRESENTATION IN THE CEREBRAL CORTEX OF MAN AS STUDIED BY ELECTRICAL STIMULATION. *Brain*, 60(4), 389–443. <https://doi.org/10.1093/BRAIN/60.4.389>

144. Penny, W., Friston, K., Ashburner, J., Kiebel, S., & Nichols, T. (2007). Statistical Parametric Mapping: The Analysis of Functional Brain Images. *Statistical Parametric Mapping: The Analysis of Functional Brain Images*. <https://doi.org/10.1016/B978-0-12-372560-8.X5000-1>
145. Percheron, G., Yelnik, J., & François, C. (1984). A Golgi analysis of the primate globus pallidus. III. Spatial organization of the striato-pallidal complex. *Journal of Comparative Neurology*, 227(2), 214–227. <https://doi.org/10.1002/CNE.902270207>
146. Permutation, Parametric and Bootstrap Tests of Hypotheses. (2005). *Permutation, Parametric and Bootstrap Tests of Hypotheses*. <https://doi.org/10.1007/B138696>
147. Peterson, D. A., Sejnowski, T. J., & Poizner, H. (2010). Convergent evidence for abnormal striatal synaptic plasticity in dystonia. *Neurobiology of Disease*, 37(3), 558. <https://doi.org/10.1016/J.NBD.2009.12.003>
148. Pinto, A. D., Lang, A. E., & Chen, R. (2003a). The cerebellothalamocortical pathway in essential tremor. *Neurology*, 60(12), 1985–1987. <https://doi.org/10.1212/01.WNL.0000065890.75790.29>
149. Pinto, A. D., Lang, A. E., & Chen, R. (2003b). The cerebellothalamocortical pathway in essential tremor. *Neurology*, 60(12), 1985–1987. <https://doi.org/10.1212/01.WNL.0000065890.75790.29>
150. Pizoli, C. E., Jinnah, H. A., Billingsley, M. L., & Hess, E. J. (2002). Abnormal Cerebellar Signaling Induces Dystonia in Mice. *The Journal of Neuroscience*, 22(17), 7825. <https://doi.org/10.1523/JNEUROSCI.22-17-07825.2002>
151. Plaha, P., Khan, S., & Gill, S. S. (2008). Bilateral stimulation of the caudal zona incerta nucleus for tremor control. *Journal of Neurology, Neurosurgery, and Psychiatry*, 79(5), 504–513. <https://doi.org/10.1136/JNNP.2006.112334>
152. Power, J. D., Mitra, A., Laumann, T. O., Snyder, A. Z., Schlaggar, B. L., & Petersen, S. E. (2014). Methods to detect, characterize, and remove motion artifact in resting state fMRI. *NeuroImage*, 84, 320–341. <https://doi.org/10.1016/J.NEUROIMAGE.2013.08.048>
153. Prudente, C. N., Pardo, C. A., Xiao, J., Hanfelt, J., Hess, E. J., LeDoux, M. S., & Jinnah, H. A. (2013). Neuropathology of Cervical Dystonia. *Experimental Neurology*, 241(1), 95. <https://doi.org/10.1016/J.EXPNEUROL.2012.11.019>



154. Quartarone, A., Rizzo, V., Terranova, C., Morgante, F., Schneider, S., Ibrahim, N., Girlanda, P., Bhatia, K. P., & Rothwell, J. C. (2009). Abnormal sensorimotor plasticity in organic but not in psychogenic dystonia. *Brain: A Journal of Neurology*, 132(Pt 10), 2871–2877. <https://doi.org/10.1093/BRAIN/AWP213>
155. Rapinesi, C., Kotzalidis, G. D., Ferracuti, S., Sani, G., Girardi, P., & Del Casale, A. (2019). Brain Stimulation in Obsessive-Compulsive Disorder (OCD): A Systematic Review. *Current Neuropharmacology*, 17(8), 787–807. <https://doi.org/10.2174/1570159X17666190409142555>
156. Reese, R., & Volkmann, J. (2017). Deep Brain Stimulation for the Dystonias: Evidence, Knowledge Gaps, and Practical Considerations. *Movement Disorders Clinical Practice*, 4(4), 486–494. <https://doi.org/10.1002/MDC3.12519>
157. Reich, M. M., Hsu, J., Ferguson, M., Schaper, F. L. W. V. J., Joutsa, J., Roothans, J., Nickl, R. C., Frankemolle-Gilbert, A., Alberts, J., Volkmann, J., & Fox, M. D. (2022). A brain network for deep brain stimulation induced cognitive decline in Parkinson's disease. *Brain: A Journal of Neurology*, 145(4), 1410–1421. <https://doi.org/10.1093/BRAIN/AWAC012>
158. Reisert, M., Mader, I., Anastasopoulos, C., Weigel, M., Schnell, S., & Kiselev, V. (2011). Global fiber reconstruction becomes practical. *NeuroImage*, 54(2), 955–962. <https://doi.org/10.1016/J.NEUROIMAGE.2010.09.016>
159. Ríos, A. S., Oxenford, S., Neudorfer, C., Butenko, K., Li, N., Rajamani, N., Boutet, A., Elias, G. J. B., Germann, J., Loh, A., Deeb, W., Wang, F., Setsompop, K., Salvato, B., Almeida, L. B. de, Foote, K. D., Amaral, R., Rosenberg, P. B., Tang-Wai, D. F., ... Horn, A. (2022). Optimal deep brain stimulation sites and networks for stimulation of the fornix in Alzheimer's disease. *Nature Communications* 2022 13:1, 13(1), 1–14. <https://doi.org/10.1038/s41467-022-34510-3>
160. Rodriguez-Rojas, R., Pineda-Pardo, J. A., Mañez-Miro, J., Sanchez-Turel, A., Martinez-Fernandez, R., del Alamo, M., DeLong, M., & Obeso, J. A. (2022). Functional Topography of the Human Subthalamic Nucleus: Relevance for Subthalamotomy in Parkinson's Disease. *Movement Disorders*, 37(2), 279–290. <https://doi.org/10.1002/MDS.28862>
161. Schnitzler, A., Münks, C., Butz, M., Timmermann, L., & Gross, J. (2009). Synchronized brain network associated with essential tremor as revealed by magnetoencephalography. *Movement Disorders: Official Journal of the Movement Disorder Society*, 24(11), 1629–1635. <https://doi.org/10.1002/MDS.22633>

162. Schrock, L. E., Ostrem, J. L., Turner, R. S., Shimamoto, S. A., & Starr, P. A. (2009). The Subthalamic Nucleus in Primary Dystonia: Single-Unit Discharge Characteristics. *Journal of Neurophysiology*, 102(6), 3740. <https://doi.org/10.1152/JN.00544.2009>
163. Sironi, V. A. (2011). Origin and Evolution of Deep Brain Stimulation. *Frontiers in Integrative Neuroscience*, 5. <https://doi.org/10.3389/FNINT.2011.00042>
164. Smith, S. M., Vidaurre, D., Beckmann, C. F., Glasser, M. F., Jenkinson, M., Miller, K. L., Nichols, T. E., Robinson, E. C., Salimi-Khorshidi, G., Woolrich, M. W., Barch, D. M., Uğurbil, K., & Van Essen, D. C. (2013). Functional connectomics from resting-state fMRI. *Trends in Cognitive Sciences*, 17(12), 666–682. <https://doi.org/10.1016/J.TICS.2013.09.016>
165. Solé-Padullés, C., Castro-Fornieles, J., De La Serna, E., Calvo, R., Baeza, I., Moya, J., Lázaro, L., Rosa, M., Bargalló, N., & Sugranyes, G. (2016). Intrinsic connectivity networks from childhood to late adolescence: Effects of age and sex. *Developmental Cognitive Neuroscience*, 17, 35–44. <https://doi.org/10.1016/J.DCN.2015.11.004>
166. Sporns, O. (2010). *Networks of the Brain*. Networks of the Brain. <https://doi.org/10.7551/MITPRESS/8476.001.0001>
167. Sporns, O. (2012). *Discovering the Human Connectome*. Discovering the Human Connectome. <https://doi.org/10.7551/MITPRESS/9266.001.0001>
168. Sporns, O. (2016). *Connectome Networks: From Cells to Systems*. *Research and Perspectives in Neurosciences*, 9783319277769, 107–127. [https://doi.org/10.1007/978-3-319-27777-6\\_8](https://doi.org/10.1007/978-3-319-27777-6_8)
169. Sporns, O., Tononi, G., & Kötter, R. (2005). The Human Connectome: A Structural Description of the Human Brain. *PLOS Computational Biology*, 1(4), e42. <https://doi.org/10.1371/JOURNAL.PCBI.0010042>
170. Steiner, L. A., & Milosevic, L. (2023). A convergent subcortical signature to explain the common efficacy of subthalamic and pallidal deep brain stimulation. *Brain Communications*, 5(2). <https://doi.org/10.1093/BRAINCOMMS/FCAD033>
171. Sussman, B. L., Wyckoff, S. N., Heim, J., Wilfong, A. A., Adelson, P. D., Kruer, M. C., Gonzalez, M. J., & Boerwinkle, V. L. (2022). Is Resting State Functional MRI Effective Connectivity in Movement Disorders Helpful? A Focused Review Across Lifespan and Disease. *Frontiers in Neurology*, 13, 734. <https://doi.org/10.3389/FNEUR.2022.847834/BIBTEX>

172. Takemura, H., Palomero-Gallagher, N., Axer, M., Gräßel, D., Jorgensen, M. J., Woods, R., & Zilles, K. (2020). Anatomy of nerve fiber bundles at micrometer-resolution in the vervet monkey visual system. *ELife*, 9, 1–102. <https://doi.org/10.7554/ELIFE.55444>
173. Thomas Yeo, B. T., Krienen, F. M., Sepulcre, J., Sabuncu, M. R., Lashkari, D., Hollinshead, M., Roffman, J. L., Smoller, J. W., Zöllei, L., Polimeni, J. R., Fisch, B., Liu, H., & Buckner, R. L. (2011). The organization of the human cerebral cortex estimated by intrinsic functional connectivity. *Journal of Neurophysiology*, 106(3), 1125–1165. <https://doi.org/10.1152/JN.00338.2011>
174. Tinaz, S., Malone, P., Hallett, M., & Horowitz, S. G. (2015). Role of the right dorsal anterior insula in the urge to tic in Tourette syndrome. *Movement Disorders : Official Journal of the Movement Disorder Society*, 30(9), 1190–1197. <https://doi.org/10.1002/MDS.26230>
175. Treu, S., Strange, B., Oxenford, S., Neumann, W. J., Kühn, A., Li, N., & Horn, A. (2020). Deep brain stimulation: Imaging on a group level. *NeuroImage*, 219, 117018. <https://doi.org/10.1016/J.NEUROIMAGE.2020.117018>
176. Tuleasca, C., Najdenovska, E., Régis, J., Witjas, T., Girard, N., Champoudry, J., Faouzi, M., Thiran, J. P., Cuadra, M. B., Levivier, M., & Van De Ville, D. (2018). Clinical response to Vim's thalamic stereotactic radiosurgery for essential tremor is associated with distinctive functional connectivity patterns. *Acta Neurochirurgica*, 160(3), 611–624. <https://doi.org/10.1007/S00701-017-3456-X>
177. Tuleasca, C., Witjas, T., Najdenovska, E., Verger, A., Girard, N., Champoudry, J., Thiran, J. P., Van de Ville, D., Cuadra, M. B., Levivier, M., Guedj, E., & Régis, J. (2017). Assessing the clinical outcome of Vim radiosurgery with voxel-based morphometry: visual areas are linked with tremor arrest! *Acta Neurochirurgica*, 159(11), 2139–2144. <https://doi.org/10.1007/S00701-017-3317-7>
178. Tuleasca, C., Witjas, T., Van de Ville, D., Najdenovska, E., Verger, A., Girard, N., Champoudry, J., Thiran, J. P., Cuadra, M. B., Levivier, M., Guedj, E., & Régis, J. (2018). Right Brodmann area 18 predicts tremor arrest after Vim radiosurgery: a voxel-based morphometry study. *Acta Neurochirurgica*, 160(3), 603–609. <https://doi.org/10.1007/S00701-017-3391-X>
179. Uğurbil, K. (2012). Development of functional imaging in the human brain (fMRI); the University of Minnesota experience. *NeuroImage*, 62(2), 613–619. <https://doi.org/10.1016/J.NEUROIMAGE.2012.01.135>

180. van Albada, S. J., & Robinson, P. A. (2007). Transformation of arbitrary distributions to the normal distribution with application to EEG test-retest reliability. *Journal of Neuroscience Methods*, 161(2), 205–211. <https://doi.org/10.1016/J.JNEUMETH.2006.11.004>
181. Vayssiere, N., Van Der Gaag, N., Cif, L., Hemm, S., Verdier, R., Frerebeau, P., & Coubes, P. (2004). Deep brain stimulation for dystonia confirming a somatotopic organization in the globus pallidus internus. *Journal of Neurosurgery*, 101(2), 181–188. <https://doi.org/10.3171/JNS.2004.101.2.0181>
182. Vidailhet, M., Vercueil, L., Houeto, J.-L., Krystkowiak, P., Benabid, A.-L., Cornu, P., Lagrange, C., Tézenas du Montcel, S., Dormont, D., Grand, S., Blond, S., De-tante, O., Pillon, B., Ardouin, C., Agid, Y., Destée, A., & Pollak, P. (2005). Bilateral deep-brain stimulation of the globus pallidus in primary generalized dystonia. *The New England Journal of Medicine*, 352(5), 459–467. <https://doi.org/10.1056/NEJMOA042187>
183. Vitek, J. L. (2002). Mechanisms of deep brain stimulation: excitation or inhibition. *Movement Disorders : Official Journal of the Movement Disorder Society*, 17 Suppl 3(SUPPL. 3). <https://doi.org/10.1002/MDS.10144>
184. Wang, D. D., de Hemptinne, C., Miocinovic, S., Ostrem, J. L., Galifianakis, N. B., Luciano, M. S., & Starr, P. A. (2018). Pallidal Deep-Brain Stimulation Disrupts Pallidal Beta Oscillations and Coherence with Primary Motor Cortex in Parkinson's Disease. *Journal of Neuroscience*, 38(19), 4556–4568. <https://doi.org/10.1523/JNEUROSCI.0431-18.2018>
185. Wang, Q., Akram, H., Muthuraman, M., Gonzalez-Escamilla, G., Sheth, S. A., Oxenford, S., Yeh, F. C., Groppa, S., Vanegas-Arroyave, N., Zrinzo, L., Li, N., Kühn, A., & Horn, A. (2021). Normative vs. patient-specific brain connectivity in deep brain stimulation. *NeuroImage*, 224. <https://doi.org/10.1016/J.NEUROIMAGE.2020.117307>
186. Wichmann, T., & Dostrovsky, J. O. (2011). Pathological basal ganglia activity in movement disorders. *Neuroscience*, 198, 232. <https://doi.org/10.1016/J.NEUROSCIENCE.2011.06.048>
187. Wills, A. J., Jenkins, L. H., Thompson, P. D., Findley, L. J., & Brooks, D. J. (1995). A positron emission tomography study of cerebral activation associated with essential and writing tremor. *Archives of Neurology*, 52(3), 299–305. <https://doi.org/10.1001/ARCHNEUR.1995.00540270095025>

188. Wright, M. D. , B. A. (2011). An Historical Review of Electroconvulsive Therapy. *Jefferson Journal of Psychiatry*, 8(2), 10. <https://doi.org/https://doi.org/10.29046/JJP.008.2.007>
189. Zuo, X. N., Anderson, J. S., Bellec, P., Birn, R. M., Biswal, B. B., Blautzik, J., Breitner, J. C. S., Buckner, R. L., Calhoun, V. D., Castellanos, F. X., Chen, A., Chen, B., Chen, J., Chen, X., Colcombe, S. J., Courtney, W., Craddock, R. C., Di Martino, A., Dong, H. M., Milham, M. P. (2014). An open science resource for establishing reliability and reproducibility in functional connectomics. *Scientific Data* 2014 1:1, 1(1), 1–13. <https://doi.org/10.1038/sdata.2014.49>

## Statutory Declaration

"I, Bassam Al-Fatly, by personally signing this document in lieu of an oath, hereby affirm that I prepared the submitted dissertation on the topic Defining Therapeutic Networks of Deep Brain Stimulation in Movement Disorders (Charakterisierung der therapeutischen Netzwerke der Tiefen Hirnstimulation bei Bewegungsstörungen), independently and without the support of third parties, and that I used no other sources and aids than those stated.

All parts which are based on the publications or presentations of other authors, either in letter or in spirit, are specified as such in accordance with the citing guidelines. The sections on methodology (in particular regarding practical work, laboratory regulations, statistical processing) and results (in particular regarding figures, charts and tables) are exclusively my responsibility.

Furthermore, I declare that I have correctly marked all of the data, the analyses, and the conclusions generated from data obtained in collaboration with other persons, and that I have correctly marked my own contribution and the contributions of other persons (cf. declaration of contribution). I have correctly marked all texts or parts of texts that were generated in collaboration with other persons.

My contributions to any publications to this dissertation correspond to those stated in the below joint declaration made together with the supervisor. All publications created within the scope of the dissertation comply with the guidelines of the ICMJE (International Committee of Medical Journal Editors; [www.icmje.org](http://www.icmje.org)) on authorship. In addition, I declare that I shall comply with the regulations of Charité – Universitätsmedizin Berlin on ensuring good scientific practice.

I declare that I have not yet submitted this dissertation in identical or similar form to another Faculty.

The significance of this statutory declaration and the consequences of a false statutory declaration under criminal law (Sections 156, 161 of the German Criminal Code) are known to me."

---

Date

---

Signature

## Declaration of your own contribution to the publications

Bassam Al-Fatly contributed the following to the below listed publications:

Publication 1: **Bassam Al-Fatly**, Siobhan Ewert, Dorothee Kübler, Daniel Kroneberg, Andreas Horn\*, Andrea A Kühn\*, Connectivity profile of thalamic deep brain stimulation to effectively treat essential tremor, *Brain*, 2019

Contribution: I conceptualized the study with my supervisors Andrea A. Kühn and Andreas Horn. I gathered data with the help of Daniel Kroneberg and Dorothee Kübler. I conducted all the analyses including MRI/CT preprocessing, deep brain stimulation electrode localization, stimulation volume estimation, connectivity estimation using connectomes and building predictive models. I created all tables and figures of this study. I wrote first draft and reviewed contributions/edit from coauthors.

Publication 2: Christos Ganos\*, **Bassam Al-Fatly\***, Jan-Frederik Fischer, Juan-Carlos Baldermann, Christina Hennen, Veerle Visser-Vandewalle, Clemens Neudorfer, Davide Martino, Jing Li, Tim Bouwens, Linda Ackermanns, Albert FG Leentjens, Nadya Pyatigorskaya, Yulia Worbe, Michael D Fox, Andrea A Kühn, Andreas Horn, A neural network for tics: insights from causal brain lesions and deep brain stimulation, *Brain*, 2022

Contribution: I conceptualized the study together with my colleague Christos Ganos and my supervisors Andrea A. Kühn and Andreas Horn. I gathered data with the help of Christos Ganos. I conducted lesion network mapping and all analyses related to deep brain stimulation parts. I created all tables and figures of this study. I wrote first draft and reviewed contributions/edit from coauthors.

Publication 3: **Bassam Al-Fatly**, Sabina J Giesler, Simon Oxenford, Ningfei Li, Till A Dembek, Johannes Achtzehn, Patricia Krause, Veerle Visser-Vandewalle, Joachim K Krauss, Joachim Runge, Vera Tadic, Tobias Bäumer, Alfons Schnitzler, Jan Vesper, Jochen Wirths, Lars Timmermann, Andrea A Kühn\*, Anne Koy\*, Neuroimaging-based analysis of DBS outcomes in pediatric dystonia: Insights from the GEPESTIM registry, *Neuroimage: Clinical*, 2023

Contribution: I conceptualized the study with my supervisor Andrea A. Kühn. I collected data with the help of Sabina J Giesler. I built a pediatric connectome and an atlas and implemented them together with openly available pediatric MNI space in [www.lead-dbs.org](http://www.lead-dbs.org) software. I conducted all the analyses including MRI/CT preprocessing, deep brain stimulation electrode localization, stimulation volume estimation, connectivity estimation using connectomes and building predictive models. I created all tables and figures of this study. I wrote first draft and reviewed contributions/edit from coauthors.

---

Signature, date and stamp of first supervising university professor / lecturer

---

Signature of doctoral candidate


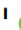

## Printing copy(s) of the publication(s)

doi:10.1093/brain/awz236

BRAIN 2019; 142; 3086–3098 | 3086

**BRAIN**  
A JOURNAL OF NEUROLOGY

# Connectivity profile of thalamic deep brain stimulation to effectively treat essential tremor

 Bassam Al-Fatly,<sup>1</sup>  Siobhan Ewert,<sup>1</sup>  Dorothee Kübler,<sup>1</sup>  Daniel Kroneberg,<sup>1</sup> Andreas Horn<sup>1,2,\*</sup> and Andrea A. Kühn<sup>1,3,\*</sup>

\*These authors contributed equally to this work.

Essential tremor is the most prevalent movement disorder and is often refractory to medical treatment. Deep brain stimulation offers a therapeutic approach that can efficiently control tremor symptoms. Several deep brain stimulation targets (ventral intermediate nucleus, zona incerta, posterior subthalamic area) have been discussed for tremor treatment. Effective deep brain stimulation therapy for tremor critically involves optimal targeting to modulate the tremor network. This could potentially become more robust and precise by using state-of-the-art brain connectivity measurements. In the current study, we used two normative brain connectomes (structural and functional) to show the pattern of effective deep brain stimulation electrode connectivity in 36 patients with essential tremor. Our structural and functional connectivity models were significantly predictive of postoperative tremor improvement in out-of-sample data ( $P < 0.001$  for both structural and functional leave-one-out cross-validation). Additionally, we segregated the somatotopic brain network based on head and hand tremor scores. These resulted in segregations that mapped onto the well-known somatotopic maps of both motor cortex and cerebellum. Crucially, this shows that slightly distinct networks need to be modulated to ameliorate head versus hand tremor and that those networks could be identified based on somatotopic zones in motor cortex and cerebellum. Finally, we propose a multi-modal connectomic deep brain stimulation sweet spot that may serve as a reference to enhance clinical care, in the future. This spot resided in the posterior subthalamic area, encroaching on the inferior borders of ventral intermediate nucleus and sensory thalamus. Our results underscore the importance of integrating brain connectivity in optimizing deep brain stimulation targeting for essential tremor.

- 1 Department of Neurology with Experimental Neurology, Movement Disorders and Neuromodulation Unit, Charité – Universitätsmedizin Berlin, corporate member of Freie Universität Berlin, Humboldt-Universität zu Berlin, and Berlin Institute of Health, Berlin, Germany
- 2 Berlin Institute of Health, Berlin, Germany
- 3 Exzellenzcluster NeuroCure, Charité – Universitätsmedizin Berlin, Berlin, Germany

Correspondence to: Bassam Al-Fatly  
Department of Neurology, Charité - Universitätsmedizin Berlin, CCM  
Neurowissenschaftliches Forschungszentrum, 2nd floor, Hufelandweg 14, 10117 Berlin  
Germany  
E-mail: bassam.al-fatly@charite.de

**Keywords:** thalamic deep brain stimulation; essential tremor; connectivity; somatotopy; sweet spot

**Abbreviations:** DBS = deep brain stimulation; FTM = Fahn-Tolosa-Marin score; VIM = ventral intermediate nucleus; VTA = volume of tissue activated



## Introduction

Essential tremor is the most common movement disorder that is encountered in clinical practice (Deuschl *et al.*, 2000). A satisfactory pharmacotherapeutic treatment is difficult if not impossible to attain in 25–55% of essential tremor cases (Flora *et al.*, 2010). Therefore, deep brain stimulation (DBS) has been accepted as an efficacious alternative to control medication-refractory tremor symptoms.

To date, multiple DBS targets have been proposed to effectively treat essential tremor (Deuschl *et al.*, 2011). Targeting the ventral intermediate (VIM) nucleus was regarded as an historical gold standard since the beginnings of modern-day DBS (Benabid *et al.*, 1991). Increasingly, the ventrally adjacent white matter has been proposed to lead to superior effects (Hamel *et al.*, 2007; Sandvik *et al.*, 2012; Eisinger *et al.*, 2018). This target has been referred to as the posterior subthalamic area (PSA). Thus, the optimal treatment coordinates are still a matter of debate.

Pathophysiological evidence has accumulated that a cerebello-thalamo-cortical tremor network plays a crucial role in mediating abnormal oscillatory tremor activity and its modulation is related to the therapeutic effects of DBS (Schnitzler *et al.*, 2009; Raethjen and Deuschl, 2012). The cortical and subcortical nodes constituting the proposed network have been described with functional MRI and MEG (Schnitzler *et al.*, 2009; Sharifi *et al.*, 2014). In light of such a network-based mechanism, strong connectivity between DBS electrodes and network tremor nodes should lead to effective treatment response. This approach has been followed in individual cases by Coenen *et al.* (2011a, b, 2017) who proposed diffusion tensor imaging (DTI)-based targeting in tremor patients focusing on the connectivity between the cerebellum and the thalamus. Recently, a different approach has been proposed to use whole brain connectivity patterns to predict clinical outcome after DBS. This was first demonstrated in Parkinson disease across cohorts, and improvement scores could be predicted across DBS centres and surgeons (Horn *et al.*, 2017a, b). In case of essential tremor, few studies addressed the relationship between DBS connectivity and clinical outcome and to date, none has actually used brain connectivity to predict the DBS effects in out-of-sample data (Pouratian *et al.*, 2011; Gibson *et al.*, 2016; Akram *et al.*, 2018; Middlebrooks *et al.*, 2018).

Here, we aimed at constructing a ‘therapeutic network’ model for DBS in essential tremor. Following the concept of Horn *et al.* (2017b), we postulated that similarity to this connectivity fingerprint could linearly predict clinical outcome in patients with essential tremor. We traced DBS-electrode connectivity to other brain regions using high resolution normative connectomes (functional and structural) as surrogate neuroimaging models in a data-driven fashion. We validated the resulting optimal connectivity fingerprints by predicting individual tremor improvements in a leave-one-out design. In a further step, we used DBS

connectivity to investigate somatotopic treatment effects. Specifically, we analysed how tremor improvement of hand and head could be associated with segregated DBS connectivity maps. Finally, we condensed findings to define an optimal surgical target for essential tremor, which is made publicly available as of a probabilistic atlas dataset.

## Materials and methods

### Patients: demographic and clinical details

Thirty-six patients underwent DBS (72 DBS electrodes) for severe, medically intractable essential tremor (13 female) were retrospectively included in the current study (mean age = 74.3 ± 11.9 years). Diagnosis of essential tremor followed the consensus criteria proposed in Deuschl *et al.* (1998). Patients with bilateral symmetric postural or kinetic tremor of the upper limb with the possibility of additional head tremor, were included as essential tremor cases. Any isolated voice, chin, tongue or leg tremor patients were excluded. Additionally, patients with dystonic, neuropathic, orthostatic, physiological or psychological tremor were excluded. Patients had a mean disease duration of 24.33 ± 4.99 years before DBS surgery. All patients received bilateral DBS implants in Charité–Universitätsmedizin, Berlin for the period between 2001 and 2017 (see Table 1 for clinical and demographic information and Supplementary Table 1 for individual patient clinical characteristics). All implanted DBS electrodes were Medtronic 3387 (except for three patients, two of which were implanted with Boston Scientific Vercice Directed and one with St Jude Medical). Preoperative MRI was used to define VIM/zona incerta DBS targets. Microelectrode recordings and test stimulation were used intraoperatively to guide DBS lead placement. Correct lead placement was confirmed by postoperative imaging using Lead-DBS to localize DBS

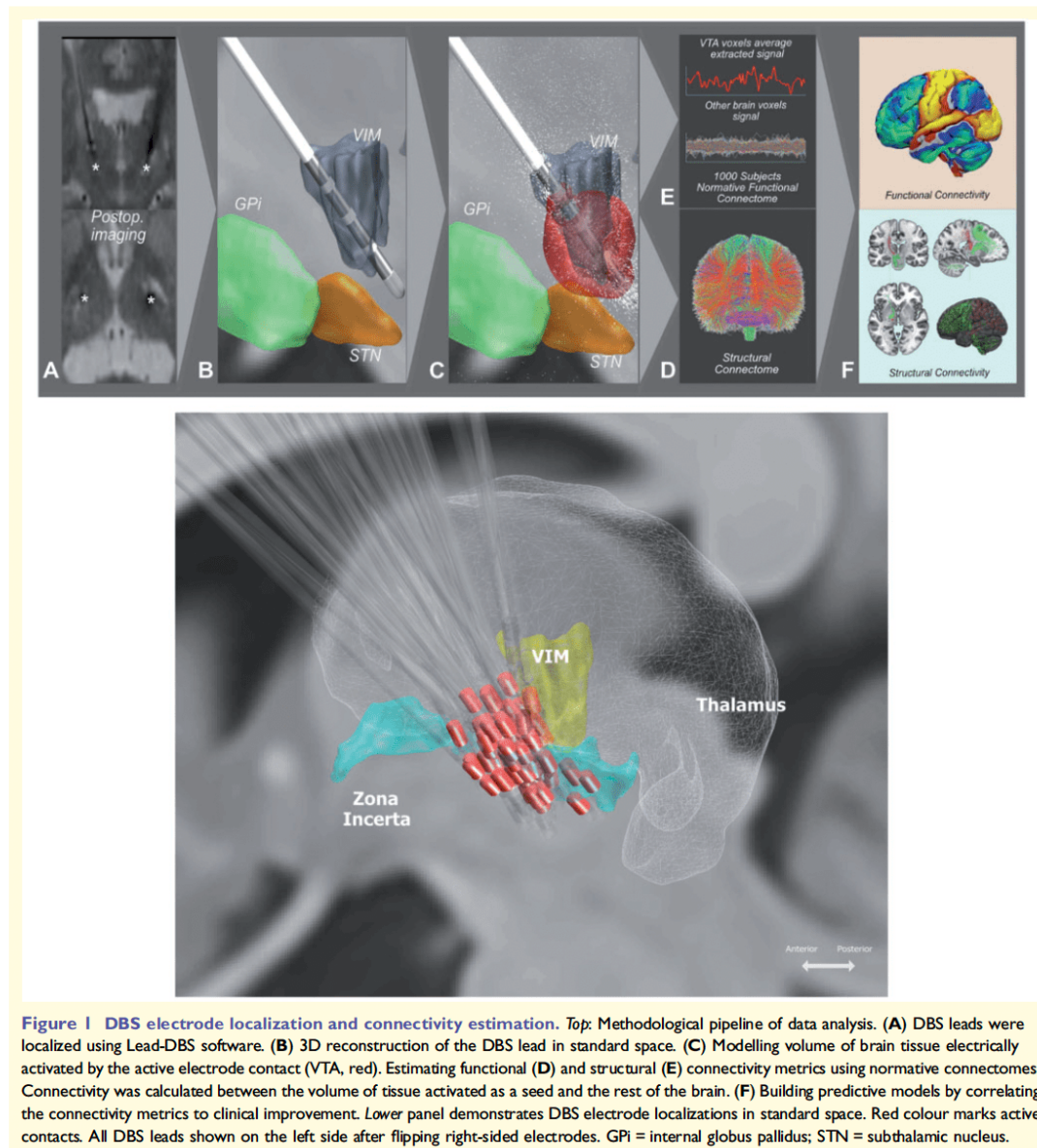
**Table 1** Cohort demographics and clinical data

Criteria	
Age, years	74.3 ± 11.9
Age at diagnosis, years	44.9 ± 18.4
Disease duration, years	24.3 ± 14.9
Male sex, n (%)	23 (72)
Baseline total FTM score	33.3 ± 9.6
Postoperative total FTM score	10.9 ± 5.5
Total FTM improvement (%)	65.1 ± 18.4
Baseline contralateral UL tremor score	13.4 ± 4.3
Postoperative contralateral UL tremor score	4.6 ± 2.9
Contralateral UL tremor improvement (%)	63.4 ± 22.9
Baseline head tremor score	3.8 ± 2.8
Postoperative head tremor score	1.0 ± 1.7
Head tremor improvement (%)	80.8 ± 29.5

UL = upper limb.

Data are presented in mean ± standard deviation (SD).

Absolute tremor scores are reported at baseline and postoperative time points while tremor improvement are reported in percentage.



electrodes in standard MNI space (Fig. 1). Per cent improvement in the Fahn-Tolosa-Marin (FTM) tremor score served as an index of clinical outcome (Fahn *et al.*, 1993). FTM scores before (baseline) and at least 3 months after electrode implantation have been obtained from archival video material. All videos have been rated by three clinicians experienced in movement disorders. Each clinician (B.A., D.Ku. and D.Ko.) rated separate parts of the cohort (i.e. no video was rated twice) and was blinded to the timing of the video (preoperative

versus postoperative). Postoperative FTM scores indicate tremor severity during the chronic DBS-on condition. Upper limb subscores contralateral to DBS electrodes were summed and used in the calculation of the main clinical outcome quantifying therapeutic effect. Upper limb subscore comprised the following items: rest tremor, postural tremor, action tremor, drawing of Archimedes spiral and repeated letter 'L' writing (modified FTM score). For somatopy-related analyses, bilateral upper limb subscores and head scores were used. The

head score consisted of the sum of head, face, tongue, speech and voice-related subscores. All patients showed a reduction in FTM score of at least ~27% with a mean decrease of  $22.4 \pm 9.9$  points of the average total FTM score (from  $33.3 \pm 9.6$  at baseline to  $10.9 \pm 5.5$  with chronic DBS). The average postoperative time at which patients were assessed for postoperative FTM scoring was  $12 \pm 9.86$  months.

The study was approved by the local ethics committee of the Charité University Medicine - Berlin.

## DBS electrode localizations

Preoperative MRI as well as postoperative MRI or CT were obtained in all patients. DBS electrodes were localized using Lead-DBS software (Horn and Kühn, 2015; [www.lead-dbs.org](http://www.lead-dbs.org)) following the enhanced methodology described in Horn *et al.* (2018) (NeuroImage). Briefly, preoperative and postoperative patients' images were linearly co-registered using Advanced Normalization Tools (ANTs, Avants *et al.*, 2008; <http://stnava.github.io/ANTs/>) and manually refined when necessary.

Pre- and postoperative images were then normalized into ICBM 2009b NLIN asymmetric space using the symmetric diffeomorphic image registration approach implemented in ANTs (Avants *et al.*, 2008). Electrodes were then localized and volumes of tissue activated (VTA) modelled using Lead-DBS based on patient-specific stimulation parameters.

## Functional and structural connectivity estimation

Using VTAs as seed regions, functional and structural connectivity estimates were computed using pipelines implemented in Lead-DBS. Two normative connectomes were used: first, a structural connectome (Horn *et al.*, 2014; Horn, 2015), which consisted of high density normative fibre tracts based on 20 subjects. Diffusion data were collected using single-shot spin-echo planar imaging sequence (repetition time = 10 000 ms, echo time = 94 ms,  $2 \times 2 \times 2$  mm<sup>3</sup>, 69 slices). Global fibre-tracking was performed using Gibb's tracking method (Reisert *et al.*, 2011) [for more methodological details, see Horn and Blankenburg (2016)]. Structural connectivity was estimated by extracting tracts passing through VTA seeds and calculating the fibre counts in a voxel-wise manner across the whole brain. Second, a functional connectome defined on resting state functional MRI scans of 1000 healthy subjects (Yeo *et al.*, 2011; <https://dataverse.harvard.edu/dataverse/GSP>) and based on data of the Brain Genomics Superstruct Project. Data were collected with 3T Siemens MRI and the resting state blood oxygen level-dependent (BOLD) processed with signal regression and application of spatial smoothing kernel of 6 mm at full-width at half-maximum (Yeo *et al.*, 2011). For the purpose of the current study, connectivity estimates were performed for each of the 72 VTAs (36 bilateral implants) after non-linearly flipping right-sided VTA to the left side using Lead-DBS.

## Models of optimal connectivity

Following the concept described in Horn *et al.* (2017b), clinical improvements in the contralateral upper limb were

correlated with structural and functional connectivity from the VTA (while these were accumulated on the left side of the brain) to each brain voxel across electrodes. This process resulted in R-maps that carry Spearman's rank-correlation coefficients for each voxel. The maps fulfil two concepts. First, they denote to which areas connectivity is associated with beneficial outcome. Second, their spatial distribution describes an optimal connectivity profile of DBS electrodes for essential tremor (Horn *et al.*, 2017b).

Thus, to make predictions, each VTA-derived structural or functional connectivity pattern was then tested for spatial similarity with this optimal connectivity model. Specifically, similarity between each VTA's connectivity profile and the 'optimal' connectivity profile (as defined by the R-map) was calculated using spatial correlation. The resulting similarity index estimates 'how optimal' each connectivity profile was and was used to explain clinical improvement in a linear regression model. To cross-validate the model, we correlated aforementioned predicted and empirical individual upper limb tremor improvements in a leave-one-out design. Furthermore, we calculated discriminative fibre tracts following the approach introduced by Baldermann *et al.* (2019). Briefly, fibre tracts connected to VTAs across the cohort were isolated from the normative group connectome. In a mass-univariate analysis, for each fibre tract, a two-sample *t*-test was performed between improvement scores of VTAs connected versus improvement of non-connected VTAs and fibres were labelled according to this *t*-score. The resulting positive *t*-score streamlines represent fibre tracts that may discriminate between poor and good responders. Again, this analysis was carried out across the left-sided accumulated VTAs using contralateral upper limb improvement subscores. This analysis was used to confirm the main analysis using a slightly different statistical concept.

## Prospective case validation

We preoperatively scanned one patient with diffusion weighted imaging (Supplementary material) to investigate the validity of our model in predicting patient improvement using patient-specific tractography. The patient received a unilateral implant on the left (Abbott's St. Jude Medical Infinity model) for treatment of refractory essential tremor affecting the upper limbs. The VTA was modelled with the same pipeline as the main patient's cohort. Patient-specific diffusion weighted imaging (diffusion MRI) data were then used to calculate fibre streamlines seeding from the modelled left-VTA. The resulting connectivity profile was then fed into the structural predictive model created on the main cohort (using the normative connectome). Patients' empirical right upper limb FTM scores were calculated pre- and postoperatively following the same methodological description as in the main cohort.

## Side effects-related connectivity profile

Connectivity seeding from electrodes associated with DBS-related side effects were also calculated in a subgroup of patients in which information about side effects were available using the same functional connectome (Yeo *et al.*, 2011). We then compared the resulting connectivity to a sample of control patients where DBS-induced side effects could be excluded.

To do so, mass-univariate voxel-wise two-sample *t*-tests were calculated between connectivity strengths seeding from VTAs associated with gait ataxia or dysarthria and that of control patients. Connectivity difference images were then masked by significant *P*-values ( $<0.05$ , uncorrected) and presented as positive *t*-scores images.

### Deriving somatotopic maps

In a further step, we segregated somatotopic maps informed by optimal functional connectivity models based on upper limb (hand) and head tremor improvements. As head tremor is an axial feature modulated by both left and right VTAs, those were combined in this analysis. Hence, bilateral VTAs were used to estimate functional somatotopic maps (i.e. connectivity was estimated seeding from both VTAs). The resulting connectivity maps were correlated with either summed bilateral hand scores or head scores. The resulting R-maps were overlaid on the cerebellum and primary motor cortex to investigate somatotopy.

### Defining an optimal DBS target

As a final step, we applied our optimal predictive structural and functional models to define an 'optimal' DBS target. We masked our functional and structural R-maps to include only voxels in the cortical and cerebellar regions. This was done as otherwise the design would have been recursive (with subcortical information already present in the R-maps). The subcortical region with maximal connectivity to those R-maps was determined using Lead-DBS. The resulting connectivity maps were then overlapped to show where exactly they converged. This spot is characterized by optimal functional and structural brain connectivity for maximal therapeutic outcome.

### Data availability

Patient datasets are not publicly available because of data privacy restrictions, but can be made available from the corresponding author upon reasonable request. All code used in the present manuscript is available within Lead-DBS software (<https://github.com/leaddbs/leaddbs>).

## Results

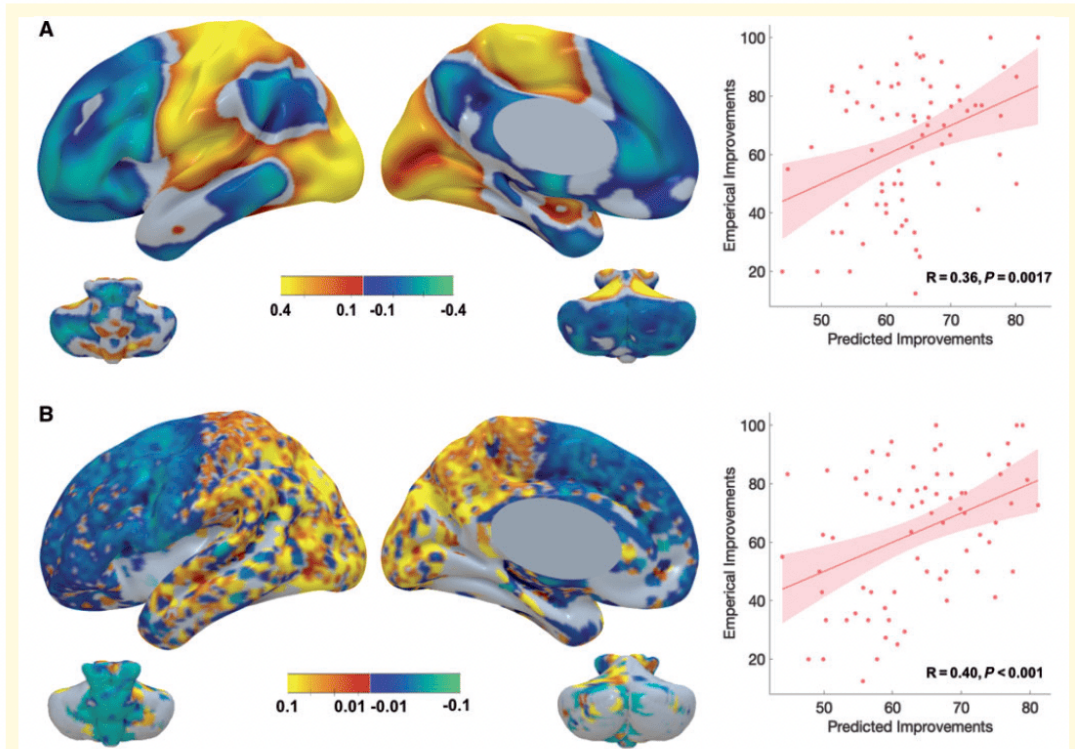
In total, 72 DBS electrodes were included in the analyses. Connectivity-based R-maps highlighted positively predictive voxels in multiple regions (Fig. 2) such as paracentral gyrus (M1 and sensory cortex), visual cortices (V1 and V2), superior temporal gyrus, and superior and inferior cerebellar lobules. Additionally, functional connectivity to part of the premotor cortex and supplementary motor area was associated with beneficial DBS outcome. On the other hand, structural optimal connectivity outlined additional regions such as superior parietal lobule and precuneus. Apart from those, the beneficial functional and structural connectivity profiles were largely congruent.

Functional connectivity profiles could explain 16.4% of the variance in DBS outcome ( $R = 0.41$ ,  $P < 0.001$ ), while structural connectivity profile could explain 25% of the variance in DBS outcome ( $R = 0.50$ ,  $P < 10^{-5}$ ). In a leave-one-out cross-validation, both structural ( $R = 0.40$ ,  $P < 0.001$ ) and functional connectivity ( $R = 0.36$ ,  $P = 0.0017$ ) remained significant predictors of individual clinical improvement. On average, predicted tremor improvements deviated from empirical improvements by  $17.98 \pm 10.73\%$  for structural and  $18.09 \pm 11.22\%$  for functional connectivity. As a proof of concept, similarity between VTA-seed connectivity in one modality and the R-map model of the other was also significantly predictive of tremor improvement (functional VTA-seed connectivity explained by structural model  $R = 0.41$ ,  $P < 0.001$ ; structural connectivity explained by functional model  $R = 0.33$ ,  $P = 0.005$ ). This may further illustrate similarities between optimal functional and structural connectivity maps. While our main analysis focused on improvements of hand-tremor scores, we repeated the main analysis for improvements of full tremor scores, which led to near identical results (Supplementary Fig. 1).

Structural DBS connectivity showed voxel clusters intersecting with a DBS target commonly used in essential tremor treatment (Papavassiliou *et al.*, 2004) and with the cerebello-thalamo-cortical tract (Fig. 3). The cluster extended from the M1 cortex down to the thalamic-subthalamic region. Discriminative fibre tract analysis delineated a well-defined tract connecting M1 and cerebellum (Fig. 5), passing through the motor thalamus. Crucially, based on our results, this tract represented the part of the cerebello-thalamo-cortical pathway that was associated with optimal improvement.

Beneficial structural connectivity (based on normative connectome) successfully predicted the magnitude of tremor improvement in a single prospective patient (empirical clinical improvement 61%, predicted clinical improvement 72%). This prediction was performed using patient-specific structural connectivity (Supplementary Fig. 2).

Next, we aimed at defining functional connectivity maps that could explain therapeutic response in different body parts (hand versus head tremor) (Fig. 4). Of note, only 22 patients were included in the functional connectivity model of head tremor as the symptom was not present in the remaining 11. All patients responded well to head tremor at baseline, thus a sub-analysis comparing good versus bad responders was not possible. The topology of M1 and cerebellar voxels predictive of hand and head tremor improvement followed the known homuncular organization of M1 and somatotopy of the cerebellum (Buckner *et al.*, 2011). Furthermore, connectivity to these somatotopy-specific subregions of the cerebellum and M1 could explain improvement of hand ( $R = 0.44$ ,  $P = 0.008$ ), and head tremor ( $R = 0.59$ ,  $P = 0.004$ ), respectively.



**Figure 2** DBS connectivity profiles predictive of tremor improvement. **(A)** Functional connectivity predictive of clinical improvement. Voxel topology predictive of DBS outcome generated using a high-definition functional connectome. The scatter plot demonstrates the correlation between predicted improvement (based on similarity between predictive functional connectivity profiles and functional connectivity profiles seeding from each VTA) and original clinical improvement scores of 66 upper limbs in a leave-one out design ( $R = 0.36$ ,  $P = 0.002$ ). **(B)** Topological distribution of structural connectivity predictive of DBS-related improvement. Connectivity generated using normative structural

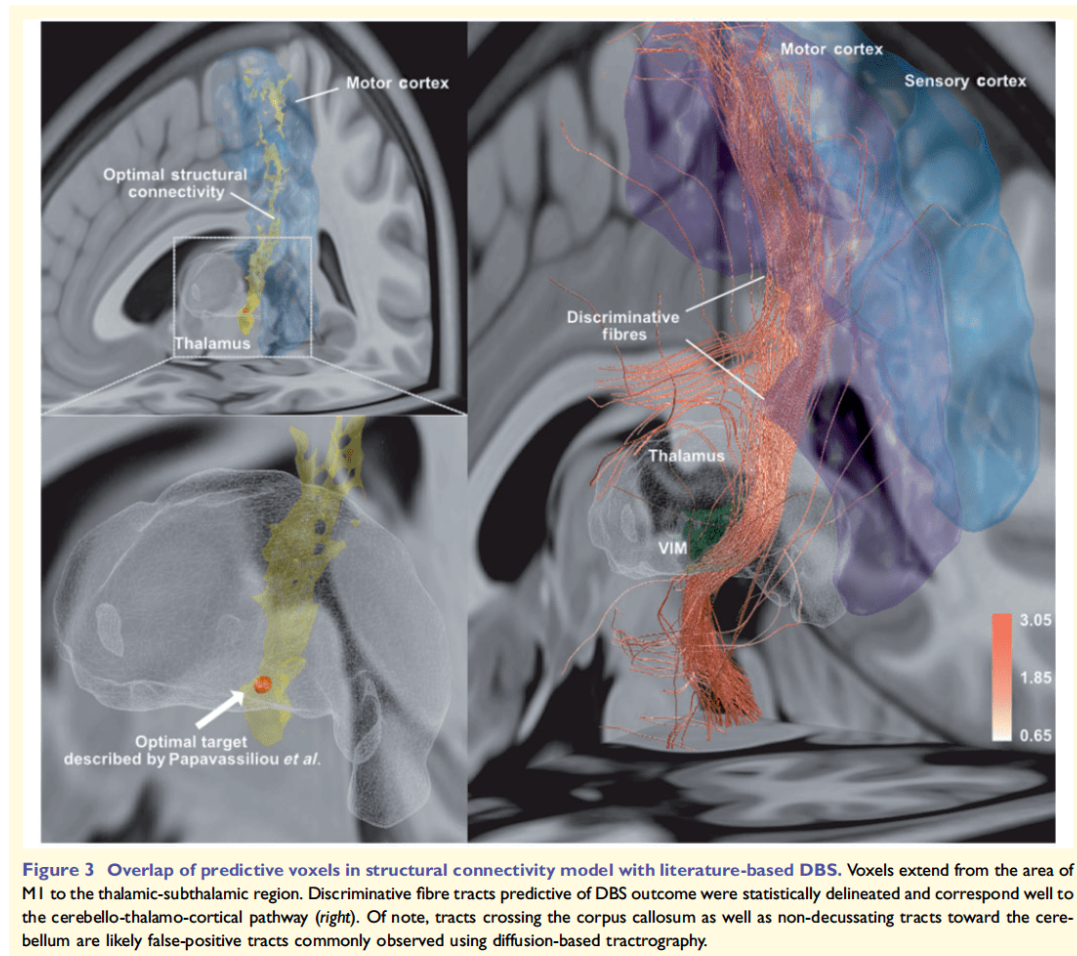
Additionally, we investigated functional connectivity patterns that could differentiate patients with DBS-related side effects (namely gait ataxia and dysarthria) from control subjects. Our analysis revealed side effect-specific clusters. Interestingly, these cortical and cerebellar clusters overlapped minimally with voxels positively correlated with optimal DBS outcome. Of note, these results are not corrected for multiple comparisons and should be interpreted with caution.

Our final goal was to define a clinically relevant surgical target that maximizes beneficial connectivity within the thalamo-subthalamic area. To obtain such a target, we seeded back from cortical voxels in our structural and functional R-maps (using their entries as a weighted connectivity seeds in Lead-DBS). Only cortical voxels were included to avoid confusion with already highlighted voxels in the sub-cortex. The resulting functional and structural connectivity patterns converged at the inferoposterior border of the VIM

and extended inferiorly and posteriorly to overlap with the dorsal part of the zona incerta (Fig. 6).

## Discussion

We demonstrated that optimal tremor reduction with DBS is significantly correlated with a specific pattern of functional and structural connectivity including sensorimotor areas and cerebellum. Importantly, the connectivity fingerprint of brain tissue activated by DBS can predict tremor improvement in out-of-sample data. Our models of optimal ‘therapeutic connectivity’ largely overlap with brain regions that were linked to essential tremor pathophysiology before. More importantly, we demonstrated that tremor in distinct body parts is optimally ameliorated by modulating a specific network that includes somatotopic regions of both M1 and the cerebellum. Finally, we defined an



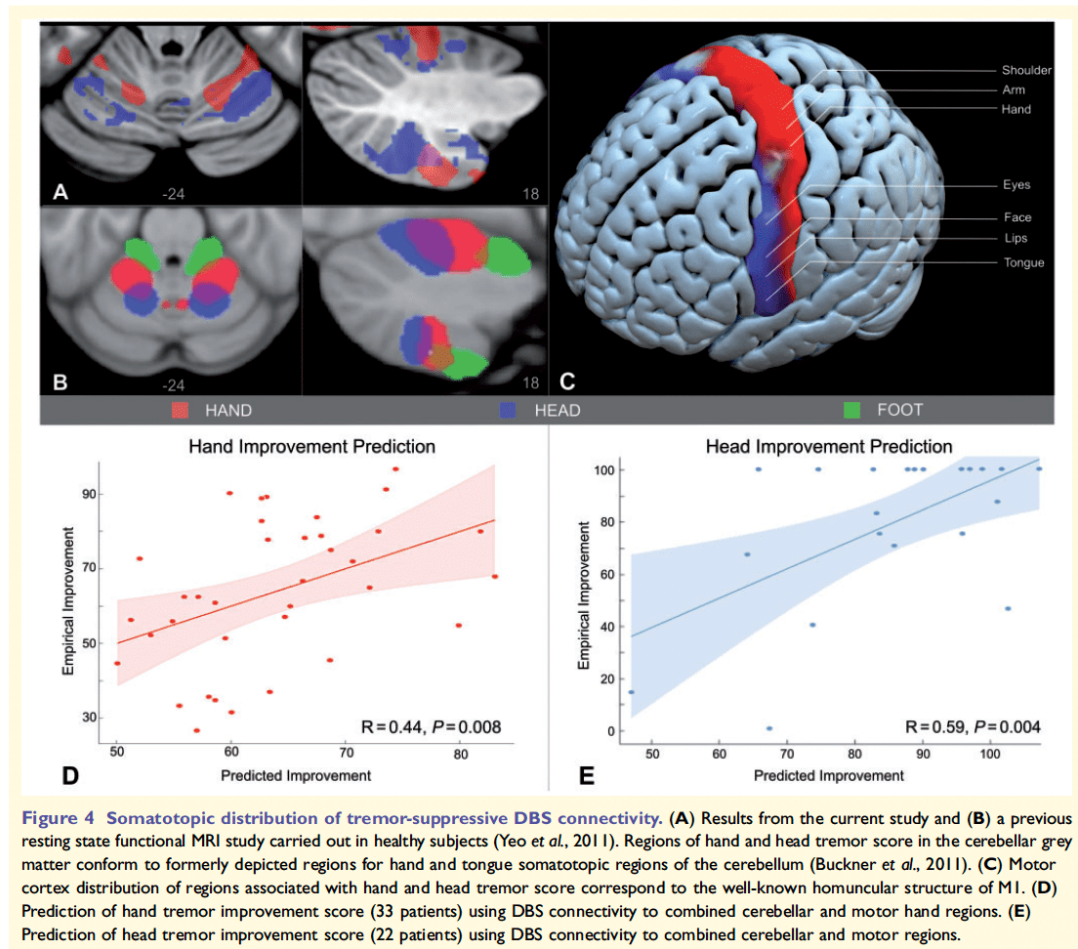
**Figure 3** Overlap of predictive voxels in structural connectivity model with literature-based DBS. Voxels extend from the area of M1 to the thalamic-subthalamic region. Discriminative fibre tracts predictive of DBS outcome were statistically delineated and correspond well to the cerebello-thalamo-cortical pathway (right). Of note, tracts crossing the corpus callosum as well as non-decussating tracts toward the cerebellum are likely false-positive tracts commonly observed using diffusion-based tractography.

‘optimal’ DBS target that maximizes beneficial functional and structural connectivity.

### The tremor network and pattern of beneficial DBS connectivity

The mechanism of tremor generation has been attributed to multiple central oscillators (Schnitzler *et al.*, 2009) that are synchronized in a tremor-specific frequency (Marsden *et al.*, 2000; Hellwig *et al.*, 2001) and distributed across nodes of the cerebello-thalamo-cortical pathway. It has been thought that the cerebellum drives tremorogenic oscillations (Deuschl *et al.*, 2000). However, several studies unveiled the involvement of cortical (sensorimotor, supplementary motor and premotor cortices) and subcortical (thalamus) nodes in tremor generation (McAuley and

Marsden, 2000; Pinto *et al.*, 2003; Schnitzler *et al.*, 2009; Helmich *et al.*, 2013). Theoretically, interference with any of these cerebello-thalamo-cortical nodes should suppress tremor oscillation. The thalamic (VIM) nucleus, which receives most of the cerebellar afferent fibres (Asanuma *et al.*, 1983), has been of much interest in tremor research (Pedrosa *et al.*, 2012; Basha *et al.*, 2014; Fang *et al.*, 2016; Milosevic *et al.*, 2018). The VIM also projects to the aforementioned tremor-related motor areas (McFarland and Haber, 2002; Haber and Calzavara, 2009). This property gives it a central position in the cerebello-thalamo-cortical tremor pathway. Historically, it was considered an excellent target for lesioning surgery (thalamotomy) yielding a satisfactory outcome of tremor control (Deuschl *et al.*, 2011). Later, DBS surgery started to replace thalamotomy in the majority of cases, given its reversible and adjustable stimulation



(Tasker, 1998). Nonetheless, clear visualization of the VIM region with conventional MRI is difficult even in contemporary DBS surgery with modern imaging protocols (Yamada *et al.*, 2010), this is why connectivity has already been used to target VIM-DBS surgeries (Anderson *et al.*, 2011; Coenen *et al.*, 2014).

This said, the optimal DBS target has to have tight functional and structural connectivity to the tremorogenic nodes in order to remotely modulate the nuisance tremor oscillations. Our results showed a connectivity pattern that agrees with this concept. Both structural and functional connectivity demonstrated areas in the pre- and postcentral gyri in addition to the superior and inferior cerebellar lobules. This is in line with the results of most studies that showed tremor-related alterations of the sensorimotor and cerebellar areas (Colebatch *et al.*, 1990; Jenkins *et al.*, 1993; Wills *et al.*, 1995; Czarnecki *et al.*, 2011; Fang *et al.*, 2013;

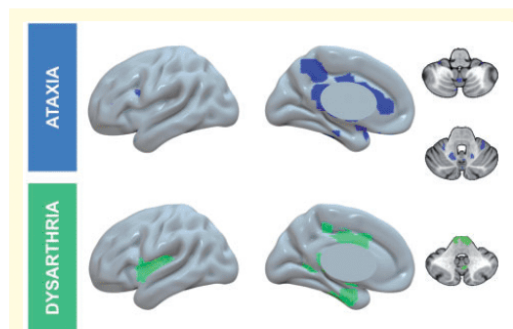
Mueller *et al.*, 2017). Additionally, target connectivity to the aforementioned areas was associated with tremor improvement in VIM-DBS and ablative (thalamotomy) surgeries (Klein *et al.*, 2012; Gibson *et al.*, 2016; Akram *et al.*, 2018; Middlebrooks *et al.*, 2018; Tuleasca *et al.*, 2018a).

Other regions that could potentially play a role based on present findings are primary and associative visual cortices. The importance of brain visual areas in tremor pathogenesis has been recently investigated by using a visual task of increasing difficulty to illustrate the impact of visuospatial network in tremor augmentation (Archer *et al.*, 2018). Furthermore, recent series of investigations suggested that structural and functional changes of the visual cortex could be a preoperative predictor of optimum tremor outcome after ablative radiosurgery (Tuleasca *et al.*, 2017, 2018b, c).

## Somatotopic organization of beneficial DBS connectivity

Finely tuned DBS targeting with respect to the somatotopy of body regions has been considered in dystonia patients (Vayssiere *et al.*, 2004). We leveraged the nature of anatomical somatotopic distributions in order to explain how DBS-related connectivity profile could vary accordingly. Our results demonstrated two distinct connectivity profiles corresponding to hand and head in M1 and cerebellar regions. Crucially, these areas corresponded to formerly determined hand and tongue brain regions in the human M1 homunculus (Penfield and Boldrey, 1937) and cerebellum (Buckner *et al.*, 2011). Furthermore, they predicted

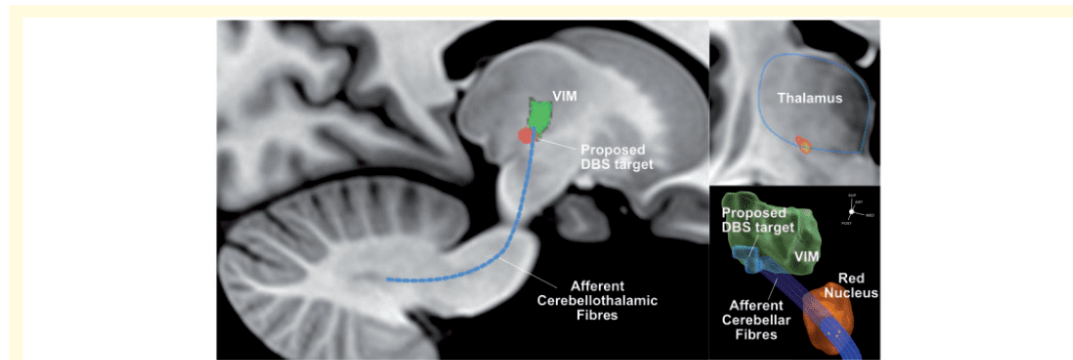
DBS tremor reduction in their respective body regions. Our finding supports the utility of hand and head tremor-driven connectivity profiles in guiding DBS targeting, which could be an important future step for further refinement of DBS treatment of focal motor symptoms. Head tremor is the second most common body distribution of tremor symptoms encountered in essential tremor patients that is highly disabling beside the predominant upper limbs tremor (Hoskovicová *et al.*, 2013; Bhatia *et al.*, 2018). Correspondingly, controlling head tremor has been an outcome issue in many patients undergoing DBS surgery (Obwegeser *et al.*, 2000; Putzke *et al.*, 2005). Our results may pave the way for personalized DBS targeting that is dependent on the tremor symptoms each patient may have. It is even conceivable to scan patients in the functional MRI while they perform (imaginary) tasks involving hand and head to identify their specific somatotopic organization of M1 and the cerebellum. These regions could then be used in single patients to define the tremor target optimally corresponding to their symptomatology.



**Figure 5** Connectivity patterns associated with gait ataxia and dysarthria as representative VIM DBS induced side-effects. Regions highlighted in the figure were associated with occurrence of these commonly encountered side effects ( $P < 0.05$ , uncorrected).

## Connectivity-derived predictive models

The beneficial connectivity profiles that were estimated in the present work were built using a completely data-driven design. This means that these profile maps can be interpreted as an answer to where in the brain connectivity may explain most of the variance in clinical improvement. The concept of using connectivity patterns to predict functional capacity and clinical symptoms has been a central dogma in contemporary studies (Beaty *et al.*, 2018; Cao *et al.*, 2018). We relied on this concept in order to draw conclusions about the optimal connectivity fingerprint that will ensure the best outcome. Of note, connectivity



**Figure 6** Connectivity-defined optimal location for DBS placement in essential tremor patients. (A) Sagittal view of MNI152 space showing VIM (green) and DBS target (red) derived from beneficial connectivity. The location of the proposed target is directly adjacent to the VIM nucleus (postero-inferiorly) in a subthalamic region where afferent cerebellothalamic fibres approach the VIM nucleus. (B) Coronal view showing the spatial relation between the connectivity-based DBS target and the thalamus (ventrolateral location). (C) 3D schematic reconstruction of VIM (green), and red nucleus (red) showing the location of connectivity-based DBS target (yellow) and its intersection with cerebello-thalamic fibres.



associated with the emergence of side effects involved inverse patterns of brain areas compared to beneficial DBS outcome. The cerebellar vermis was shown as a key region in ataxia-related analysis, which is in accordance with previous results (Reich *et al.*, 2016). Our models could significantly predict tremor improvement in out-of-sample data as well as in a single prospective patient using patient-specific diffusion MRI data. Future work should focus on validating such connectivity fingerprints in a larger sample of prospective patients. Furthermore, the isolated discriminative tract emphasized the importance of targeting cerebello-thalamo-cortical pathways for determining DBS outcome (Coenen *et al.*, 2014; Sammartino *et al.*, 2016).

### A connectomic DBS target for essential tremor

The exact DBS target for optimal therapeutic benefit in essential tremor is not yet entirely clear. Four main surgical targets have been suggested for essential tremor treatment. Located within the thalamus, the VIM nucleus has been regarded as the mainstay therapeutic target (Benabid *et al.*, 1991; Pahwa *et al.*, 2006; Zhang *et al.*, 2010; Baizabal-Carvallo *et al.*, 2014), while the other three targets within the subthalamic area (the PSA, which encompasses the caudal zona incerta, the radiatio prelemniscalis and subthalamic nucleus) were the focus of other studies (Herzog *et al.*, 2004; Plaha *et al.*, 2008; Fytogoridis and Blomstedt, 2010). VIM DBS has proven to be an effective tremor target since the beginnings of modern-day DBS (Benabid *et al.*, 1991; Deuschl *et al.*, 2011). On the other hand, there is growing evidence that DBS to the directly adjacent PSA is similarly effective (Plaha *et al.*, 2004, 2011; Fytogoridis *et al.*, 2012; Barbe *et al.*, 2018). Deciding which target is optimal for tremor suppression is a critical step in stereotactic surgery. The results of the present study showed that the discussed targets may in fact be the same—fibres that pass along the red nucleus toward the thalamus and in doing so traverse through the PSA and zona incerta. Structural and functional connectivity maps converged in a region that impinges the inferior-thalamic border and extend to the PSA. Moreover, the proposed DBS spot is located ventrolateral to the thalamus, in an area medial to the internal capsule and directly inferior to the VIM and sensory thalamic nuclei, encroaching on their inferior borders. This area has been described in the literature as the entry of the afferent cerebellar fibres to the thalamus (particularly, the VIM nucleus) (Gallay *et al.*, 2008). Our results further imply the importance of the cerebellothalamic tremor pathway and encourage tract-based targeting for essential tremor treatment (Sammartino *et al.*, 2016; Fenoy and Schiess, 2018). Intriguingly, the identified spot is in accordance with a recently described optimal location for focused ultrasound thalamotomy in essential tremor treatment (Boutet *et al.*,

2018) and with a previously published sweet spot (Papavassiliou *et al.*, 2004).

### Limitations of the study

We used normative connectome data to estimate seed-based connectivity in individual patients. This concept has been introduced for studies in clinical domains such as stroke (Darby *et al.*, 2018; Joutsa *et al.*, 2018a, b), DBS (Fox *et al.*, 2014; Horn *et al.*, 2017b) or transcranial magnetic stimulation (Weigand *et al.*, 2018) where patient-specific connectivity data are often lacking. Although these connectome atlases do not represent patient-specific connectivity, they in turn have the benefit of high signal-to-noise ratios. The functional connectome we used was defined on a high  $n$  (1000 subjects) and was acquired using specialized magnetic resonance hardware (Yeo *et al.*, 2011). In addition, the structural connectome was calculated using a modern approach that was best performer among 10 different tractography processing algorithms in an open competition (Fillard *et al.*, 2011). Finally, this limitation should bias our results toward non-significance to predict out-of-sample data, but instead, the models proved highly robust in cross-validation.

Second, the retrospective design of our study poses a limitation. Needless to say, our exemplary attempt to validate the model on a single case scanned with patient-specific diffusion MRI should only be considered as anecdotal evidence. Despite the good performance of our models in predicting individual outcome, a prospective multicentre study is needed to translate our results into clinical practice. Additionally, our side effects connectivity analysis was based on a small number of patients and did not involve a quantitative assessment of side effects. As a consequence, results did not survive correction for multiple comparisons. Nevertheless, these results could be used to form hypotheses for further studies that may specifically address the connectivity fingerprints of VIM-DBS induced side effects.

Third, interindividual anatomical variability implies another challenge in predicting individual optimal DBS target using an optimal target from a group analysis. Nevertheless, our target was built on a connectome-based model, which emphasizes the importance of targeting structural and functional connectivity between DBS electrode and regions delineated by the predictive models (specifically M1 and the cerebellum).

Lastly, our cohort assumed a single category of tremor syndromes, namely essential tremor. This could be of concern as other tremor syndromes equally benefit from DBS surgery (Kumar *et al.*, 2003; Herzog *et al.*, 2004; Foote *et al.*, 2006; Mandat *et al.*, 2010; Kilbane *et al.*, 2015; Cury *et al.*, 2017). For example, parkinsonian tremor is successfully treated with subthalamic nucleus (Diamond *et al.*, 2007) and VIM (Kumar *et al.*, 2003) DBS. How connectivity patterns of effective DBS therapy could predict tremor reduction across different targets and tremor semiology remains to be established.

## Conclusion

We identified patterns of connectivity that allow us to predict individual clinical outcomes of DBS in essential tremor patients. More specifically, we introduced somatotopic connectivity maps that bear the potential of steering DBS targeting and programming toward patient-specific profiles with respect to the body distribution of symptoms. Finally, we estimated an ‘optimal’ DBS target and set it in relation to known essential tremor-DBS targets. Our target is based on the convergence of beneficial functional and structural connectivity patterns and is available as a probabilistic, deformable atlas that we have made openly available within the Lead-DBS software. Our results add to the ongoing effort of connectivity-based DBS targeting and foster the advance of connectomic surgery.

## Acknowledgements

We would like to thank Igor Ilinsky and Kristy-Kultas Ilinsky (University of Iowa) for their helpful comments on our results. We also thank Wolf-Julian Neumann (Charité – University Medicine Berlin) for his valuable advice and comments.

## Funding

The study is supported by German Research Foundation grants (DFG grant SPP2041 to A.K.K. and Emmy Noether DFG grant 410169619 to A.H.). B.A. is supported by a Doctoral Research Grant from the German Academic Exchange Service - DAAD.

## Competing interests

A.H. reports one-time lecture fee by Medtronic unrelated to the present work. A.A.K. reports personal fees and non-financial support from Medtronic, personal fees from Boston Scientific, personal fees from Ipsen Pharma, grants and personal fees from St. Jude Medical outside the current work. B.A., D.Ku, D.Kr and S.E. have nothing to disclose.

## Supplementary material

Supplementary material is available at *Brain* online.

## References

Akram H, Dayal V, Mahlkecht P, Georgiev D, Hyam J, Foltynic T, et al. Connectivity derived thalamic segmentation in deep brain stimulation for tremor. *NeuroImage Clin* 2018; 18: 130–42.  
Anderson JS, Dhatt HS, Ferguson MA, Lopez-Larson M, Schrock LE, House PA, et al. Functional connectivity targeting for deep brain

stimulation in essential tremor. *Am J Neuroradiol* 2011; 32: 1963–8.  
Archer DB, Coombes SA, Chu WT, Chung JW, Burciu RG, Okun MS, et al. A widespread visually-sensitive functional network relates to symptoms in essential tremor. *Brain* 2018; 141: 472–85.  
Asanuma C, Thach WT, Jones EG. Brainstem and spinal projections of the deep cerebellar nuclei in the monkey, with observations on the brainstem projections of the dorsal column nuclei [review]. *Brain Res Rev* 1983; 5: 299–322.  
Avants B, Epstein C, Grossman M, Gee J. Symmetric diffeomorphic image registration with cross-correlation: evaluating automated labeling of elderly and neurodegenerative brain. *Med Image Anal* 2008; 12: 26–41.  
Baizabal-Carvallo JF, Kagnoff MN, Jimenez-Shahed J, Fekete R, Jankovic J. The safety and efficacy of thalamic deep brain stimulation in essential tremor: 10 years and beyond. *J Neurol Neurosurg Psychiatry* 2014; 85: 567–72.  
Baldermann JC, Melzer C, Zapf A, Kohl S, Timmermann L, Tittgenmeyer M, et al. Connectivity profile predictive of effective deep brain stimulation in obsessive-compulsive disorder. *Biol Psychiatry* 2019; 85: 735–43.  
Barbe MT, Reker P, Hamacher S, Franklin J, Kraus D, Dembek TA, et al. DBS of the PSA and the VIM in essential tremor. *Neurology* 2018; 91: e543–50.  
Basha D, Dostrovsky JO, Lopez Rios AL, Hodaie M, Lozano AM, Hutchison WD. Beta oscillatory neurons in the motor thalamus of movement disorder and pain patients. *Exp Neurol* 2014; 261: 782–90.  
Beatty RE, Kenett YN, Christensen AP, Rosenberg MD, Benedek M, Chen Q, et al. Robust prediction of individual creative ability from brain functional connectivity. *Proc Natl Acad Sci USA* 2018; 115: 1087–92.  
Benabid AL, Pollak P, Hoffmann D, Gervason C, Hommel M, Perret JE, et al. Long-term suppression of tremor by chronic stimulation of the ventral intermediate thalamic nucleus. *Lancet* 1991; 337: 403–6.  
Bhatia KP, Bain P, Bajaj N, Elble RJ, Hallett M, Louis ED, et al. Consensus Statement on the classification of tremors. from the task force on tremor of the International Parkinson and Movement Disorder Society. *Mov Disord* 2018; 33: 75–87.  
Boutet A, Ranjan M, Zohng J, Germann J, Xu D, Schwart ML, et al. Focused ultrasound thalamotomy location determines clinical benefits in patients with essential tremor. *Brain* 2018; 141: 3405–3414.  
Buckner RL, Krienen FM, Castellanos A, Diaz JC, Yeo BT. The organization of the human cerebellum estimated by intrinsic functional connectivity. *J Neurophysiol* 2011; 106: 2322–45.  
Cao H, Chen OY, Chung Y, Forsyth JK, McEwen SC, Gee DG, et al. Cerebello-thalamo-cortical hyperconnectivity as a state-independent functional neural signature for psychosis prediction and characterization. *Nat Commun* 2018; 9: 3836.  
Coenen VA, Allert N, Mädler B. A role of diffusion tensor imaging fiber tracking in deep brain stimulation surgery: DBS of the dentato-rubro-thalamic tract (drt) for the treatment of therapy-refractory tremor. *Acta Neurochir (Wien)* 2011a; 153: 1579–85.  
Coenen VA, Allert N, Paus S, Kronenbürger M, Urbach H, Mädler B. Modulation of the cerebello-thalamo-cortical network in thalamic deep brain stimulation for tremor. *Neurosurgery* 2014; 75: 657–70.  
Coenen VA, Mädler B, Schiffbauer H, Urbach H, Allert N. Individual fiber anatomy of the subthalamic region revealed with diffusion tensor imaging: a concept to identify the deep brain stimulation target for tremor suppression. *Neurosurgery* 2011b; 68: 1069–76.  
Coenen VA, Varkuti B, Parpaley Y, Skodda S, Prokop T, Urbach H, et al. Postoperative neuroimaging analysis of DRT deep brain stimulation revision surgery for complicated essential tremor. *Acta Neurochir (Wien)* 2017; 159: 779–87.  
Colebatch J, Findley LJ, Frackowiak RS, Marsden CD, Brooks DJ. Preliminary report: activation of the cerebellum in essential tremor. *Lancet* 1990; 336: 1028–30.

- Cury RG, Fraix V, Castrioto A, Pérez Fernández MA, Krack P, Chabardes S, et al. Thalamic deep brain stimulation for tremor in Parkinson disease, essential tremor, and dystonia. *Neurology* 2017; 89: 1416–23.
- Czarnecki K, Jones DT, Burnett MS, Mullan B, Matsumoto JY. SPECT perfusion patterns distinguish psychogenic from essential tremor. *Parkinsonism Relat Disord* 2011; 17: 328–32.
- Darby RR, Horn A, Cushman F, Fox MD. Lesion network localization of criminal behavior. *Proc Natl Acad Sci USA* 2018; 115: 601–6.
- Deuschl G, Bain P, Brin M. Consensus statement of the Movement Disorder Society on Tremor. *Ad Hoc Scientific Committee. Mov Disord* 1998; 13: 2–23.
- Deuschl G, Raethjen J, Hellriegel H, Elble R. Treatment of patients with essential tremor [review]. *Lancet Neurol* 2011; 10: 148–61.
- Deuschl G, Wenzelburger R, Löffler K, Raethjen J, Stolze H. Essential tremor and cerebellar dysfunction clinical and kinematic analysis of intention tremor. *Brain* 2000; 123: 1568–80.
- Diamond A, Shahed J, Jankovic J. The effects of subthalamic nucleus deep brain stimulation on parkinsonian tremor. *J Neurol Sci* 2007; 260: 199–203.
- Eisinger RS, Wong J, Almeida L, Ramirez-Zamora A, Cagle JN, Giugni JC, et al. Ventral intermediate nucleus versus zona incerta region deep brain stimulation in essential tremor. *Mov Disord Clin Pract* 2018; 5: 75–82.
- Fahn S, Tolosa E, Conception M. Clinical rating scale for tremor In: Jankovic J, Tolosa E, editors. *Parkinson's disease and movement disorders*. Baltimore, MD: Williams and Wilkins; 1993. p. 271–80.
- Fang W, Chen H, Wang H, Zhang H, Puneet M, Liu M, et al. Essential tremor is associated with disruption of functional connectivity in the ventral intermediate Nucleus-Motor Cortex-Cerebellum circuit. *Hum Brain Mapp* 2016; 37: 165–78.
- Fang W, Lv F, Luo T, Cheng O, Liao W, Sheng K, et al. Abnormal regional homogeneity in patients with essential tremor revealed by resting-state functional MRI. *PLoS One* 2013; 8: e69199.
- Fenoy AJ, Schiess MC. Comparison of tractography-assisted to atlas-based targeting for deep brain stimulation in essential tremor. *Mov Disord* 2018; 33: 1–7.
- Fillard P, Descoteaux M, Goh A, Gouttard S, Jeurissen B, Malcol J, et al. Quantitative evaluation of 10 tractography algorithms on a realistic diffusion MR phantom. *Neuroimage* 2011; 56: 220–34.
- Flora ED, Perera CL, Cameron AL, Maddern GJ. Deep brain stimulation for essential tremor: a systematic review. *Mov Disord* 2010; 25: 1550–9.
- Fox MD, Buckner RL, Liu H, Chakravarty MM, Lozano AM, Pascual-Leone A, et al. Resting-state networks link invasive and noninvasive brain stimulation across diverse psychiatric and neurological diseases. *Proc Natl Acad Sci USA* 2014; 111: E4367–75.
- Foote KD, Seignourel P, Fernandez HH, Romrell J, Whidden E, Jacobson C, et al. Dual electrode thalamic deep brain stimulation for the treatment of posttraumatic and multiple sclerosis tremor. *Neurosurgery* 2006; 58: 280–5.
- Fytogoridis A, Blomstedt P. Complications and side effects of deep brain stimulation in the posterior subthalamic area. *Stereotact Funct Neurosurg* 2010; 88: 88–93.
- Fytogoridis A, Sandvik U, Åström M, Bergenheim T, Blomstedt P. Long term follow-up of deep brain stimulation of the caudal zona incerta for essential tremor. *J Neurol Neurosurg Psychiatry* 2012; 83: 258–62.
- Gallay MN, Jeanmonod D, Liu J, Morel A. Human pallidothalamic and cerebellothalamic tracts: anatomical basis for functional stereotactic neurosurgery. *Brain Struct Funct* 2008; 212: 443–63.
- Gibson WS, Jo HJ, Testini P, Cho S, Felmler JP, Welker KM, et al. Functional correlates of the therapeutic and adverse effects evoked by thalamic stimulation for essential tremor. *Brain* 2016; 139: 2198–210.
- Haber SN, Calzavara R. The cortico-basal ganglia integrative network: the role of the thalamus. *Brain Res Bull* 2009; 16;78: 69–74.
- Hamel W, Herzog J, Kopper F, Pinsker M, Weinert D, Müller D, et al. Deep brain stimulation in the subthalamic area is more effective than nucleus ventralis intermedius stimulation for bilateral intention tremor. *Acta Neurochir (Wien)* 2007; 149: 749–58.
- Hellwig B, Häußler S, Schelter B, Lauk M, Guschlbauer B, Timmer J, et al. Tremor-correlated cortical activity in essential tremor. *Lancet* 2001; 357: 519–23.
- Helmich RC, Toni I, Deuschl G, Bloem BR. The pathophysiology of essential tremor and parkinson's tremor [review]. *Curr Neurol Neurosci Rep* 2013; 13: 378.
- Herzog J, Fietzek U, Hamel W, Morsnowski A, Steigerwald F, Schrader B, et al. Most effective stimulation site in subthalamic deep brain stimulation for Parkinson's disease. *Mov Disord* 2004; 19: 1050–4.
- Horn A. A structural group-connectome in standard stereotactic (MNI) space. *Data Brief* 2015; 5: 292–6.
- Horn A, Blankenburg F. Toward a standardized structural-functional group connectome in MNI space. *Neuroimage* 2016; 124: 310–22.
- Horn A, Kühn AA. Lead-DBS: a toolbox for deep brain stimulation electrode localizations and visualizations. *Neuroimage* 2015; 107: 127–35.
- Horn A, Kühn AA, Merkl A, Shih L, Alterman R, Fox M. Probabilistic conversion of neurosurgical DBS electrode coordinates into MNI space. *Neuroimage* 2017a; 150: 395–404.
- Horn A, Li N, Dembek TA, Kappel A, Boulay C, Ewert S, et al. Lead-DBS v2: towards a comprehensive pipeline for deep brain stimulation imaging. *Neuroimage* 2018; 184: 293–316.
- Horn A, Ostwald D, Reisert M, Blankenburg F. The structural-functional connectome and the default mode network of the human brain. *Neuroimage* 2014; 102: 142–51.
- Horn A, Reich M, Vorwerk J, Li N, Wenzel G, Fang Q, et al. Connectivity predicts deep brain stimulation outcome in Parkinson disease. *Ann Neurol* 2017b; 82: 67–78.
- Hoskovicová M, Ulmanová O, Šprdlík O, Sieger T, Nováková J, Jech R, et al. Disorders of balance and gait in essential tremor are associated with midline tremor and age. *Cerebellum* 2013; 12: 27–34.
- Jenkins IH, Bain PG, Colebatch JG, Thompson PD, Findley LJ, Frackowiak RSJ, et al. A positron emission tomography study of essential tremor: evidence for overactivity of cerebellar connections. *Ann Neurol* 1993; 34: 82–90.
- Joutsa J, Horn A, Hsu J, Fox MD. Localizing parkinsonism based on focal brain lesions. *Brain* 2018a; 141: 2445–56.
- Joutsa J, Shih LC, Horn A, Reich MM, Wu O, Rost NS, et al. Identifying therapeutic targets from spontaneous beneficial brain lesions. *Ann Neurol* 2018b; 84: 153–7.
- Kilbane C, Ramirez-Zamora A, Ryapolova-Webb E, Qasim S, Glass GA, Starr PA, et al. Pallidal stimulation for Holmes tremor: clinical outcomes and single-unit recordings in 4 cases. *J Neurosurg* 2015; 122: 1306–14.
- Klein JC, Barbe MT, Seifried C, Baudrexel S, Runge M, Maarouf M, et al. The tremor network targeted by successful VIM deep brain stimulation in humans. *Neurology* 2012; 78: 787–95.
- Kumar R, Lozano AM, Sime E, Lang AE. Long-term follow-up of thalamic deep brain stimulation for essential and parkinsonian tremor. *Neurology* 2003; 61: 1601–4.
- Mandat T, Koziara H, Tutaj M, Rola R, Bonicki W, Nauman P. Thalamic deep brain stimulation for tremor among multiple sclerosis patients. *Neurol Neurochir Pol* 2010; 44: 542–5.
- Marsden JF, Ashby P, Limousin-Dowsey P, Rothwell JC, Brown P. Coherence between cerebellar thalamus, cortex and muscle in man: cerebellar thalamus interactions. *Brain* 2000; 123: 1459–70.
- McAuley JH, Marsden CD. Physiological and pathological tremors and rhythmic central motor control [review]. *Brain* 2000; 123: 1545–67.
- McFarland NR, Haber SN. Thalamic relay nuclei of the basal ganglia form both reciprocal and nonreciprocal cortical connections, linking

- multiple frontal cortical areas [review]. *J Neurosci* 2002; 22: 8117–32.
- Middlebrooks EH, Tuna IS, Almeida L, Grewal SS, Wong J, Heckman MG, et al. Structural connectivity-based segmentation of the thalamus and prediction of tremor improvement following thalamic deep brain stimulation of the ventral intermediate nucleus. *NeuroImage Clin* 2018; 20: 1266–73.
- Milosevic L, Kalia SK, Hodaie M, Lozano AM, Popovic MR, Hutchison WD. Physiological mechanisms of thalamic ventral intermediate nucleus stimulation for tremor suppression. *Brain* 2018; 141: 2142–55.
- Mueller K, Jech R, Hoskovicová M, Ulmanová O, Urgošik D, Vymazal J, et al. General and selective brain connectivity alterations in essential tremor: a resting state fMRI study. *NeuroImage Clin* 2017; 16: 468–76.
- Obwegeser AA, Uitti RJ, Turk MF, Strongosky AJ, Wharen RE. Thalamic stimulation for the treatment of midline tremors in essential tremor patients. *Neurology* 2000; 54: 2342–4.
- Pahwa R, Lyons KE, Wilkinson SB, Simpson RK, Ondo WG, Tarsy D, et al. Long-term evaluation of deep brain stimulation of the thalamus. *J Neurosurg* 2006; 104: 506–12.
- Papavassiliou E, Rau G, Heath S, Abosch A, Barbaro NM, Larson PS, et al. Thalamic deep brain stimulation for essential tremor: relation of lead location to outcome. *Neurosurgery* 2004; 54: 1120–29.
- Pedrosa DJ, Reck C, Florin E, Pauls KAM, Maarouf M, Wojtecki L, et al. Essential tremor and tremor in Parkinson's disease are associated with distinct 'tremor clusters' in the ventral thalamus. *Exp Neurol* 2012; 237: 435–43.
- Penfield W, Boldrey E. Somatic motor and sensory representation in the cerebral cortex of man as studied by electrical stimulation. *Brain* 1937; 60: 389–443.
- Pinto AD, Lang AE, Chen R. The cerebellothalamocortical pathway in essential tremor. *Neurology* 2003; 60: 1985–7.
- Plaha P, Javed S, Agombar D, O'Farrell G, Khan S, Whone A, et al. Bilateral caudal zona incerta nucleus stimulation for essential tremor: outcome and quality of life. *J Neurol Neurosurg Psychiatry* 2011; 82: 899–904.
- Plaha P, Khan S, Gill SS. Bilateral stimulation of the caudal zona incerta nucleus for tremor control. *J Neurol Neurosurg Psychiatry* 2008; 79: 504–13.
- Plaha P, Patel NK, Gill SS. Stimulation of the subthalamic region for essential tremor. *J Neurosurg* 2004; 101: 48–54.
- Pouratian N, Zheng Z, Bari AA, Behnke E, Elias WJ, Desalles AAF. Multi-institutional evaluation of deep brain stimulation targeting using probabilistic connectivity-based thalamic segmentation. *J Neurosurg* 2011; 115: 995–1004.
- Putzke JD, Uitti RJ, Obwegeser AA, Wszolek ZK, Wharen RE. Bilateral thalamic deep brain stimulation: midline tremor control. *J Neurol Neurosurg Psychiatry* 2005; 76: 684–90.
- Raethjen J, Deuschl G. The oscillating central network of Essential tremor [review]. *Clin Neurophysiol* 2012; 123: 61–4.
- Reich MM, Brumberg J, Pozzi NG, Marotta G, Roothans J, Åström M, et al. Progressive gait ataxia following deep brain stimulation for essential tremor: adverse effect or lack of efficacy? *Brain* 2016; 139: 2948–56.
- Reisert M, Mader I, Anastasopoulos C, Weigel M, Schnell S, Kiselev V. Global fiber reconstruction becomes practical. *Neuroimage* 2011; 54: 955–62.
- Sammartino F, Krishna V, King NKK, Lozano AM, Schwartz ML, Huang Y, et al. Tractography-based ventral intermediate nucleus targeting: novel methodology and intraoperative validation. *Mov Disord* 2016; 31: 1217–225.
- Sandvik U, Koskinen L-O, Lundquist A, Blomstedt P. Thalamic and subthalamic deep brain stimulation for essential tremor. *Neurosurgery* 2012; 70: 840–6.
- Schnitzler A, Münks C, Butz M, Timmermann L, Gross J. Synchronized brain network associated with essential tremor as revealed by magnetoencephalography. *Mov Disord* 2009; 24: 1629–35.
- Sharifi S, Nederveen AJ, Booi J, van Rootselaar A-F. Neuroimaging essentials in essential tremor: a systematic review [review]. *NeuroImage Clin* 2014; 5: 217–31.
- Tasker RR. Deep brain stimulation is preferable to thalamotomy for tremor suppression. *Surg Neurol* 1998; 49: 145–54.
- Tuleasca C, Najdenovska E, Régis J, Witjas T, Girard N, Champoudry J, et al. Pretherapeutic functional neuroimaging predicts tremor arrest after thalamotomy. *Acta Neurol Scand* 2018a; 137: 500–8.
- Tuleasca C, Najdenovska E, Régis J, Witjas T, Girard N, Champoudry J, et al. Clinical response to Vim's thalamic stereotactic radiosurgery for essential tremor is associated with distinctive functional connectivity patterns. *Acta Neurochir (Wien)* 2018b; 160: 611–24.
- Tuleasca C, Witjas T, Najdenovska E, Verger A, Girard N, Champoudry J, et al. Assessing the clinical outcome of Vim radiosurgery with voxel-based morphometry: visual areas are linked with tremor arrest! *Acta Neurochir (Wien)* 2017; 159: 2139–44.
- Tuleasca C, Witjas T, Van de Ville D, Najdenovska E, Verger A, Girard N, et al. Right Brodmann area 18 predicts tremor arrest after Vim radiosurgery: a voxel-based morphometry study. *Acta Neurochir (Wien)* 2018c; 160: 603–9.
- Vayssiere N, van der Gaag N, Cif L, Hemm S, Verdier R, Frerebeau P, et al. Deep brain stimulation for dystonia confirming a somatotopic organization in the globus pallidus internus. *J Neurosurg* 2004; 101: 181–8.
- Weigand A, Horn A, Caballero R, Cooke D, Stern AP, Taylor SF, et al. Prospective validation that subgenual connectivity predicts antidepressant efficacy of transcranial magnetic stimulation sites. *Biol Psychiatry* 2018; 84: 28–37.
- Wills AJ, Jenkins LH, Thompson PD, Findley LJ, Brooks DJ. A Positron emission tomography study of cerebral activation associated with essential and writing tremor. *Arch Neurol* 1995; 52: 299–305.
- Yamada K, Akazawa K, Yuen S, Goto M, Matsushima S, Takahata A, et al. MR Imaging of ventral thalamic nuclei. *Am J Neuroradiol* 2010; 31: 732–5.
- Yeo BY, Krienen FM, Sepulcre J, Sabuncu MR, Lashkari D, Hollinshead M, et al. The organization of the human cerebral cortex estimated by intrinsic functional connectivity. *J Neurophysiol* 2011; 106: 1125–65.
- Zhang K, Bhatia S, Oh MY, Cohen D, Angle C, Whiting D. Long-term results of thalamic deep brain stimulation for essential tremor. *J Neurosurg* 2010; 112: 1271–6.



# A neural network for tics: insights from causal brain lesions and deep brain stimulation

Christos Ganos,<sup>1,†</sup> Bassam Al-Fatly,<sup>1,†</sup> Jan-Frederik Fischer,<sup>1</sup> Juan-Carlos Baldermann,<sup>2,3</sup> Christina Hennen,<sup>2</sup> Veerle Visser-Vandewalle,<sup>4</sup> Clemens Neudorfer,<sup>1</sup> Davide Martino,<sup>5,6</sup> Jing Li,<sup>7</sup> Tim Bouwens,<sup>8</sup> Linda Ackermanns,<sup>8</sup> Albert F. G. Leentjens,<sup>9</sup> Nadya Pyatigorskaya,<sup>10</sup> Yulia Worbe,<sup>11</sup> Michael D. Fox,<sup>7,12</sup> Andrea A. Kühn<sup>1,†</sup> and Andreas Horn<sup>1,7,†</sup>

<sup>†</sup>These authors contributed equally to this work.

Brain lesions are a rare cause of tic disorders. However, they can provide uniquely causal insights into tic pathophysiology and can also inform on possible neuromodulatory therapeutic targets. Based on a systematic literature review, we identified 22 cases of tics causally attributed to brain lesions and employed 'lesion network mapping' to interrogate whether tic-inducing lesions would be associated with a common network in the average human brain. We probed this using a normative functional connectome acquired in 1000 healthy participants. We then examined the specificity of the identified network by contrasting tic-lesion connectivity maps to those seeding from 717 lesions associated with a wide array of neurological and/or psychiatric symptoms within the Harvard Lesion Repository. Finally, we determined the predictive utility of the tic-inducing lesion network as a therapeutic target for neuromodulation. Specifically, we collected retrospective data of 30 individuals with Tourette disorder, who underwent either thalamic ( $n = 15$ ; centromedian/ventrooralis internus) or pallidal ( $n = 15$ ; anterior segment of globus pallidus internus) deep brain stimulation and calculated whether connectivity between deep brain stimulation sites and the lesion network map could predict clinical improvements.

Despite spatial heterogeneity, tic-inducing lesions mapped to a common network map, which comprised the insular cortices, cingulate gyrus, striatum, globus pallidus internus, thalami and cerebellum. Connectivity to a region within the anterior striatum (putamen) was specific to tic-inducing lesions when compared with control lesions. Connectivity between deep brain stimulation electrodes and the lesion network map was predictive of tic improvement, regardless of the deep brain stimulation target.

Taken together, our results reveal a common brain network involved in tic generation, which shows potential as a therapeutic target for neuromodulation.

- 1 Charité – Universitätsmedizin Berlin, corporate member of Freie Universität Berlin and Humboldt-Universität zu Berlin, Movement Disorders and Neuromodulation Unit, Department of Neurology with Experimental Neurology, 10117 Berlin, Germany
- 2 Department of Psychiatry and Psychotherapy, Faculty of Medicine and University Hospital Cologne, University of Cologne, 50931 Cologne, Germany
- 3 Department of Neurology, Faculty of Medicine and University Hospital Cologne, University of Cologne, 50931 Cologne, Germany
- 4 Department of Stereotactic and Functional Neurosurgery, Faculty of Medicine and University Hospital Cologne, University of Cologne, 50931 Cologne, Germany
- 5 Department of Clinical Neurosciences, University of Calgary, Calgary 3330, AB, Canada

Received September 7, 2021. Revised November 14, 2021. Accepted December 16, 2021. Advance access publication January 13, 2022

© The Author(s) 2022. Published by Oxford University Press on behalf of the Guarantors of Brain. All rights reserved. For permissions, please e-mail: [journals.permissions@oup.com](mailto:journals.permissions@oup.com)

- 6 Hotchkiss Brain Institute, Calgary 3330, AB, Canada  
 7 Center for Brain Circuit Therapeutics, Department of Neurology, Psychiatry, and Radiology, Brigham and Women's Hospital, Harvard Medical School, Boston, MA 02115, USA  
 8 Department of Neurosurgery, Maastricht University Medical Centre, 6229 HX Maastricht, The Netherlands  
 9 Department of Psychiatry, Maastricht University Medical Centre, 6229 HX Maastricht, The Netherlands  
 10 Sorbonne University, Paris Brain Institute - ICM, Inserm, CNRS, Department of Radiology, Hôpital de la Pitié Salpêtrière (DMU 6), AP-HP, 75013, Paris, France  
 11 Sorbonne University, ICM, Inserm, CNRS, Department of Neurophysiology, Hôpital Saint Antoine (DMU 6), AP-HP, 75013 Paris, France  
 12 Athinoula A. Martinos Centre for Biomedical Imaging, Department of Neurology and Radiology, Massachusetts General Hospital, Charlestown, MA 02129, USA

Correspondence to: Andreas Horn  
 Movement Disorders and Neuromodulation Unit  
 Department of Neurology  
 Charité University Medicine Berlin  
 Charitéplatz 1, 10117 Berlin, Germany  
 E-mail: andreas.horn@charite.de

**Keywords:** brain lesions; tic disorders; lesion network mapping; deep brain stimulation

## Introduction

Tics are brief and sudden movements or sounds that resemble voluntary actions but occur repetitively and without embedment to discernible context.<sup>1</sup> Tics may have multiple aetiologies, but they are most encountered as part of a neurodevelopmental disorder spectrum, including Tourette disorder, which affects ~1% of children. There has been a long-standing debate about the pathophysiological underpinnings of tics and in the past few decades there have been numerous efforts to identify the neuronal locus—or network—that leads to their emergence.<sup>2,3</sup>

The basal ganglia have been suggested as key neuronal structures in tic genesis.<sup>4</sup> This was driven by neuropathological studies, which identified abnormalities within motor and associative functional domains of the striatum and globus pallidus internus (GPi),<sup>5,6</sup> and therapeutic interventions, such as deep brain stimulation (DBS) that targeted these areas. Building on ablational studies by Hassler and Dieckmann,<sup>7</sup> a first report on a patient treated with DBS targeting the border between centromedian and ventrooralis internus nuclei of the thalamus (CM-Voi) was published in 1999.<sup>8</sup> Since then, DBS targeting (i) this target<sup>9,10</sup>, (ii) the anterior versus posterior ventrooralis nuclei in Hassler nomenclature<sup>11</sup> (or ventroanterior/ventrolateral thalamus according to Jones nomenclature<sup>12</sup>); (iii) the anteromedial<sup>13,14</sup>; and (iv) the posteroventral<sup>15</sup> GPi has been demonstrated to effectively reduce tics. More recently low-frequency tic-related neuronal activity was recorded in GPi and CM-Voi in Tourette patients undergoing DBS suggesting an electrophysiological correlate in tic pathophysiology.<sup>16,17,18</sup>

Outside the basal ganglia, cortical neurophysiology studies have implicated the supplementary motor area and primary motor cortex in tic occurrence.<sup>17–19,20,21,22</sup> Structural and functional neuroimaging studies further revealed an extensive network of additional brain areas involved in the generation of tics (reviewed by Martino *et al.*<sup>23</sup>), including the prefrontal and cingulate cortices,<sup>24,25,26</sup> the primary somatosensory area,<sup>24,25–27,28,29,30</sup> the parietal operculum<sup>31,32</sup> and the insula.<sup>27–31,32,33</sup>

These and other studies suggest that tics are not the result of a single dysfunctional brain region, but rather emerge in consequence of critical alterations at different cortical and subcortical hubs within a widespread neural circuit.<sup>24–34</sup> However, a causal

role of different brain regions for tic generation remains elusive. Moreover, while some regions described in functional (correlative) studies may contribute to tic expression, others could indeed be involved in symptom compensation.

Studies of brain lesions and brain stimulation results are among the few general concepts that may justify causal inference.<sup>35</sup> More recently, it has become possible to map the impact of specific lesions on distributed 'brain networks'. The technique, termed 'lesion network mapping'<sup>36</sup> uses normative functional connectomes acquired in large samples of healthy participants to investigate into which network a specific lesion would fall in the average human brain. So far, the method has provided insights into different neuropsychiatric symptoms,<sup>35</sup> including movement disorders<sup>37,38,39</sup> and disorders of volition.<sup>40,41</sup> In a similar vein, a novel concept termed 'DBS network mapping' has applied the same concept to stimulation sites.<sup>42</sup> Again, the method asks the question of which functional brain network a specific DBS stimulation site would fall within the average human brain. So far, the method has provided insights into effective neuromodulation networks in neurological disorders of movement<sup>42,43,44</sup> and psychiatric disorders.<sup>45,46</sup> Importantly, several papers have shown that both lesion and DBS network mapping provide convergent results, as for example in parkinsonism,<sup>38</sup> dystonia<sup>39</sup> and depression.<sup>47</sup>

The aim of this study was to shed light onto the networks associated with tic generation using combined brain lesion and DBS network mapping. To this end, we carried out a systematic review of the medical literature to collect brain lesions that were involved in the occurrence of tics and determined the common functional network underlying most lesions. To assess the therapeutic relevance of this network, we predicted clinical outcomes in patients with Tourette disorder who received therapeutic DBS (either in the CM-Voi of thalamus or GPi) from three different centres (Cologne, Paris and Maastricht).

## Materials and methods

### Cases and lesion definition

Methods of the review were developed by two members of the author team (C.G., J.F.F.) prior to conducting the review. In March 2020

PubMed (MEDLINE 1966–2020) and EMBASE (1947–2020) were searched with a combination of free-text, MeSH terms, and truncated words (Supplementary material). To be included, papers needed to meet predefined inclusion criteria: (i) English reports; describing (ii) patients (case reports, case series, letters and observational studies); with (iii) new-onset tics; attributed to (iv) lesions of the CNS; and (v) lesion location shown by neuroimaging that was further described in writing. After removal of duplicates results were screened by title and abstract. The first 50 abstracts were screened by two reviewers (J.F.F., C.G.) to control for interpersonal agreement and subsequent results were screened by one author (J.F.F.). Eligible, and available records were then read in full text subsequently. If the single reviewer had questions about the potential full-text inclusion of an article, the full text was then reviewed with the first author (C.G.) for discussion. Risk of bias assessment was not applicable. Details on the number of results and the process of literature search are listed in Supplementary Fig. 1. We did not apply a temporal restriction criterion between the clinical manifestation of tics and the documentation of brain lesions to capture as many different aetiologies as possible. In cases where the manifestation of tics was the only clinical event associated with a brain lesion, we captured the latency between the two. In all other cases, where an additional clinical syndrome preceded the onset of tics and was attributed to documented brain damage, we captured the time lag between this event, tic behaviours and lesion confirmation. We excluded reports about 'tic-like' phenomena, which may subsume functional tic disorders or overlap syndromes, as well as drug-induced tics and cases of tics associated with traumatic events of the peripheral nervous system. Reports of tic improvement associated with brain lesions (e.g. through neurosurgery) were not considered. Cases with characteristic brain malformations associated with known, mostly neurodevelopmental, genetic syndromes and tic disorders were also excluded. Review articles were included for cross-referencing in the first step.

From the included reports we extracted the following data: (i) study characteristics (study type, year of publication); (ii) patient characteristics (age of assessment, sex, medical history, type of clinical event and age at time of occurrence); (iii) clinical characteristics of tics (predisposing factors, pre-existing tics and their characteristics, latency between first confirmation of lesions and tic onset/worsening, motor/vocal forms, tic somatotopy, suppressibility/premonitory urges, waxing and waning course, neuropsychiatric comorbidities, therapeutic strategy and outcome and additional video documentation); and (iv) characteristics of documented brain lesion (attributed aetiology, anatomical localization and modality of neuroimaging, age at confirmation of lesion).

Lesion locations were identified from corresponding publication figures and manually traced using 3D Slicer (www.slicer.org) on a common T<sub>1</sub> template available within ICBM2009b NLIN Asym ('MNI') space.

### Lesion network mapping

Each binary lesion mask was entered as a seed using the Lead connectome mapper toolbox openly available within Lead-DBS (www.lead-dbs.org<sup>48</sup>). Seed-based connectivity was calculated using a normative functional MRI connectome acquired at rest in 1000 participants<sup>49</sup> that had been preprocessed as described elsewhere.<sup>50</sup> For each subject in the connectome, blood oxygen level-dependent (BOLD) signal fluctuations across all voxels within the lesion mask were averaged and correlated to the BOLD signal of all other brain voxels using the Pearson correlation coefficient. This resulted in

1000 R-values for each brain voxel (one per subject) which were Fisher z-transformed. Using voxel-wise one-sample T-tests, these 1000 z-values were summed up to an average connectivity profile map of T-scores. We will refer to this map as the T-map. Every lesion specific T-map was then thresholded to a T-score of 7 and binarized to represent the significant positive T-scores in each T-map. This threshold level was chosen based on previous experience in multiple lesion network mapping publications (see Cohen and Fox<sup>51</sup> for a discussion). Choosing a range of different thresholds largely did not alter the overall pattern of the result (Supplementary Fig. 2). In a next step, all lesion-specific binarized T-maps ( $n=22$ ) were summed up into a single N-map which represented a tic-inducing lesion network map (LNM). The LNM was then thresholded to include only voxels that received contribution from  $\geq 19/22$  lesions (86% of cases). This threshold was chosen upon visual inspection and the number of retained voxels, to define a set of regions most specifically connected to a maximum number of lesion cases (higher thresholds  $>20$  or  $>21$  retained little to no voxels, see Supplementary Fig. 3 for results with different thresholds).

### Specificity of tic lesion network

We then aimed to explore whether specific sites within the tic-lesion network were not only sensitive but also specific to tics compared to other naturally occurring brain lesions. In order to do so, connectivity T-maps derived from tic-inducing lesions were compared to the ones from a total of 717 other brain lesions from the Harvard Lesion Repository.<sup>35</sup> This repository contains lesions associated with various neurological and/or psychiatric symptoms which are (numbers indicate lesion counts in each specific category): Akinetic Mutism, 28; Alien Limb, 53; Amnesia, 53; Aphasia, 12; Asterixis, 30; Cervical Dystonia, 25; Criminality, 17; Delusions, 32; Depression, 58; Freezing of gait, 14; Hemichorea 29, Hallucination: 89, Holmes' tremor, 36; Infantile Spasms, 74; Loss of consciousness, 16; Mania, 56; Pain, 22; Parkinsonism, 29; Prosopagnosia, 44. The specificity map was calculated using a voxel-wise permutation-based two-sample T-test performed (with 1000 permutations) within FSL PALM (https://fsl.fmrib.ox.ac.uk/fsl/fslwiki/Randomise/UserGuide). A rigorous voxel-wise family-wise error (FWE) correction was then applied at  $\alpha < 0.05$  to reduce false positive results<sup>52</sup> and highlight only the significant findings. Based on these results, we subsequently computed a 'conjunction map', on which voxels that were both specific and sensitive to tics were retained by multiplying the sensitivity (lesion network) map and the specificity map.

### Relationship to DBS treatment

In a further step, we sought to investigate the relevance and potential clinical utility of the tic-inducing lesion network. We tested whether specific stimulation sites in a retrospective cohort of Tourette disorder patients treated with DBS that were maximally connected to the lesion network map would be associated with optimal outcomes. Pre- and postoperative imaging data from a total of 30 adult patients from three DBS centres with a diagnosis of Tourette disorder that underwent DBS surgery were used to localize DBS electrodes and specify stimulation sites in each patient.

Fifteen adult patients with Tourette disorder underwent DBS to thalamus nuclei (Cologne cohort;  $n=12$  in the centromedian-ventro-oralis and  $n=3$  in the nucleus ventroanterior/ventrolateral nucleus with the most distal contacts residing in the field of Forel/subthalamic nucleus) and 15 to the GPi (Paris and

Maastricht cohorts). Localization of electrodes and estimation of stimulation volumes were carried out using Lead-DBS software ([www.lead-dbs.org](http://www.lead-dbs.org))<sup>48</sup>. We applied default parameters of the revised pipeline.<sup>53</sup> Briefly, this involved co-registration between post-operative MRI ( $n = 2$ ) or CT ( $n = 28$  patients) to preoperative anatomical MRIs using advanced normalization tools (ANTs; <http://stnava.github.io/ANTs/>)<sup>54</sup>. The resulting co-registered images were then normalized to MNI space using the ANTs SyN Symmetric Diffeomorphic algorithm<sup>54</sup> using the 'effective: low variance + sub-cortical refinement' preset in Lead-DBS. Electrodes were reconstructed using the PaCER<sup>55</sup> algorithm and manually refined, if necessary. Stimulation volumes were estimated using a finite element approach based on a four-compartment tetrahedral mesh (including white or grey matter, electrode insulating and conducting regions).<sup>53</sup> The estimated E-field was thresholded to a heuristic value of 0.2 V/mm to calculate the extent of a binary volume. These were then used as seed regions to calculate functional connectivity average T-scores, representing average connectivity strength, to voxels within the tic-inducing lesion network. T-scores were z-transformed to a Gaussian distribution following the approach of van Albada et al.<sup>56</sup> to serve as predictors of DBS associated tic-improvements.

In a last step, we sought to investigate how connectivity strength from stimulation sites of DBS cohorts to both sensitive and specific voxels of the maps, and their overlap (conjunction map) could explain tic-improvement. Similar to the analysis above, connectivity strength was again calculated between DBS stimulation sites and the respective map. These coefficients were then correlated to tic-improvement.

### DBS network mapping

In a final analysis, we aimed at characterizing the networks optimally modulated by each DBS site in a data-driven fashion. To do so, we applied DBS network mapping following the approach by Horn et al.,<sup>42</sup> which follows a highly similar logic as the lesion network mapping approach. Briefly, DBS network maps were calculated in identical fashion to lesion network maps. We then correlated connectivity strength in each voxel with tic improvements, across patients, resulting in R-map models that approximate optimal connectivity profiles. Voxels with high values on these maps embody locations to which DBS electrodes that led to optimal improvement were strongly connected. We calculated these R-map models for each target cohort separately (pallidal and thalamic target). In a second step, we multiplied resulting maps with each other, but only retaining voxels that were positive on both maps. In doing so, we were able to pinpoint the network from two angles (pallidal and thalamic DBS sites). Therefore, this approach would likely clean the result from some spurious correlations and retain a higher fraction of regions that could indeed have causal implications.<sup>57</sup>

### Data availability

The DBS MRI/CT datasets generated and analysed during the current study are not publicly available due to data privacy regulations of patient data but are available from the corresponding author upon reasonable request. Lesion network map and code used to analyse the datasets is available within Lead-DBS/Connectome software (<https://github.com/leaddbs/leaddbs>).

## Results

The systematic review (see [Supplementary Fig. 1](#) for flow chart) identified 22 cases with new onset of tics attributed to brain lesions ([Supplementary Table 1](#)). The mean age at tic onset was 25.3 years [ $\pm 20.7$  standard deviation (SD), range 5–73 y; in two cases tic-onset age was not provided]. In 12 cases, the latency between brain injury and tic onset could be reconstructed ([Supplementary Table 1](#)). There were two cases with isolated motor tics and two with isolated vocal tics. The remaining 18 cases had both motor and vocal tics. Premonitory urges and tic suppressibility were documented in 10 and 12 cases, respectively. In 10 cases, additional movement disorders were also noted, including dystonia ( $n = 4$ ), parkinsonism ( $n = 3$ ), cerebellar ataxia ( $n = 2$ ), tremor ( $n = 1$ ) and stereotypies ( $n = 1$ ). However, again, in these cases occurrence of tics was salient and novel following the brain lesion. Neuropsychiatric features, such as impulsivity and/or hyperactivity ( $n = 9$ ), obsessive-compulsive ( $n = 5$ ) and self-injurious behaviours ( $n = 3$ ) were also reported.

Although the basal ganglia were the most commonly documented lesion site ( $n = 17$ ), the locus of neuronal damage varied among cases, and often involved multiple brain areas ([Fig. 1](#)). Other brain areas included the temporal and parietal lobes, the insula, corpus callosum, thalamus, internal capsule, midbrain, pons and medulla oblongata. Brain lesions occurred for different aetiological reasons, ranging from traumatic brain injury to stroke, as well as infectious and inflammatory causes ([Supplementary Table 1](#) provides the complete list of clinical and paraclinical case characteristics).

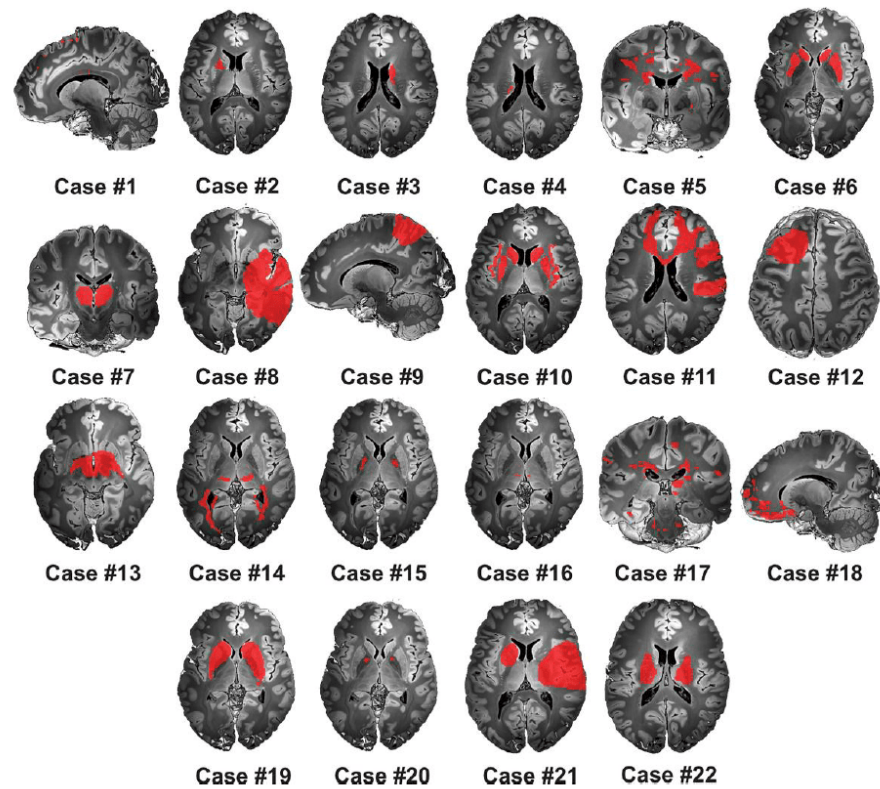
Although tic-inducing brain lesions expressed spatial heterogeneity, they mapped to a common functional brain network ([Figs 2 and 3](#)). Namely, voxels within a network comprising the insular cortices, cingulate gyrus, striatum, GPI, thalami, and the cerebellum were connected to a majority of lesions ([Fig. 3 and Table 1](#)). This included thalamic and pallidal DBS targets ([Fig. 3](#) insets).

However, while the identified network seemed sensitive to tic-inducing lesions, it did not provide insights into how specific it would be to tics. In other words, while spontaneously occurring lesions associated with tics formed part of the network, this did not preclude lesions associated with different symptoms would not fall into the network, as likely. To account for this, we probed the specificity of the identified network by contrasting tic lesion connectivity maps with connectivity maps seeding from 717 lesions within the Harvard Lesion Repository that were associated with a wider array of neurological and/or psychiatric symptoms. This showed significantly higher connectivity of tic-inducing (versus control) lesions to the anterior striatum ([Fig. 4B](#)). Subsequent conjunction analysis identified voxels that were both sensitive and specific to tics ([Fig. 4C](#)).

To probe the predictive utility and therapeutic significance of the identified tic-inducing network, we calculated connectivity between DBS stimulation sites in 30 patients with Tourette disorder ([Fig. 5](#)) and the lesion network. Connectivity strength correlated with respective tic improvements in both pallidal and thalamic cohorts when analysed together ( $R = 0.45$  at  $P = 0.01$ ) and each DBS target separately (thalamic target:  $R = 0.54$  at  $P = 0.01$ ; GPI target:  $R = 0.45$  at  $P = 0.04$ ; [Fig. 6](#)). Connectivity between DBS stimulation sites and the specific and conjunction maps also correlated with clinical improvements ( $R = 0.43$  at  $P = 0.004$ ,  $R = 0.43$  at  $P = 0.006$ ; [Fig. 6B](#)).

In a final analysis, we wanted to probe optimal DBS connectivity profiles in a data-driven fashion. We did so by correlating connectivity values with clinical improvements for each cohort, in a voxel-wise fashion (following the approach of Horn et al.<sup>42</sup>). This resulted in a set of connections with differences and similarities for the





**Figure 1** Tic-inducing lesions. The spatial distribution of lesion masks extracted from 22 case reports included in the current study mapped to a wide extent of brain regions. All binary masks were drawn in MNI space and visualized on an ultra-high resolution post-mortem template for anatomical reference.<sup>58</sup>

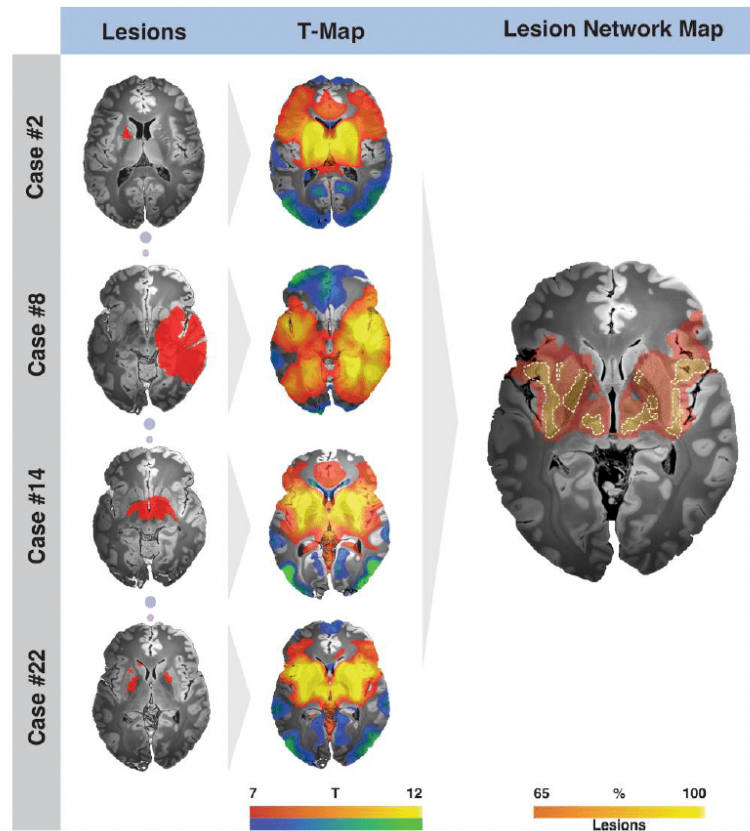
pallidal and thalamic DBS sites. While some sites of optimal connectivity agreed between DBS sites, the two maps were largely different (Fig. 7). However, when probing which regions had positive associations with clinical outcomes for both sites (thalamic and pallidal DBS), this carved out a network that included a highly similar pattern of regions as did the lesion network (Fig. 7 and Table 1). Hence, by pinpointing the sites of optimal connectivity for effective DBS from two DBS targets, a more specific network emerged that matched the one defined by tic-inducing brain lesions.

## Discussion

Three major conclusions can be drawn from this study. First, our results confirm that a network of brain regions is involved in tic generation. Second, we show that a sub-region of the anterior striatum shows specificity to tics when comparing lesion network results to a larger database of lesions associated with other neurological and/or psychiatric symptoms. Third, the identified network was able to predict outcomes following DBS in cohorts with two subcortical stimulation targets.

## A tic-inducing neural network

Contemporary neurology and neuropsychiatry in part explain pathological changes of behaviour as a result of damage to distributed brain networks rather than to isolated brain regions.<sup>35</sup> In this sense, behavioural brain network disorders have been described as ‘circuitopathies’ or ‘connectopathies’.<sup>59,60</sup> In the rare cases of lesion-induced tics identified by our systematic search, the inciting lesions were connected to a common neural circuit, which encompassed structures of the cortico-basal-ganglia-thalamo-cortical circuit, as well as the insular and anterior cingulate cortex (ACC). These regions have previously been implicated in the pathophysiology of tic disorders.<sup>23</sup> For example, in their seminal functional MRI study on the neural correlates of tics, Bohlhalter *et al.*<sup>31</sup> identified a network that preceded tic onset which largely overlapped with the present network, including the insular cortex, ACC, putamen, and thalamus. The relevance of these structures was confirmed in a subsequent study, which employed a similar design with careful time-locked monitoring of tics, providing further support to their involvement in tic occurrence.<sup>32</sup> Moreover, the insular cortex and the ACC have also been associated with specific pathophysiological aspects of tic occurrence, including premonitory urges<sup>33</sup> and vocalizations.<sup>61</sup> Of note, the role of the input and output



**Figure 2** Exemplary cases illustrating the methodological steps used to create the lesion network map. Each lesion mask (left) extracted from the literature ( $n=22$ ) served as a seed region using normative rs-fMRI connectivity data acquired in 1000 healthy participants. The resulting connectivity profiles (in form of T-maps aggregated across the 1000 rs-fMRI scans) were then thresholded and summed to identify regions connected to most tic-inducing lesions (right). The final lesion network map features brain regions connected to voxels encompassed by at least 19 of the 22 identified patient-specific lesion maps.

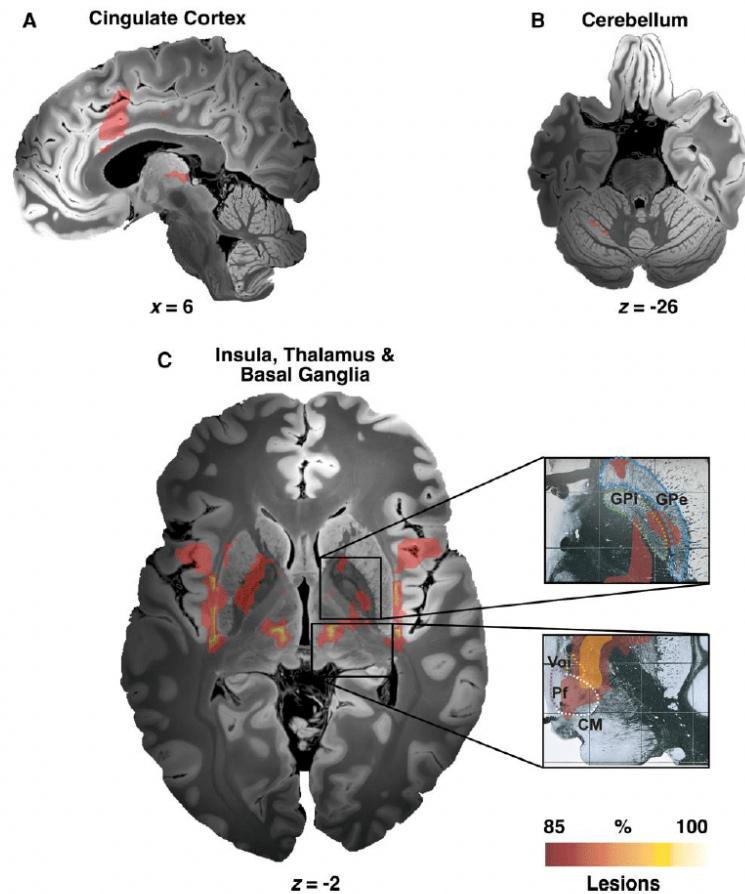
structures of the basal ganglia in tic emergence had already been highlighted by pioneering neuropathological studies in the field<sup>5,6-62</sup> and Hassler's and Dieckman's early neurosurgical therapeutic interventions for tics and obsessive-compulsive symptoms.<sup>7</sup> Indeed, the thalamic and GPi clusters of the network we have identified precisely matched the ablational lesion locations probed by these pioneering studies and showed overlap with the common DBS targets used for the treatment of Tourette disorder (which were inspired by them).<sup>63</sup>

Finally, the network associated with tics identified here covers the claustrum, which could be of potential interest. While the function of the claustrum remains somewhat elusive (and it has been seen as an additional cortical layer by some authors, e.g. Swanson<sup>64</sup>), lesion network mapping has associated a specific part of the claustrum with the occurrence of lesion-induced parkinsonism.<sup>38</sup> Similar to all parts of the basal ganglia, the claustrum is a widespread structure with inputs and outputs from and to various cortical regions, including connecting the anterior insula with the ACC.<sup>65</sup> Hence, specific parts of the structure could be involved in

motor processing (and potentially the occurrence of tics), while others would be involved in cognitive or limbic processes.

#### A specific role for the anterior striatum in tic induction

The comparison between individual tic lesion network profiles and a large database of cases with lesions associated with neurological and psychiatric disorders revealed a specific role of the anterior striatum in tic induction, which was identified as a subset of the tic-related lesion network. Conjunction analysis identified a region within the anterior putamen, which was both sensitive and specific to tics. This region mapped to the associative-limbic functional zone of the striatum,<sup>66</sup> well within the projection site of CM-Voi. Importantly, this pre-commissural sub-region of the putamen constitutes a complex information processing hub, driven by its exceptional level of input heterogeneity.<sup>67</sup> Similarly, CM-Voi nuclei receive input from and diffusely project to the entire cerebral cortex.<sup>68</sup> A compelling pathological study of brains of adults with



**Figure 3** Tic-inducing lesion network map. Lesion network mapping highlighted different cortical and subcortical regions including cingulate cortex (A), cerebellum (lobule VI) (B), insula, thalamus, striatum, and the pallidum (C). Of note, main DBS neuroanatomical targets (GPI and CM-Pf-Voi) used to treat primary tic-syndrome are included within the network. CM = centromedian nucleus of thalamus; GPe = globus pallidus externus; GPI = globus pallidus internus; Pf = parafascicular nucleus of thalamus; Voi = ventralis oralis nucleus of thalamus.

Tourette disorder reported pronounced decreases of different interneuronal populations in the associative and, to a lesser degree, sensorimotor striatum.<sup>6</sup> At the same time, animal models of pharmacologically-induced GABAergic disinhibition within this sub-region of the striatum led to tic-like behaviors.<sup>69,70</sup> This body of pathological and behavioural animal model data suggests that information processing within this striatal hub, and its functional connectivity with other subcortical structures, could be altered in primary tic disorders.

#### A tic-lesion network as a potential target for neuromodulation

Tic disorders are characterized by clinical heterogeneity and variability in treatment response, including response to DBS.<sup>63</sup> According to a recent estimate, ~30% of adults with Tourette disorder and moderate to severe tics are refractory to non-invasive

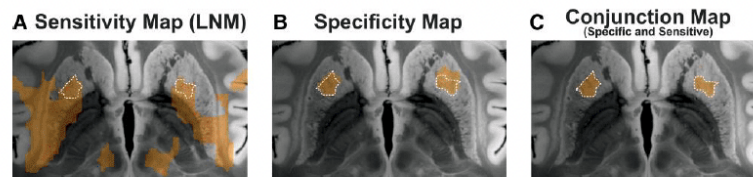
interventions, and would be eligible for DBS. In the USA alone, this corresponds to more than 6000 individuals.<sup>71</sup> However, robust predictors of treatment outcome following DBS have not yet been established, motivating the application of both the lesion and DBS network mapping approaches in the present study. Indeed, combining the two methods (as done here) allowed to predict clinical outcomes following DBS in the treatment of Parkinson's disease and major depression based on lesions causing parkinsonism<sup>38</sup> and depression.<sup>72</sup> Another study focusing on dystonia<sup>39</sup> demonstrated anatomical overlap between a lesion-based network and the network associated with positive outcome after DBS.

In Tourette disorder, a first study has applied DBS network mapping, before,<sup>73</sup> but did not relate DBS network patterns to lesions associated with tics. Furthermore, the study applied normative structural (instead of functional) connectivity and hence results may not be directly comparable to ours. In the study, structural

Table 1 Peak coordinates

Region	Hemisphere	Thalamus R-Map	GPI R-Map	Agreement R-Map	Lesion network map
		X/Y/Z (R-value)	X/Y/Z (R-value)	X/Y/Z (R-value)	X/Y/Z (T-value)
Sub-lobar insula (BA13)	LH	-42/-8/2 (0.66)	-34/-28/14 (0.45)	-34/-28/14 (0.28)	-44/10/-8 (20)
	RH	46/-6/0 (0.67)	42/-18/14 (0.48)	46/-16/10 (0.27)	44/12/-8 (19)
Putamen	LH	-32/-14/-2 (0.68)	-18/6/-6 (0.63)	-30/-6/-8 (0.25)	-20/4/-14 (20)
	RH	34/-18/6 (0.64)	24/4/-10 (0.59)	32/-12/12 (0.20)	20/4/-14 (20)
Cingulate gyrus (limbic lobe)	LH	-6/-6/40 (0.63)	-4/-2/34 (0.64)	0/-10/42 (0.31)	0/12/24 (19)
	RH	4/-14/44 (0.65)	4/-2/34 (0.55)	2/-12/42 (0.27)	10/22/24 (19)
Precentral gyrus	LH	-66/0/10 (0.66)	-68/0/26 (0.46)	-68/0/26 (0.26)	-42/12/2 (19)
	RH	70/4/6 (0.67)	44/18/34 (0.63)	70/6/4 (0.30)	44/8/2 (19)
Mammillary body	LH	-10/-16/-2 (0.77)	-8/-20/-2 (0.08)	-10/-16/-2 (0.06)	-8/-20/-2 (20)
	RH	12/-20/0 (0.57)	12/-22/-2 (0.04)	12/-22/-2 (0.02)	12/-16/-2 (20)
Midbrain	LH	-8/-16/-4 (0.71)	0/-34/0 (0.44)	-6/-30/0 (0.12)	-8/-22/-4 (20)
	RH	16/-22/-4 (0.62)	2/-34/0 (0.53)	16/-26/-4 (0.17)	10/-22/-4 (20)
Medial dorsal nucleus	LH	-10/-18/4 (0.62)	-4/-12/8 (0.58)	-4/-14/6 (0.27)	-6/-20/2 (20)
	RH	14/-20/4 (0.58)	4/-14/10 (0.57)	4/-12/4 (0.25)	8/-20/2 (20)
Ventral posterior medial nucleus	LH	-14/-18/-2 (0.68)	-14/-18/8 (0.17)	-14/-18/8 (0.08)	-16/-22/4 (20)
	RH	18/-20/-2 (0.62)	20/-20/8 (0.26)	18/-20/8 (0.13)	18/-22/6 (20)
Cingulate gyrus (BA24)	LH	-10/-4/40 (0.64)	-2/0/34 (0.65)	-4/-14/40 (0.34)	-2/12/24 (19)
	RH	12/-4/40 (0.64)	4/0/34 (0.59)	4/0/34 (0.27)	8/14/24 (19)
Claustrum	LH	-36/-22/4 (0.65)	-28/6/12 (0.47)	-34/-24/8 (0.21)	-38/-20/-8 (20)
	RH	38/-20/4 (0.65)	34/-14/14 (0.44)	34/-14/14 (0.25)	38/-14/-10 (20)
Pulvinar	LH	-20/-24/2 (0.65)	-6/-28/4 (0.40)	-10/-24/12 (0.17)	-18/-24/4 (20)
	RH	20/-28/2 (0.60)	12/-26/12 (0.30)	20/-22/14 (0.15)	20/-24/6 (20)
Inferior frontal gyrus	LH	-64/12/12 (0.66)	-60/22/26 (0.52)	-64/10/26 (0.22)	-48/14/-10 (19)
	RH	68/10/12 (0.61)	62/30/-4 (0.59)	68/14/24 (0.28)	50/16/-6 (19)
Globus pallidus, pars externa	LH	-26/-16/0 (0.48)	-14/6/-2 (0.48)	-26/-18/0 (0.08)	-20/-4/-10 (19)
	RH	30/-12/-2 (0.50)	22/2/-8 (0.50)	30/-14/-6 (0.14)	18/4/-10 (20)
Globus pallidus, pars interna	LH	-18/-10/0 (0.28)	-12/2/-2 (0.17)	-20/-10/-6 (0)	-16/-8/-10 (0)
	RH	24/-14/-4 (0.32)	16/-2/-6 (0.18)	24/-12/-6 (0.02)	18/-2/-10 (19)

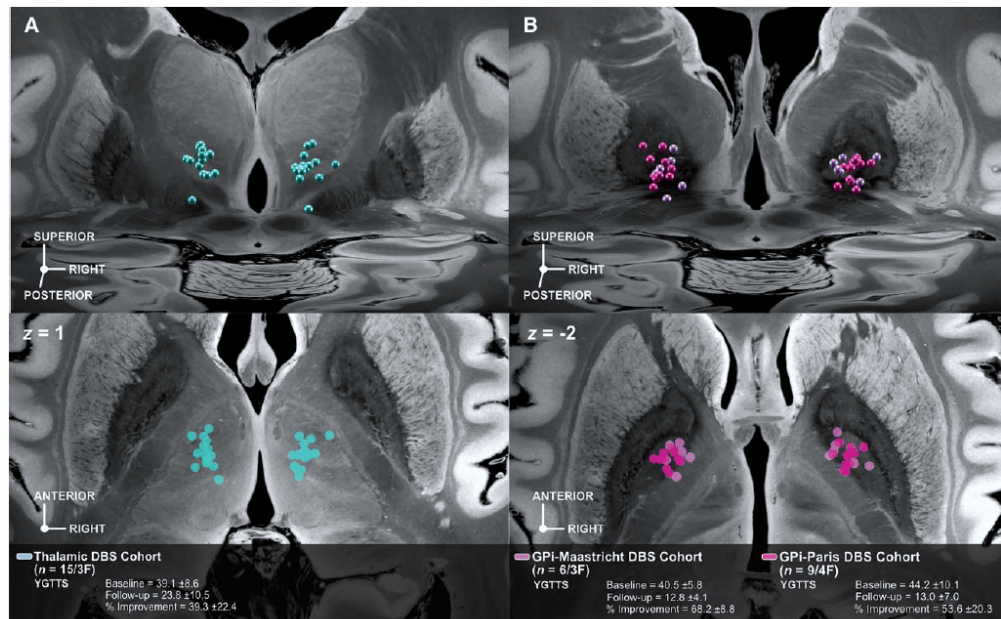
Table summarizes MNI coordinates of regions visualized on different brain connectivity maps presented in the study (Figs 3 and 7). LH = left hemisphere; RH = right hemisphere.



**Figure 4** Regions connected to tic-inducing lesions: sensitivity and specificity analysis. Lesion network map (LNM; A) represents voxels that were connected to tic-inducing lesions. Specificity of connectivity to lesions associated with occurrence of tics was calculated by contrasting connectivity profiles of lesions associated with tics to a total of 717 lesions from the Harvard Lesion Repository (B). This analysis highlighted a region within the anterior striatum that would be specifically linked to tic-occurrence. Voxels that were both specific and sensitive to tic occurrence are demonstrated in C. This conjunction map contained voxels that were shown in both A and B.

connectivity to an extensive array of brain areas was associated with DBS-related modulation of tic severity, including limbic, associative, and sensorimotor networks. Interestingly, structural connectivity patterns were largely inverse between the pallidal and thalamic stimulation targets. Although a strong connectivity to limbic and associative networks, including the cingulate cortex, caudate and thalamus, predicted post-DBS tic improvement in patients who received GPi stimulation ( $n = 34$ ), this was not the case for the thalamic stimulation cohort. In the latter group ( $n = 32$ ), connectivity to primary sensorimotor and parietal-temporal-occipital networks, as well as the putamen, correlated with reduction in tic severity. In part, this matches with our results which showed different optimal connectivity profiles for both pallidal and thalamic target sites—however, here, networks were not inverse to each

other, and their common denominator set of regions precisely matched the network identified by lesions. Crucially, structural connectivity analyses as carried out in the aforementioned study<sup>73</sup> cannot detect indirect (i.e. polysynaptic) connections. In our sample, functional connectivity of both pallidal and thalamic cohorts to the same tic-related lesion network was associated with greater tic improvement. Moreover, while in a data-driven analysis of DBS sites, the two optimal connectivity profiles between pallidal and thalamic targets differed, their agreement mapped exactly to the network identified by the lesion analysis. First, these results validate the significance of the tic lesion network in the pathophysiology of tic generation. Second, they provide a functional network template that could inform effective neuromodulatory interventions aimed at reducing tics.



**Figure 5** DBS cohorts electrode placement. Each DBS cohort comprises bilaterally implanted electrodes targeting different subcortical regions. The thalamic DBS cohort (A) consisted of  $n=15$  patients from the Cologne clinical centre while the GPI cohort (B) consisted of six patients from the Maastricht and nine from the Paris clinical centres. Panels show active contact locations relative to anatomical planes defined by the 100  $\mu\text{m}$  post-mortem ultra-high resolution post-mortem template in an oblique 3D view from posterodorsal (top) and axial slice (bottom) view (where contact sites were orthogonally projected onto the plane).<sup>58</sup>

### Limitations

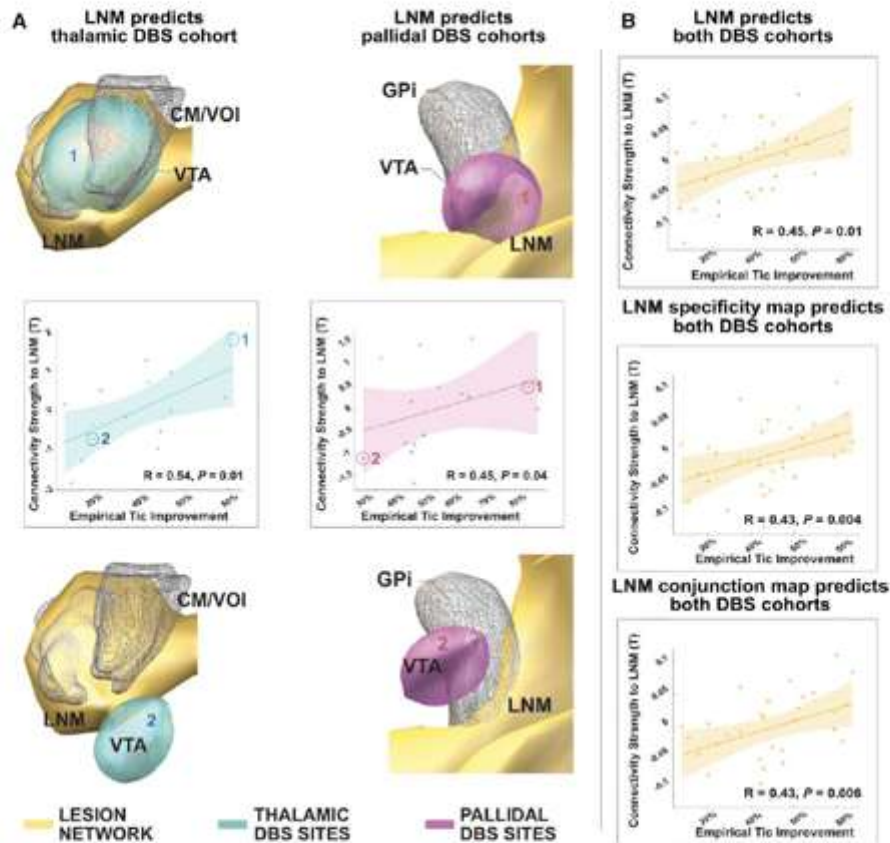
Some noteworthy limitations apply to this study. First, both literature-derived network maps and DBS cases were acquired retrospectively. In the former, causality between brain lesions and occurrence of tics cannot be established with absolute certainty. This has been a longstanding limitation of studying case reports across symptoms and constitutes a true limitation. However, lesions resulting in the emergence of tics are rare and from 22 identified cases, 19 mapped to a shared network. We manually segmented lesion locations on the MNI template, resulting in 2D regions. Prior analyses showed that this would lead to similar connectivity profiles as corresponding 3D lesions<sup>36,74</sup> and the same procedure has been carried out in several lesion network mapping studies that showed robust findings.<sup>38,41–72</sup> Prospective validation of network maps to explain variance in clinical outcome will be crucial to move forward.

Second, we carried out network mapping for both lesions and DBS cases using normative functional connectivity acquired in healthy individuals. This has been done successfully in previous studies yielding results that were used to cross-predict clinical improvement in independent cohorts in a variety of diseases.<sup>42,43,44,45,46–59</sup> At the same time, this approach applies a 'broad lens' view on human brain function and may not reveal patient- or disease-specific details of brain connectivity. The method determines the networks underlying DBS sites or lesions within the average healthy human brain. This notion is crucial when interpreting results but indeed has multiple practical advantages: for

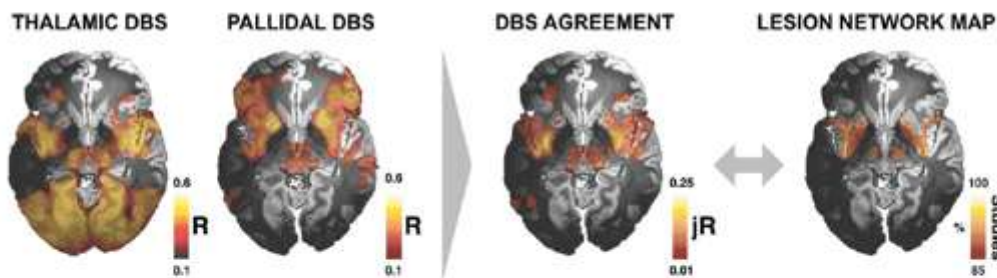
instance, lesions (with ischemic tissue) would not show patient-specific network connectivity, even if patient-specific functional scans were available (since the lesion site is not active after stroke). In other words, functional connectivity from stroke sites is not present and cannot be calculated using patient-specific functional MRI data. In both stroke and DBS, distributed brain networks would be altered by the incidents (infarction or neurostimulation) themselves. Here, we ask which networks of the pre-stroke/pre-DBS brain would be affected by both incidents and argue that this would identify exactly the networks with therapeutic value.

Third, the process of DBS electrode reconstruction is prone to inaccuracies that can be relevant, as previously discussed.<sup>53</sup> Moreover, the model applied to estimate stimulation volumes surrounding DBS electrodes applied here may be over-simplistic compared to more elaborate methods.<sup>75,76,77</sup> However, in the context of functional MRI mapping (with an isotropic resolution of 2 mm), subtle inaccuracies of the applied model may not be as impactful as in more fine-grained analyses.

Finally, we note that while both lesions and DBS sites identified a shared network with high spatial overlap, lesions that fell into the network induced tics while DBS to the network alleviated tics. With the methods at hand, we may currently only speculate why that is the case. For one, we believe that the disruption of the network is involved in producing tics and such a disruption could be induced by lesions that corrupt the functionality of the network. How exactly this 'disruption' is mechanistically implemented cannot be investigated with the methods of the present study, but local field potential recordings from both thalamic and pallidal DBS



**Figure 6** DBS associated tic improvement associates with connectivity to the lesion network map. (A) Postoperative percentage improvement of primary tic syndrome from three clinical centres (Cologne-thalamic DBS cohort/turquoise and Paris and Maastricht-pallidal DBS cohort/magenta) associated with the degree of connectivity between either the thalamic or pallidal DBS stimulation sites and the lesion network map. Four example cases of optimal and poor improvements are shown, each demonstrating either strong or weak functional connectivity between the DBS site and the lesion network map, respectively. The lesion network map is shown in yellow, and thalamic stimulation sites in cyan, pallidal ones in purple. Respective example cases are marked in scatter plots. (B) Correlation plots between the degree of connectivity of the entire patient cohort and the lesion network map (top), the sensitivity map (middle), and the conjunction map (bottom), respectively. CM/VOI = centromedian nucleus/ventro-oralis nucleus of thalamus; GPI = globus pallidus internus; LNM = lesion network map.



**Figure 7** Agreement between DBS and lesion-informed mapping. In a final data-driven analysis, functional connectivity between DBS targets and all other brain areas that correlated with optimal clinical improvement was separately calculated for the thalamic and pallidal cohorts. This led to different connectivity profiles but also included overlapping regions. These are shown as dashed lines in the two maps and by the agreement map. In the agreement map, only regions with positive association in both targets were retained.

electrodes showed that prolonged theta bursts in both targets were associated with preoperative motor tic severity.<sup>16</sup> In other diseases such as Parkinson's disease and dystonia, DBS is known to tone down such aberrant elevated network activity.<sup>78</sup> Hence, our current working model constitutes that lesions (or other aetiologies) could lead to network dysfunction (including the occurrence of noisy feedback carrier signals<sup>79,80</sup>) and DBS could in turn selectively tone down/compensate these aberrant signals, freeing up bandwidth for physiological communication within the network.

## Conclusions

This study could associate a functional network including striatal, thalamic, and insular regions of the human brain with (i) the occurrence of tics resulting from brain lesions; and (ii) successful tic reduction following DBS treatment. We could demonstrate that the connectivity between DBS electrodes implanted in two different target sites and our network identified by tic-inducing lesions was able to predict significant amounts of variance in tic improvements. In a data-driven approach, the regions associated with improvement following both pallidal and thalamic DBS mapped to the exact same set of regions identified by the lesion network analysis.

## Funding

C.G. is supported by a Freigeist Fellowship of the VolkswagenStiftung. He has received honoraria for educational activities from the Movement Disorder Society. He has served as ad hoc advisory board to Biomar Pharmaceutical and Lundbeck. J.C.B. and V.V.V. are funded by the Deutsche Forschungsgemeinschaft (DFG, German Research Foundation)—Project-ID 431549029—SFB 1451. M.D.F. was supported by the Nancy Lurie Marks Foundation, the Kaye Family Research Endowment, the Ellison/Baszucki Foundation and the NIH (R01MH113929, R21MH126271, R56AG069086, R01MH115949, and R01AG060987). A.H. was supported by the German Research Foundation (Deutsche Forschungsgemeinschaft, Emmy Noether Stipend 410169619 and 424778381—TRR 295) as well as Deutsches Zentrum für Luft- und Raumfahrt (DynaSti grant within the EU Joint Programme Neurodegenerative Disease Research, JPND). A.H. is participant in the BIH-Charité Clinician Scientist Program funded by the Charité – Universitätsmedizin Berlin and the Berlin Institute of Health. B.A.F., J.F.F., C.H., C.N., D.M., J.L., T.B., L.A., N.P. and Y.W. report no relevant funding for this work.

## Competing interests

A.K.K. is a consultant to Boston Scientific and has received honoraria for speaking from Medtronic, Boston Scientific and Abbott, as well as grants from Medtronic, all outside the submitted work. A.F.L. receives royalties from 'Springer Media' and 'De Tijdstroom' Publishers. A.H. reports lecture fees by Boston Scientific unrelated to the present work. The other authors report no competing interests.

## Supplementary material

Supplementary material is available at *Brain* online.

## References

1. Kurvits L, Martino D, Ganos C. Clinical features that evoke the concept of disinhibition in Tourette syndrome. *Front Psychiatry*. 2020;11:21.
2. Ganos C, Roessner V, Munchau A. The functional anatomy of Gilles de la Tourette syndrome. *Neurosci Biobehav Rev*. 2013;37:1050–1062.
3. Hashemiyouon R, Kuhn J, Visser-Vandewalle V. Putting the pieces together in Gilles de la Tourette syndrome: exploring the link between clinical observations and the biological basis of dysfunction. *Brain Topogr*. 2017;30:3–29.
4. Mink JW. Basal ganglia dysfunction in Tourette's syndrome: a new hypothesis. *Pediatr Neurol*. 2001;25:190–198.
5. Kalanithi PSA, Zheng W, Kataoka Y, et al. Altered parvalbumin-positive neuron distribution in basal ganglia of individuals with Tourette syndrome. *Proc Natl Acad Sci U S A*. 2005;102:13307–13312.
6. Kataoka Y, Kalanithi PSA, Grantz H, et al. Decreased number of parvalbumin and cholinergic interneurons in the striatum of individuals with Tourette syndrome. *J Comp Neurol*. 2010;518:277–291.
7. Hassler R, Dieckmann G. [Stereotaxic treatment of tics and inarticulate cries or coprolalia considered as motor obsessional phenomena in Gilles de la Tourette's disease]. *Rev Neurol (Paris)*. 1970;123:89–100.
8. Vandewalle V, van der Linden C, Groenewegen HJ, Caemaert J. Stereotactic treatment of Gilles de la Tourette syndrome by high frequency stimulation of thalamus. *The Lancet*. 1999;353:724.
9. Ackermans L, Duits A, van der Linden C, et al. Double-blind clinical trial of thalamic stimulation in patients with Tourette syndrome. *Brain*. 2011;134(Pt 3):832–844.
10. Baldemann JC, Kuhn J, Schuller T, et al. Thalamic deep brain stimulation for Tourette Syndrome: A naturalistic trial with brief randomized, double-blinded sham-controlled periods. *Brain Stimul*. 2021;14:1059–1067.
11. Baldemann JC, Hennen C, Schüller T, et al. A functional network target for tic reduction during thalamic stimulation for Tourette Syndrome. *bioRxiv*, 2021.
12. Huys D, Bartsch C, Koester P, et al. Motor improvement and emotional stabilization in patients with Tourette syndrome after deep brain stimulation of the ventral anterior and ventrolateral motor part of the thalamus. *Biol Psychiatry*. 2016;79:392–401.
13. Kefalopoulou Z, Zrinzo L, Jahanshahi M, et al. Bilateral globus pallidus stimulation for severe Tourette's syndrome: a double-blind, randomised crossover trial. *Lancet Neurol*. 2015;14:595–605.
14. Welter ML, Houeto JL, Thobois S, et al. Anterior pallidal deep brain stimulation for Tourette's syndrome: a randomised, double-blind, controlled trial. *Lancet Neurol*. 2017;16:610–619.
15. Martínez-Ramírez D, Jiménez-Shahed J, Leckman JF, et al. Efficacy and safety of deep brain stimulation in tourette syndrome: The international Tourette syndrome deep brain stimulation public database and registry. *JAMA Neurol*. 2018;75:353–359.
16. Neumann WJ, Huebl J, Brucke C, et al. Pallidal and thalamic neural oscillatory patterns in tourette's syndrome. *Ann Neurol*. 2018;84:505–514.
17. Cagle JN, Okun MS, Opri E, et al. Differentiating tic electrophysiology from voluntary movement in the human thalamocortical circuit. *J Neurol Neurosurg Psychiatry*. 2020;91:533–539.
18. Priori A, Giannicola G, Rosa M, et al. Deep brain electrophysiological recordings provide clues to the pathophysiology of Tourette syndrome. *Neurosci Biobehav Rev*. 2013;37:1063–1068.

19. Karp BI, Porter S, Toro C, Hallett M. Simple motor tics may be preceded by a premotor potential. *J Neurol Neurosurg Psychiatry*. 1996;61:103–106.
20. van der Salm SM, Tijssen MA, Koelman JH, van Rootselaar AF. The Bereitschaftspotential in jerky movement disorders. *J Neurol Neurosurg Psychiatry*. 2012;83:1162–1167.
21. Orth M, Munchau A, Rothwell JC. Corticospinal system excitability at rest is associated with tic severity in tourette syndrome. *Biol Psychiatry*. 2008;64:248–251.
22. Franzkowiak S, Pollok B, Biermann-Ruben K, et al. Motor-cortical interaction in Gilles de la Tourette syndrome. *PLoS One*. 2012;7:e27850.
23. Martino D, Ganos C, Worbe Y. Neuroimaging applications in Tourette's syndrome. *Int Rev Neurobiol*. 2018;143:65–108.
24. Worbe Y, Gerardin E, Hartmann A, et al. Distinct structural changes underpin clinical phenotypes in patients with Gilles de la Tourette syndrome. *Brain*. 2010;133(Pt 12):3649–3660.
25. Draganski B, Martino D, Cavanna AE, et al. Multispectral brain morphometry in Tourette syndrome persisting into adulthood. *Brain*. 2010;133(Pt 12):3661–3675.
26. Liu Y, Miao W, Wang J, et al. Structural abnormalities in early Tourette syndrome children: a combined voxel-based morphometry and tract-based spatial statistics study. *PLoS One*. 2013;8:e76105.
27. Draper A, Jackson GM, Morgan PS, Jackson SR. Premonitory urges are associated with decreased grey matter thickness within the insula and sensorimotor cortex in young people with Tourette syndrome. *J Neuropsychol*. 2016;10:143–153.
28. Thomalla G, Siebner HR, Jonas M, et al. Structural changes in the somatosensory system correlate with tic severity in Gilles de la Tourette syndrome. *Brain*. 2009;132(Pt 3):765–777.
29. Fahim C, Yoon U, Das S, et al. Somatosensory–motor bodily representation cortical thinning in Tourette: effects of tic severity, age and gender. *Cortex*. 2010;46:750–760.
30. Sowell ER, Kan E, Yoshii J, et al. Thinning of sensorimotor cortices in children with Tourette syndrome. *Nat Neurosci*. 2008;11:637–639.
31. Bohlhalter S, Goldfine A, Matteson S, et al. Neural correlates of tic generation in Tourette syndrome: an event-related functional MRI study. *Brain*. 2006;129(Pt 8):2029–2037.
32. Neuner I, Werner CJ, Arrubla J, et al. Imaging the where and when of tic generation and resting state networks in adult Tourette patients. *Front Hum Neurosci*. 2014;8:362.
33. Tinaz S, Malone P, Hallett M, Horowitz SG. Role of the right dorsal anterior insula in the urge to tic in Tourette syndrome. *Mov Disord*. 2015;30:1190–1197.
34. Worbe Y, Sgambato-Faure V, Epinat J, et al. Towards a primate model of Gilles de la Tourette syndrome: anatomo-behavioural correlation of disorders induced by striatal dysfunction. *Cortex*. 2013;49:1126–1140.
35. Fox MD. Mapping symptoms to brain networks with the human connectome. *N Engl J Med*. 2018;379:2237–2245.
36. Boes AD, Prasad S, Liu H, et al. Network localization of neurological symptoms from focal brain lesions. *Brain*. 2015;138(Pt 10):3061–3075.
37. Laganieri S, Boes AD, Fox MD. Network localization of hemichorea-hemiballismus. *Neurology*. 2016;86:2187–2195.
38. Joutsa J, Horn A, Hsu J, Fox MD. Localizing parkinsonism based on focal brain lesions. *Brain*. 2018;141:2445–2456.
39. Corp DT, Joutsa J, Darby RR, et al. Network localization of cervical dystonia based on causal brain lesions. *Brain*. 2019;142:1660–1674.
40. Darby RR, Joutsa J, Burke MJ, Fox MD. Lesion network localization of free will. *Proc Natl Acad Sci U S A*. 2018;115:10792–10797.
41. Darby RR, Horn A, Cushman F, Fox MD. Lesion network localization of criminal behavior. *Proc Natl Acad Sci U S A*. 2018;115:601–606.
42. Horn A, Reich M, Vorwerk J, et al. Connectivity predicts deep brain stimulation outcome in Parkinson disease. *Ann Neurol*. 2017;82:67–78.
43. Irmen F, Horn A, Mosley P, et al. Left prefrontal connectivity links subthalamic stimulation with depressive symptoms. *Ann Neurol*. 2020;87:962–975.
44. Al-Fatly B, Ewert S, Kubler D, Kroneberg D, Horn A, Kuhn AA. Connectivity profile of thalamic deep brain stimulation to effectively treat essential tremor. *Brain*. 2019;142:3086–3098.
45. Baldermann JC, Melzer C, Zapf A, et al. Connectivity profile predictive of effective deep brain stimulation in obsessive-compulsive disorder. *Biol Psychiatry*. 2019;85:735–743.
46. Li N, Baldermann JC, Kibleur A, et al. A unified connectomic target for deep brain stimulation in obsessive-compulsive disorder. *Nat Commun*. 2020;11:3364.
47. Siddiqi SH, Schaper FLWVJ, Horn A, et al. Brain stimulation and brain lesions converge on common causal circuits in neuropsychiatric disease. *Nat Hum Behav*. 2021;5(12):1707–1716.
48. Horn A, Kuhn AA. Lead-DBS: a toolbox for deep brain stimulation electrode localizations and visualizations. *Neuroimage*. 2015;107:127–135.
49. Holmes AJ, Hollinshead MO, O'Keefe TM, et al. Brain Genomics Superstruct Project initial data release with structural, functional, and behavioral measures. *Sci Data*. 2015;2:150031.
50. Yeo BT, Krienen FM, Sepulcre J, et al. The organization of the human cerebral cortex estimated by intrinsic functional connectivity. *J Neurophysiol*. 2011;106:1125–1165.
51. Cohen AL, Fox MD. Reply: the influence of sample size and arbitrary statistical thresholds in lesion-network mapping. *Brain*. 2020;143:e41.
52. Eklund A, Nichols TE, Knutsson H. Cluster failure: why fMRI inferences for spatial extent have inflated false-positive rates. *Proc Natl Acad Sci U S A*. 2016;113:7900–7905.
53. Horn A, Li N, Dembek TA, et al. Lead-DBS v2: towards a comprehensive pipeline for deep brain stimulation imaging. *Neuroimage*. 2019;184:293–316.
54. Avants BB, Epstein CL, Grossman M, Gee JC. Symmetric diffeomorphic image registration with cross-correlation: evaluating automated labeling of elderly and neurodegenerative brain. *Med Image Anal*. 2008;12:26–41.
55. Husch A, Petersen MV, Gemmar P, Goncalves J, Hertel F. PaCER - a fully automated method for electrode trajectory and contact reconstruction in deep brain stimulation. *Neuroimage Clin*. 2018;17:80–89.
56. van Albada SJ, Robinson PA. Transformation of arbitrary distributions to the normal distribution with application to EEG test-retest reliability. *J Neurosci Methods*. 2007;161:205–211.
57. Li N, Hollunder B, Baldermann JC, et al. A unified functional network target for deep brain stimulation in obsessive-compulsive disorder. *Biol Psychiatry*. 2021;90:701–713.
58. Edlow BL, Mareyam A, Horn A, et al. 7 Tesla MRI of the ex vivo human brain at 100 micron resolution. *Sci Data*. 2019;6:244.
59. Horn A, Fox MD. Opportunities of connectomic neuromodulation. *Neuroimage*. 2020;221:117180.
60. Lozano AM, Lipsman N. Probing and regulating dysfunctional circuits using deep brain stimulation. *Neuron*. 2013;77:406–424.
61. McCairn KW, Nagai Y, Hori Y, et al. A primary role for nucleus accumbens and related limbic network in vocal tics. *Neuron*. 2016;89:300–307.
62. Balthasar K. [The anatomical substratum of the generalized tic disease (maladie des tics, Gilles de la Tourette); arrest of



- development of the corpus striatum]. *Arch Psychiatr Nervenkr Z Gesamte Neurol Psychiatr*. 1957;195:531–549.
63. Johnson KA, Fletcher PT, Servello D, et al. Image-based analysis and long-term clinical outcomes of deep brain stimulation for Tourette syndrome: a multisite study. *J Neurol Neurosurg Psychiatry*. 2019;90:1078–1090.
  64. Swanson LW. Cerebral hemisphere regulation of motivated behavior. *Brain Res*. 2000;886:113–164.
  65. Chia Z, Augustine GJ, Silberberg G. Synaptic connectivity between the cortex and claustrum is organized into functional modules. *Curr Biol*. 2020;30:2777–2790.e4.
  66. Choi EY, Yeo BTT, Buckner RL. The organization of the human striatum estimated by intrinsic functional connectivity. *J Neurophysiol*. 2012;108:2242–2263.
  67. McCutcheon RA, Abi-Dargham A, Schizophrenia HO. Schizophrenia, dopamine and the striatum: from biology to symptoms. *Trends Neurosci*. 2019;42:205–220.
  68. Nieuwenhuys R, Voogd J, van Huijzen C. *The human central nervous system*. 4th ed. Springer; 2008:xiv, 967 p.
  69. McCairn KW, Iriki A, Isoda M. Global dysrhythmia of cerebro-basal ganglia-cerebellar networks underlies motor tics following striatal disinhibition. *J Neurosci*. 2013;33:697–708.
  70. Tremblay L, Worbe Y, Thobois S, Sgambato-Faure V, Feger J. Selective dysfunction of basal ganglia subterritories: from movement to behavioral disorders. *Mov Disord*. 2015;30:1155–1170.
  71. Martino D, Deeb W, Jimenez-Shahed J, et al. The 5 pillars in Tourette syndrome deep brain stimulation patient selection: present and future. *Neurology*. 2021;96:664–676.
  72. Padmanabhan JL, Cooke D, Joutsa J, et al. A human depression circuit derived from focal brain lesions. *Biol Psychiatry*. 2019;86:749–758.
  73. Johnson KA, Duffley G, Anderson DN, et al. Structural connectivity predicts clinical outcomes of deep brain stimulation for Tourette syndrome. *Brain*. 2020;143:2607–2623.
  74. Darby RR, Laganieri S, Pascual-Leone A, Prasad S, Fox MD. Finding the imposter: brain connectivity of lesions causing delusional misidentifications. *Brain*. 2017;140:497–507.
  75. Gunalan K, Chaturvedi A, Howell B, et al. Creating and parameterizing patient-specific deep brain stimulation pathway-activation models using the hyperdirect pathway as an example. *PLoS One*. 2017;12:e0176132.
  76. Duffley G, Anderson DN, Vorwerk J, Dorval AD, Butson CR. Evaluation of methodologies for computing the deep brain stimulation volume of tissue activated. *J Neural Eng*. 2019;16:066024.
  77. Howell B, Gunalan K, McIntyre CC. A driving-force predictor for estimating pathway activation in patient-specific models of deep brain stimulation. *Neuromodulation*. 2019;22:403–415.
  78. Kuhn AA, Volkmann J. Innovations in deep brain stimulation methodology. *Mov Disord*. 2017;32:11–19.
  79. Horn A, Al-Fatly B, Neumann WJ, Neudorfer C. Chapter 1 - Connectomic DBS: an introduction. In: Horn A, ed. *Connectomic Deep Brain Stimulation*. Academic Press; 2022:3–23.
  80. Brown P. Oscillatory nature of human basal ganglia activity: relationship to the pathophysiology of Parkinson's disease. *Mov Disord*. 2003;18(4):357–363.



Contents lists available at ScienceDirect

NeuroImage: Clinical

journal homepage: [www.elsevier.com/locate/ynicl](http://www.elsevier.com/locate/ynicl)



## Neuroimaging-based analysis of DBS outcomes in pediatric dystonia: Insights from the GEPESTIM registry

Bassam Al-Fatly<sup>a,\*</sup>, Sabina J. Giesler<sup>b</sup>, Simon Oxenford<sup>a</sup>, Ningfei Li<sup>a</sup>, Till A. Dembek<sup>c</sup>, Johannes Achtzehn<sup>a</sup>, Patricia Krause<sup>a</sup>, Veerle Visser-Vandewalle<sup>d</sup>, Joachim K. Krauss<sup>e</sup>, Joachim Runge<sup>e</sup>, Vera Tadic<sup>f</sup>, Tobias Bäumer<sup>g</sup>, Alfons Schnitzler<sup>h,i</sup>, Jan Vesper<sup>h</sup>, Jochen Wirths<sup>d</sup>, Lars Timmermann<sup>j</sup>, Andrea A. Kühn<sup>a,1,\*</sup>, Anne Koy<sup>b,k,1</sup>, on behalf of the GEPESTIM consortium

<sup>a</sup> Charité-Universitätsmedizin Berlin, Corporate Member of Freie Universität Berlin and Humboldt-Universität zu Berlin, Department of Neurology, Berlin, Germany

<sup>b</sup> Department of Pediatrics, Faculty of Medicine and University Hospital Cologne, University of Cologne, Cologne, Germany

<sup>c</sup> Department of Neurology, Faculty of Medicine, University of Cologne, Cologne, Germany

<sup>d</sup> Department of Stereotactic and Functional Neurosurgery, Faculty of Medicine and University Hospital Cologne, University of Cologne, Cologne, Germany

<sup>e</sup> Department of Neurosurgery, Hannover Medical School, Hannover, Germany

<sup>f</sup> Department of Neurology, University Medical Center Schleswig Holstein, Lübeck Campus, Lübeck, Germany

<sup>g</sup> Institute of System Motor Science, University Medical Center Schleswig Holstein, Lübeck Campus, Lübeck, Germany

<sup>h</sup> Department of Neurology, Institute of Clinical Neuroscience and Medical Psychology, Medical Faculty, Heinrich Heine University Düsseldorf, Düsseldorf, Germany

<sup>i</sup> Department of Neurology, Medical Faculty, Heinrich Heine University Düsseldorf, Düsseldorf, Germany

<sup>j</sup> Department of Neurology, University Hospital of Marburg, Marburg, Germany

<sup>k</sup> Center for Rare Diseases, Faculty of Medicine and University Hospital Cologne, University of Cologne, Cologne, Germany

### ARTICLE INFO

#### Keywords:

Dystonia  
Pediatric  
Deep brain stimulation  
Connectomics  
Sweetspot

### ABSTRACT

**Introduction:** Deep brain stimulation (DBS) is an established treatment in patients of various ages with pharmacoresistant neurological disorders. Surgical targeting and postoperative programming of DBS depend on the spatial location of the stimulating electrodes in relation to the surrounding anatomical structures, and on electrode connectivity to a specific distribution pattern within brain networks. Such information is usually collected using group-level analysis, which relies on the availability of normative imaging resources (atlases and connectomes). Analysis of DBS data in children with debilitating neurological disorders such as dystonia would benefit from such resources, especially given the developmental differences in neuroimaging data between adults and children. We assembled pediatric normative neuroimaging resources from open-access datasets in order to comply with age-related anatomical and functional differences in pediatric DBS populations. We illustrated their utility in a cohort of children with dystonia treated with pallidal DBS. We aimed to derive a local pallidal sweetspot and explore a connectivity fingerprint associated with pallidal stimulation to exemplify the utility of the assembled imaging resources.

**Methods:** An average pediatric brain template (the MNI brain template 4.5–18.5 years) was implemented and used to localize the DBS electrodes in 20 patients from the GEPESTIM registry cohort. A pediatric subcortical atlas, analogous to the DISTAL atlas known in DBS research, was also employed to highlight the anatomical structures of interest. A local pallidal sweetspot was modeled, and its degree of overlap with stimulation volumes was calculated as a correlate of individual clinical outcomes. Additionally, a pediatric functional connectome of 100 neurotypical subjects from the Consortium for Reliability and Reproducibility was built to allow network-based analyses and decipher a connectivity fingerprint responsible for the clinical improvements in our cohort.

**Results:** We successfully implemented a pediatric neuroimaging dataset that will be made available for public use as a tool for DBS analyses. Overlap of stimulation volumes with the identified DBS-sweetspot model correlated

\* Corresponding authors at: Director of Movement Disorders and Neuromodulation Unit, Charité, Universitätsmedizin Berlin, Department of Neurology, Campus Mitte, Charitéplatz 1, 10117 Berlin, Germany (A.A. Kühn). Department of Neurology, Charité- Universitätsmedizin Berlin, CCM, Neurowissenschaftliches Forschungszentrum, 2nd floor, Hufelandweg 14, 10117 Berlin, Germany.

E-mail addresses: [bassam.al-fatly@charite.de](mailto:bassam.al-fatly@charite.de) (B. Al-Fatly), [andrea.kuehn@charite.de](mailto:andrea.kuehn@charite.de) (A.A. Kühn).

<sup>1</sup> These authors contributed equally.

<https://doi.org/10.1016/j.nicl.2023.103449>

Received 16 February 2023; Received in revised form 16 May 2023; Accepted 2 June 2023

Available online 10 June 2023

2213-1582/© 2023 The Author(s). Published by Elsevier Inc. This is an open access article under the CC BY license (<http://creativecommons.org/licenses/by/4.0/>).

significantly with improvement on a local spatial level ( $R = 0.46$ , *permutated*  $p = 0.019$ ). The functional connectivity fingerprint of DBS outcomes was determined to be a network correlate of therapeutic pallidal stimulation in children with dystonia ( $R = 0.30$ , *permutated*  $p = 0.003$ ).

**Conclusions:** Local sweetspot and distributed network models provide neuroanatomical substrates for DBS-associated clinical outcomes in dystonia using pediatric neuroimaging surrogate data. Implementation of this pediatric neuroimaging dataset might help to improve the practice and pave the road towards a personalized DBS-neuroimaging analyses in pediatric patients.

## 1. Introduction

Imaging-based analyses of the effects of deep brain stimulation (DBS) have gained popularity over the last decade (Horn and Fox, 2020; Treu et al., 2020). Compared to neuroimaging analyses in adult populations, developmental differences could play a major role in the analysis of pediatric neuroimaging data (Fonov et al., 2011). For example, the basal ganglia and the thalamus widen and elongate with increasing age, in addition to many other morphological changes in gray and white matter (Fonov et al., 2011). There is also an uneven growth of brain structures that cannot be entirely represented using an average adult brain template (Thompson et al., 2000; Gogtay et al., 2004). Thus, mapping the effects of DBS on a group level necessitates use of a common pediatric brain template as a reference (Tödt et al., 2022; Dembek et al., 2019; Horn et al., 2017; Al-Fatly et al., 2019), which has never been adopted in neuroimaging analyses of DBS in children (Coblenz et al., 2021; Tambirajoo et al., 2021; Lumsden et al., 2022). Although transforming a pediatric brain image to an adult brain template is technically possible, the anatomical precision and visualization of basal ganglia structures may differ substantially, especially with regard to localizing DBS electrodes where millimeter differences matter (Horn et al., 2019; Wilke et al., 2002). Furthermore, the use of an adult template could lead to a higher degree of warping and distortion compared to a pediatric template (Wilke et al., 2003; Molfese et al., 2021). Many studies in adult populations have also demonstrated that DBS-associated remote networks can predict clinical improvement (Horn et al., 2017; Al-Fatly et al., 2019; Horn et al., 2022; Ganos et al., 2022; Sobesky et al., 2022). A pediatric connectome that is representative of age-related developmental variances would be beneficial to the application of such predictive network model in children treated with DBS. An example of these variances is increased motor network functional connectivity (particularly in the basal ganglia) during childhood, which correlates with the increasing age of the child (Sussman et al., 2022; Solé-Padullés et al., 2016).

Neurological disorders can affect various age groups. Dystonia is a good example, as it can manifest in different stages throughout life. The disorder is characterized by sustained or intermittent muscle contractions causing abnormal, often repetitive, movements, postures, or both in one or more body regions (Albanese et al., 2013). Clinically, dystonia is defined as isolated dystonia if it is the only feature, or as combined dystonia when associated with other movement disorders. The etiology of dystonia can be inherited, idiopathic, or acquired. Moreover, the pathophysiological background is complex in this network disease, involving abnormal inhibition, plasticity and other features on different levels of the nervous system (Koy et al., 2016; Sanger et al., 2010). Pediatric dystonia is a difficult condition with a negative impact on a patient's quality of life and on caregivers (van Egmond et al., 2015; Koy et al., 2022). Pharmacotherapy is limited due to the lack of efficacy or intolerable side effects (Lumsden et al., 2016). DBS has been established as a safe and effective treatment alternative for pharmacorefractory dystonia (Volkmann et al., 2012). Multiple studies have investigated the beneficial outcomes of DBS in children with idiopathic or inherited dystonia, with the globus pallidus internus (GPi) as the most common target for electrode implantation (Olaya et al., 2013; Ghosh et al., 2013; Krause et al., 2016). Despite several studies on optimal targeting for the best clinical outcomes in adults, data on how neuroimaging-based

analyses could improve targeting of electrodes and clinical outcomes after pallidal DBS in pediatric cohorts are scarce (Coblenz et al., 2021; Tambirajoo et al., 2021; Lumsden et al., 2022). It is therefore of paramount importance to investigate whether such analyses could elucidate the local distribution and remote connections of efficacious pallidal stimulation in children with dystonia.

In our study, we sought to build a set of age-respective, neuroimaging resources for imaging-based analyses in a pediatric DBS population. We used an age-specific, pediatric MNI template to comply with our cohort's age. The latter allows for accumulating the imaging information of patients into a common stereotactic space and hence eases group-level analyses. We also built a pediatric basal ganglia atlas that suits the pediatric template and better demonstrates basal ganglia nuclei of relevance to pallidal DBS-surgery. Finally, we assembled a pediatric functional connectome from 100 neurotypical children. We wanted to demonstrate the utility of these neuroimaging resources in mapping the clinical effects of pallidal DBS, using DBS-data of 20 children from the German Registry on Pediatric DBS (GEPESTIM) (Koy et al., 2017). The clinical effects of DBS were then locally mapped using a statistical sweetspot model. Electrode localization and sweetspot distribution were visualized in relation to the pediatric basal ganglia atlas. Lastly, a whole-brain connectivity model was estimated by correlating clinical outcomes with stimulation-related connectivity in a voxel-wise fashion using the pediatric functional connectome.

## 2. Methods

### 2.1. Pediatric neuroimaging dataset assembly

To overcome the co-registration/normalization bias that can be introduced by warping pediatric images onto an adult brain template, we incorporated an unbiased pediatric MNI template (Fonov et al., 2011) in Lead-DBS pipelines (Horn et al., 2019). To ensure coverage of the full span of pediatric ages, a template representative of the age group 4.5–18.5 years was chosen. To comply with the routine of spatially normalizing individual brain images into the adult MNI space in Lead-DBS, the asymmetric version of the aforementioned age-range template was chosen. This template has a  $1 \times 1 \times 1$  mm resolution and represents an average of 324 enrolled children. In addition, the template is available in multispectral versions (T1, T2 and proton density (PD)). All were included to take advantage of the multispectral option of spatial normalization routines.

Visualizing DBS electrodes in relation to the surrounding anatomical structures is highly important to clinicians and researchers. A pediatric DISTAL atlas was introduced as a new atlas in Lead-DBS, warping specific structures from the adult DISTAL atlas (Ewert et al., 2018) relevant to the current work. First, the pediatric MNI space was co-registered and normalized to the default adult space used in Lead-DBS (MNI152 NLIN 2009b). Manual refinement of the normalization step was performed on structures incorporated in the pediatric DISTAL atlas, using WarpDrive (Oxenford et al., 2022). Specifically, the GPi, globus pallidus externus (GPe), subthalamic nucleus (STN), and red nucleus (RN) were included in the new pediatric atlas as DBS target structures (GPi/GPe) and to further assure quality of alignment (using the STN and RN). In addition to facilitating electrode visualization, this atlas allowed us to precisely assess the relation of locally-mapped DBS effects to anatomical

structures of interest (in this case, the GPi/GPe complex) using sweet-spot analysis. The resulting inverse warp field was used to extract atlas structures in the pediatric MNI space.

As one of the neuroimaging-based analyses is to delineate the distributed functional network associated with beneficial DBS therapy, we sought to create a normative resting-state functional MRI (rs-fMRI) connectome. To do so, we downloaded and processed an rs-fMRI dataset from the nyu2 sub-cohort of the Consortium for Reliability and Reproducibility (CoRR) (Zuo et al., 2014), which contained neuroimaging data collected from neurotypical adult and pediatric subjects ([https://fcon\\_1000.projects.nitrc.org/indi/CoRR/html/nyu\\_2.html](https://fcon_1000.projects.nitrc.org/indi/CoRR/html/nyu_2.html)) (Zuo et al., 2014). Only data from 107 subjects aged 6–18 years were included (an earlier version of the connectome is mentioned in (Neudorfer et al., 2023); for demographics and imaging protocols, please see (Zuo et al., 2014); for scan parameters, see [Supplementary Table 1](#)). The participants had been informed by the investigators to rest with their eyes open during the whole scanning period. All participants underwent exhaustive psychometric tests to determine their neurotypical development. MRI scanning was performed during two different sessions on two different dates to conform with the aim of the original study (CoRR). However, for the purpose of our connectome aggregation, we exclusively used data from session 1, as only a few children had completed two sessions.

## 2.2. Normative connectome processing

The anatomical and functional MRI data from each subject were first preprocessed using a collection of tools from different software (namely FSL, SPM, and Lead-Connectome from the Lead-DBS neuroimaging suite, <https://www.lead-dbs.org/about/lead-connectome/>). Slice time correction (FSL; <https://fsl.fmrib.ox.ac.uk>) was applied to the data. Realignment and initial motion correction of the rs-fMRI time series was then performed using mcflirt (FSL; <https://fsl.fmrib.ox.ac.uk>) (Jenkinson et al., 2012). Subjects were excluded if they had a framewise-displacement of >0.5 mm in >50 % of the volumes (Power et al., 2014) (seven subjects were excluded based on this criterion). Detrimental motion effects were regressed out from the data using code implemented in Lead-Connectome (<https://www.lead-dbs.org/about/lead-connectome/>). Spatial smoothing was performed using a Gaussian kernel of 6 mm full width at half maximum, after which a high-pass filter of 0.01 Hz and a low pass filter of 0.08 Hz were applied to the data to mitigate the effects of scanner drift and high-frequency noise fluctuations.

Finally, we regressed out the average BOLD time series over cerebrospinal fluid (CSF) and white matter (Caballero-Gaudes and Reynolds, 2017). To do this, the corresponding T1-weighted structural image for each subject was segmented using the SPM “*newsegment*” function (Friston et al., 1994). The resultant masks were linearly aligned (coregistered) to the rs-fMRI images, from which masks of white matter, CSF, and gray matter were obtained. The average signal over the CSF and white matter masks was then calculated and regressed from the rs-fMRI time series via linear regression. Regression of the global signal was also performed using Lead-Connectome Matlab code (Fox et al., 2009). Normalization of functional volumes to the pediatric MNI space was then performed using FSL-FNIRT to nonlinearly warp the anatomical T1 images to the pediatric MNI space, and later apply the warp to the coregistered rs-fMRI volumes. Following the normalization of each fMRI acquisition, a  $285,903 \times 180$  matrix – containing the BOLD signal of every voxel ( $n = 285,903$ ) for each volume in the time series ( $n = 180$ ) – was computed using Lead-Connectome. The data were then masked to only include voxels within the brain in a readable format for seed-based connectivity analyses in *Lead-Mapper* (another toolbox from Lead-DBS neuroimaging suite).

## 2.3. Study cohort

Twenty children with a diagnosis of dystonia were selected from the GEPESTIM registry. Original trial data was provided by German DBS centers. After screening the available imaging data from the GEPESTIM cohort, the current data for analysis was collected from five different neurological centers across Germany. Reasons for exclusion of data from the original GEPESTIM cohort were lack of pre- and/or postoperative imaging datasets or poor-quality scans (scans with artefacts) that were insufficient for electrode reconstruction and localization, lack of documented DBS settings corresponding to documented clinical scores, and an insufficient period of postoperative clinical follow-up. Ethical approvals were provided by each participating center. Each patient was preoperatively assessed by an expert pediatric neurologist, and at least one follow-up was performed postoperatively at 6 months or later (given a latency of approximately 6 months for pallidal DBS to take effect). A preoperative and postoperative Burke-Fahn-Marsden Dystonia Rating Scale (BFMDRS) score was collected for each patient (Burke et al., 1985), and the improvement under DBS was calculated as the percentage ratio of the difference between these scores. Preoperative MRI scans were also acquired from each respective clinical center, in addition to a postoperative computed tomography (CT) or MRI scan to confirm the final DBS lead locations. There were regular postoperative follow-up visits to try to program the most clinically beneficial DBS settings. We used the most clinically stable DBS programming parameters. Detailed information and trial protocols can be found in the original GEPESTIM registry publication (Koy et al., 2017).

## 2.4. Estimation of electrode localization and stimulation volumes

The DBS electrodes were localized using the open-source software Lead-DBS (<https://www.lead-dbs.org>) (Horn et al., 2019). The postoperative MRI or CT were co-registered to the corresponding preoperative MRI of each patient using Statistical Parametric Mapping software (SPM12; <https://www.fil.ion.ucl.ac.uk/spm/software/spm12/>) (Friston et al., 1994) or the Advanced Normalization Tools (ANTs; <https://stnava.github.io/ANTs/>) (Avants et al., 2008), respectively. The latter tools are integrated within the Lead-DBS software. Next, the co-registered images from all patients were warped to the pediatric MNI space using the ANTs symmetric normalization (SyN) strategy. Both co-registered and normalized images were visualized and quality controlled for any mismatch. Importantly, we used a new feature of Lead-DBS WarpDrive (Neudorfer et al., 2023) to control for any minute differences in specific brain regions that were still misaligned in the pediatric MNI space, by manually warping segments of the image. To minimize effects of brain-shift due to perioperative pneumocephalus, we applied brain-shift correction as implemented within Lead-DBS (Horn et al., 2019). This strategy refines linear mappings between postoperative and preoperative scans using consecutive alignment routines focused on the target regions (basal ganglia). Accordingly, nonlinear shifts introduced by pneumocephalus (usually present in frontal regions, since patients are in a supine position during scans) were substantially minimized. DBS electrodes were automatically pre-reconstructed using the PaCER algorithm (Husch et al., 2018) for postoperative CT and the TRAC/CORE algorithm (Horn et al., 2019) for postoperative MRI, and later manually refined as implemented in Lead-DBS.

The stimulation volume surrounding active contacts was modeled using the SimBio/FieldTrip approach (Horn et al., 2017) implemented in Lead-DBS. Briefly, the electric fields (E-fields) were estimated in the native space based on the individual optimized stimulation parameters using the finite element method. This was done by solving the static formulation of the Laplace equation on a discretized domain, represented by a tetrahedral four-compartment mesh (composed of gray and white matter, metal and insulating electrode parts). Uniform conductivity of 0.14 S/m was applied to model gray and white matter. We adopted a simplified heuristic strategy, which thresholds electric fields

at a vector magnitude above 0.2 V/mm (Åström et al., 2015) and considers the resulting volume as “activated”. Below, we refer to these thresholded volumes as “stimulation volumes”. Volumes were transferred to the pediatric MNI space using the deformation field calculated during spatial normalization. All the steps of the imaging data processing performed in Lead-DBS are illustrated in Fig. 1A.

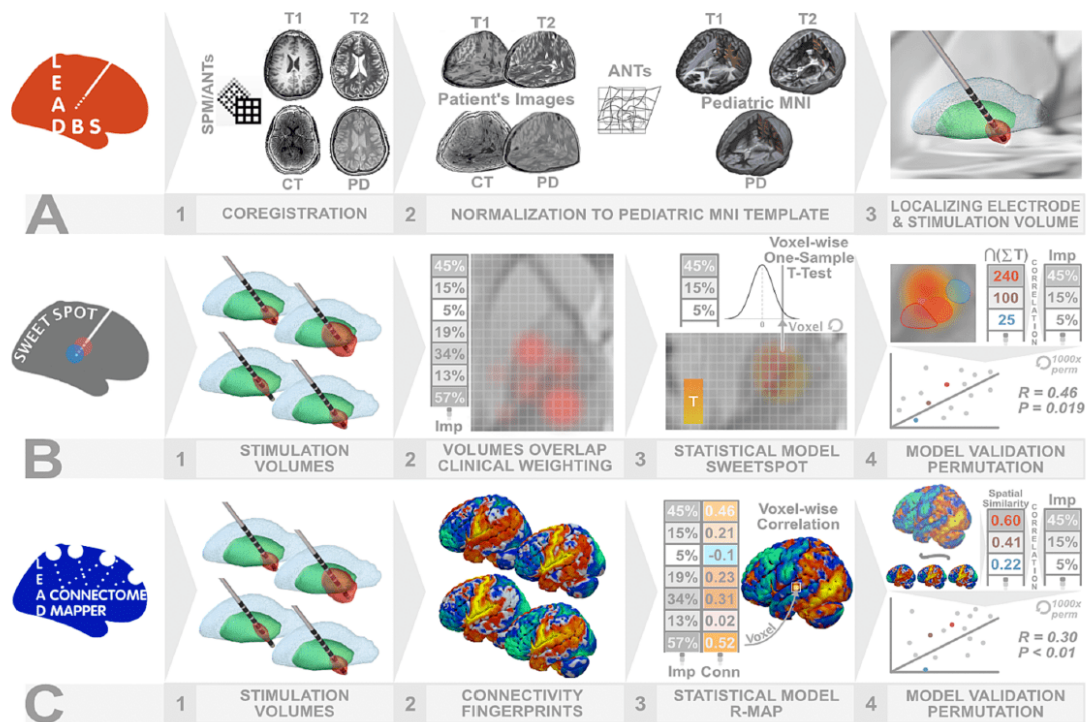
### 2.5. Sweetspot analysis

A group analysis was performed on stimulation volumes to locally map the effects of DBS in the pallidum. Previous studies used different sweetspot calculation methods (Dembek et al., 2022). In our analysis, we used a recent method that was able to map outcomes in Parkinson’s patients implanted with DBS early in their disease progression (Tödt et al., 2022). Briefly, every binarized mask of each stimulation volume was weighted by its corresponding improvement score. Aggregated together, weighted volumes were statistically tested with a one-sample  $t$ -test to test the average score of each voxel against zero. The null hypothesis here assumes no effect of DBS on clinical outcomes. This enabled formation of a sweetspot statistical map containing  $t$ -scores (T-model). To do so, voxels receiving contribution from less than 20 % of

the total stimulation volumes were excluded to ensure robustness of the statistical test. We then calculated the sum of  $t$ -scores from the T-model voxels overlapping with each stimulation volume. These sum values were correlated with percentage improvement-scores using a 1000x permutation test (permuting improvement scores). The permutation test was implemented to correct for multiple comparisons and test against null distribution, and is free from assumptions about the distributions, which are typically violated in small sample sizes (Permutation, 2005; Li et al., 2020). We repeated the same analysis on a subgroup of patients that included cases with a diagnosis of inherited or idiopathic dystonia ( $n = 14$ ). The latter analysis was meant to control for a possible effect of brain lesions in the acquired dystonia cases. For a diagrammatic representation of the sweetspot analysis, please refer to Fig. 1B.

### 2.6. Network analysis

On the whole-brain level, we wanted to test where the DBS electrodes should be connected on a functional network scale to obtain a beneficial DBS outcome. In a similar analysis to previous work (Horn et al., 2017; Al-Fatly et al., 2019), we estimated the functional connectivity profile of each stimulation volume to the rest of the brain using



**Fig. 1.** Methodological pipeline summarizing the main steps used in the current study. **A** All available neuroimaging data (pre- and postoperative MRI/CT) of all patients have undergone spatial coregistration (using SPM/ANTs - A1) in Lead-DBS toolbox. Multispectral normalization was applied using ANTs SyN Diffeomorphic Mapping (A2) implemented in Lead-DBS to ensure a precise warping of all preoperative volumes (T1, T2 and PD when available) to the pediatric MNI template. This spatial normalization was also applied to postoperative CT and followed by 3D reconstruction of DBS electrode model and modeling of stimulation volume (A3). **B** Sweetspot model estimation starts with aggregating stimulation volumes (B1) and weighting them by their respective clinical improvement (B2). Voxel-wise, one-sample  $t$ -test was then performed to calculate  $t$ -score of each voxel stimulated in at least  $n > 4$  patients (20 %) to ensure robust results. This yielded a statistical sweetspot that carries a  $t$ -score in each of its voxels (a T-model, B3). Pearson correlation with 1000x permutation was used to validate the sweetspot model (B4) correlating the sum  $t$ -scores of the voxels overlapping with each stimulation volume (exemplified by the red, currant and blue volumes of good, mediocre and bad responding patients respectively) with their respective percent improvement. **C** Connectivity analysis was carried out using Lead Connectome Mapper. Each stimulation volume (C1) was used as a seed in the 100 subjects, normative pediatric connectome. Connectivity fingerprint maps of all stimulation volumes have been exported (C2) and voxel-wise Pearson correlation between functional connectivity strength and respective percent improvement was calculated (C3) yielding a whole-brain statistical model (R-map). R-map has been validated again by Pearson correlation with 1000x permutation correlating spatial similarities between connectivity fingerprints of stimulation volumes with their respective percent improvement. Conn, connectivity; CT, computed tomography; Imp, improvement; PD, proton density. (For interpretation of the references to colour in this figure legend, the reader is referred to the web version of this article.)

our assembled pediatric normative rs-fMRI connectome. In brief, the average BOLD signal of the bilateral stimulation volumes for each patient was correlated to every other voxel BOLD signal in the brain from each of the connectome subjects. The average voxel-wise R values of 100 subjects were Fisher Z scored to represent the connectivity profile of each patient in our cohort. A voxel-wise correlation of connectivity strengths to the corresponding DBS-related improvement values was then carried out across subjects to yield a statistical R map (Horn et al., 2017). The R map represents the optimal connectivity map, which deciphers important regions of the DBS functional network in children with dystonia. The spatial similarity of each stimulation volume-associated connectivity profile to the R-map was then correlated with a percentage improvement across all 20 subjects using a 1000x permutation test similar to the method described above. Spatial similarities were calculated as the R coefficient of Pearson correlation between the voxel-wise connectivity values in the DBS-connectivity signature map and the voxel-wise R values in the R map. The same analysis was repeated for the subgroup mentioned under the sweetspot analysis section above (inherited/idiopathic subgroup of 14 cases). Fig. 1C summarizes the method used in the network analysis pipeline.

### 2.7. Data availability

Sensitive individual patient data cannot be shared for data protection reasons. All Lead-DBS codes can be accessed on <https://github.com/nets-tim/leaddbs>. Neuroimaging resources collected and processed in this manuscript, including the pediatric MNI space/atlas and the connectome, can be downloaded and queried from the Lead-DBS interface.

## 3. Results

### 3.1. Patient characteristics

The patients included in our analysis were part of a cohort from a registered trial (GEPESTIM) (Koy et al., 2017). Five DBS centers from Germany provided data on 20 children who underwent DBS until the age of 18 years between the 2008–2020. In our cohort of 11 males and nine females, the mean age of dystonia onset was  $2.9 \pm 3.21$  years, the mean duration of disease at the time of surgery was  $8.65 \pm 5.06$  years, and the mean age at DBS implantation was  $11.55 \pm 3.91$  years. The average postoperative BFMDRS ( $56.43 \pm 32.95$  points) was significantly lower ( $t(19) = -2.99$ ,  $p = 0.007$ ; average percentage improvement  $23.89 \pm 30.95\%$ ) than the preoperative BFMDRS ( $71.68 \pm 26.51$  points). The average time to postoperative follow-up to calculate the percentage improvement was  $16.20 \pm 12.89$  months.

Nine patients were diagnosed with inherited dystonia, six patients suffered from acquired dystonia, and in five patients no underlying cause could be identified (idiopathic dystonia). The etiology of dystonia within the group of inherited dystonia was classified as follows: DYT-TOR1A ( $n = 3$ ), DYT-KMT2B ( $n = 1$ ), DYT-SGCE ( $n = 1$ ), DYT-PRKRA ( $n = 1$ ), DYT-ANO3 ( $n = 1$ ), GNAO1 gene mutations ( $n = 2$ ). Among the group of acquired dystonia, all patients experienced perinatal brain injury, including perinatal asphyxia leading to dystonia. Overall, two patients with acquired and one patient with idiopathic dystonia were preterm (31, 32, and 36 weeks of gestation). In addition, we included one patient with hemi-dystonia, whereas 19 patients had generalized dystonia. Ten patients had isolated dystonia, while the other ten presented with dystonia combined with another movement disorder. Pre- and postoperative BFMDRS scores were available for all 20 patients (see Table 1 for demographics and clinical data; detailed individual patient-related information can be found in Supplementary Table 2; stimulation parameters in Supplementary Table 3).

### 3.2. Pediatric common brain space and subcortical atlas

An important step in our study was to implement a common pediatric

**Table 1**  
Patients demographic and clinical data.

Criteria	N (%) or mean $\pm$ SD
Gender (male/female)	11 (55)/9 (45)
Age at onset (years)	$2.9 \pm 3.21$
Age at implantation of DBS-system (years)	$11.55 \pm 3.91$
Duration of disease (years)	$8.65 \pm 5.06$
Etiology of dystonia (inherited/acquired/idiopathic)	9 (45)/6 (30)/5 (25)
Postoperative follow-ups	$6.9 \pm 2.55$
Postoperative surveillance period after initial DBS implantation (years)	$5.05 \pm 2.7$
Baseline BFMDRS score	$71.68 \pm 26.51$
Postoperative BFMDRS score	$56.43 \pm 32.95$
Improvement (%)	$23.89 \pm 30.59$

BFMDRS, Burke-Fahn-Marsden Dystonia Rating Scale; DBS, deep brain stimulation; SD, standard deviation.

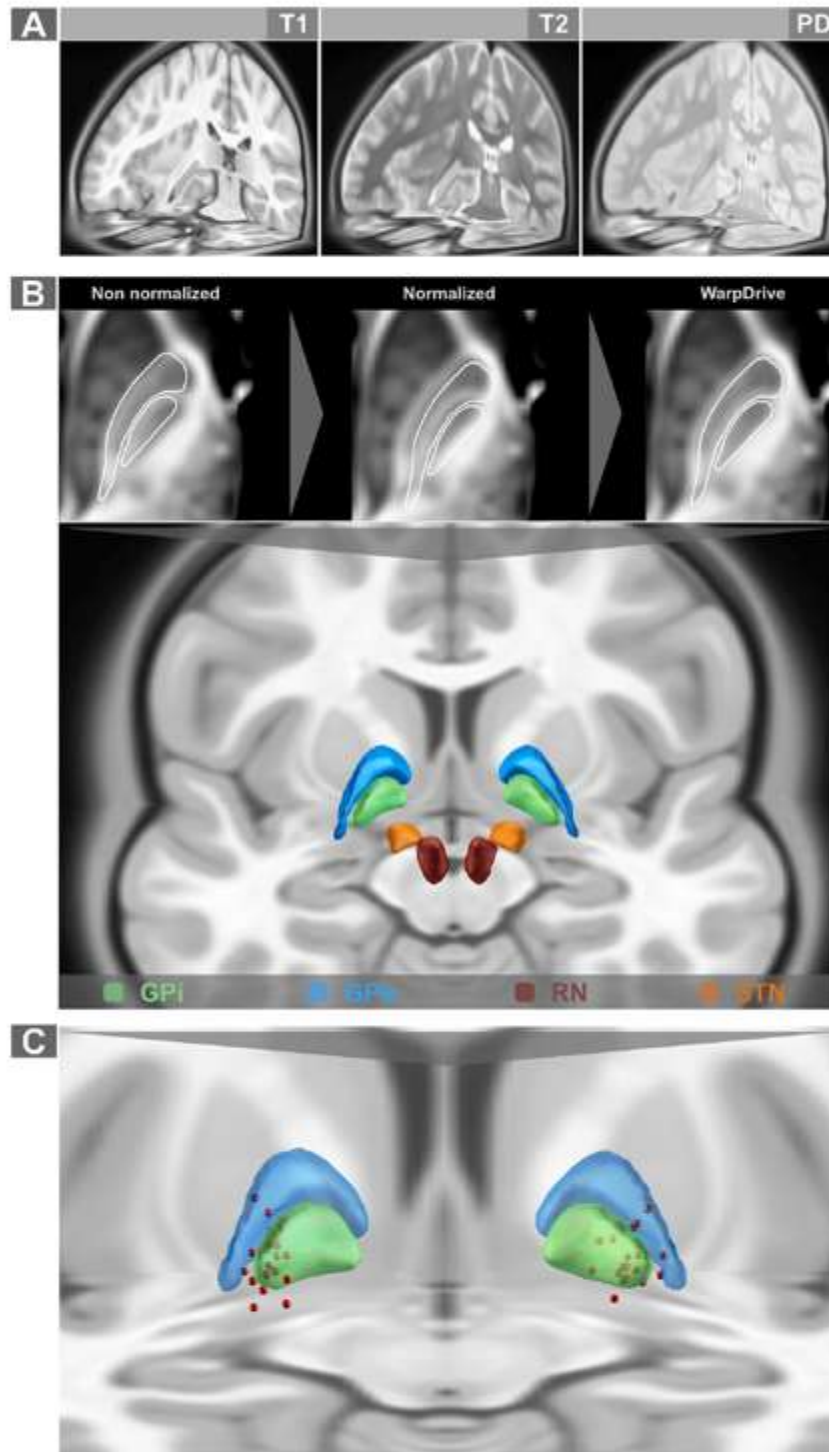
brain template that could be used in DBS group analysis. A multispectral version of the MNI pediatric space (Fig. 2A) was incorporated and openly distributed within the analysis pipeline of Lead-DBS software, for use in future research. In addition, a pediatric atlas similar to the DISTAL adult atlas was created to highlight important subcortical structures that were surgically targeted or were in the vicinity of the surgical target of DBS for dystonia. Precise transformation of the GPi, GPe, STN, and RN from the DISTAL adult atlas to our pediatric atlas was made possible by using the WarpDrive tool, which enabled manual refinement (Fig. 2B). This in turn ensured precise visualization of the patients' active contacts in relation to their anatomical structures in space (Fig. 2C).

### 3.3. Degree of overlap with the DBS sweetspot correlates with clinical improvement

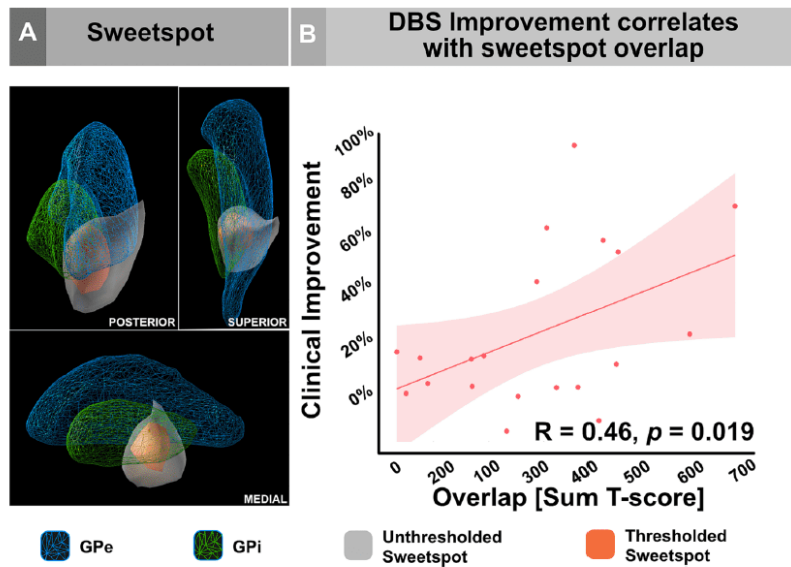
The calculated statistical model (T-model) of the sweetspot was found to lie in the region of the GPi, with a tendency to encroach on the ventral and lateral border of the GPi (on its interface with the GPe) and slightly extending toward the subpallidal region (see Fig. 3A). Overlap of each combined bilateral stimulation volumes with the sweetspot correlated with the corresponding DBS-associated clinical improvement ( $R = 0.46$ ,  $permutated\ p = 0.019$ , Fig. 3B). The results were stable when the analysis was repeated in inherited/idiopathic dystonia subgroup ( $R = 0.79$ ,  $permutated\ p = 0.001$ ; Supplementary Fig. 1). The center of gravity coordinates of the sweetspots of the whole- and the idiopathic/inherited-group are  $x = 21.6$ ,  $y = -7.44$ ,  $z = -4.99$  and  $x = 20.2$ ,  $y = -6.84$ ,  $z = -5.63$ , respectively. It should be noted that these coordinates are based on the pediatric MNI template used in the current work and could not be directly compared to an adult template-based results.

### 3.4. A pediatric functional connectome

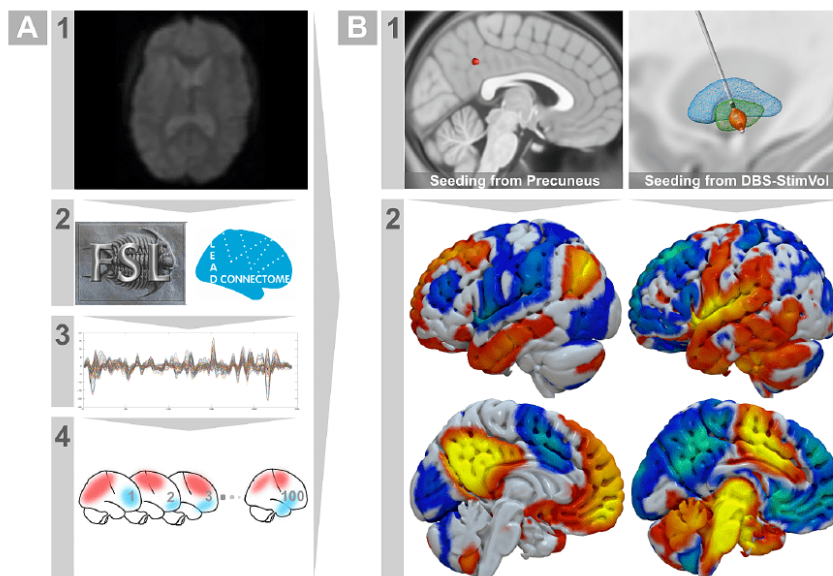
rs-fMRI data from normally developing children were successfully processed and assembled as a ready-to-use functional connectome for seed-based connectivity (Fig. 4). To pretest the robustness of the connectome, we seeded from a precuneal location (spherical seed size, 4 mm). The seed was manually placed using Mango software (<https://www.nitrc.org/projects/mango/>) and later fed to Lead-Mapper to estimate the related-connectivity profile. The latter was in agreement with the canonical pattern of the default mode network (Fox et al., 2005). This was a confirmatory step to ensure the vigor of the connectome. In addition, stimulation-related connectivity profiles were visually inspected to give an example of pallidal functional connectivity (see Fig. 4B). It is worth noting that the time-series data of this rs-fMRI connectome were sampled in the pediatric MNI space.



**Fig. 2.** Pediatric standard (MNI) space and subcortical atlas. A. Multispectral MRI acquisitions of the pediatric MNI space (Fonov et al., 2011) were implemented as a standard space in Lead-DBS toolbox. B. Warping of relevant structures from the adult DISTAL atlas (Ewert et al., 2016), with manual fine-tuning using the WarpDrive tool, enabled the pediatric DISTAL atlas to be constructed. C. Active contacts (red spheres) from the GEPSTIM cohort included in our study are depicted in relation to the globus pallidus internus (green) and externus (blue). GPe, globus pallidus externus; GPI, globus pallidus internus; RN, red nucleus; STN, subthalamic nucleus. (For interpretation of the references to colour in this figure legend, the reader is referred to the web version of this article.)



**Fig. 3. Sweetspot analysis.** A. Spatial location of the DBS sweetspot in relation to the right GPI/GPe complex from the current pediatric DISTAL atlas. Of note, the sweetspot spanned a region lateral to the GPI on its interface to the GPe in its posterior ventrolateral border. It also extended ventrally to the subpallidal white matter. The sweetspot was presented as a t-score cluster (T-model, see Methods) in unthresholded (gray) and thresholded (red,  $T \geq 3$ ) to demonstrate a consistent extent regardless of threshold. B. Overlap of the combined DBS stimulation volumes with the sweetspot (T-model) on local level correlated significantly with the DBS-ON clinical improvement. The latter correlation was validated by permuting the percentage improvement scores 1000 times. DBS, deep brain stimulation; GPe, globus pallidus externus; GPI, globus pallidus internus. (For interpretation of the references to colour in this figure legend, the reader is referred to the web version of this article.)



**Fig. 4. Resting-state normative pediatric connectome.** A. Pipeline for connectome preprocessing. Raw fMRI scans (1) were downloaded and preprocessed with associated T1 MRI using FSL and Lead-Connectome tools (2) to extract BOLD signals (3) across 100 neurotypical children. Matrices of time-series were stored in a form usable by Lead-Mapper tool for seed connectivity analysis in each subject of the connectome (4). B. Estimation of average seed connectivity. (1) Example seed locations from the precuneus and a stimulation volume modeled from one of the patients in our study cohort. (2) Using the Lead-Mapper tool, estimation of seed connectivity profiles (averaged across 100 subjects in the connectome) successfully replicated the default mode network in case of the precuneal seed, and relevant connectivity from GPI region was calculated using stimulation volume as a seed. DBS, deep brain stimulation; GPI, globus pallidus internus.

### 3.5. Connectivity pattern of DBS effect

To obtain further insight from a network perspective, a connectivity analysis was performed harnessing data from the pediatric functional connectome. While the sweetspot analysis looked at the clinical effects of DBS from an electrode localization perspective, functional network analysis extends this concept and extracts related information from whole-brain regions that are indirectly and remotely (polysynaptically) connected to the DBS electrode location. In this regard, the estimated group-level R map demonstrated a peculiar topology where connectivity to areas like the sensorimotor cortex, frontal cortex, and posterior cerebellum was negatively correlated with the clinical effects of DBS (i.e., patients would worsen if their DBS electrodes were more connected to

these regions). On the other hand, connectivity to the parietal and anterior cingulate cortices were positively correlated with postoperative improvement. The brainstem and medial and superior parts of the cerebellum also displayed a similar pattern of connectivity that correlated with improvement. In general, the similarity of the individual stimulation-related connectivity profile to the R-map model was significantly positively correlated with DBS improvement across our study cohort ( $R = 0.30$ , *permutated*  $p = 0.003$ ; Fig. 5). The model also yielded significant correlation using permutation testing when repeated on the inherited/idiopathic subgroup ( $R = 0.40$ , *permutated*  $p = 0.001$ ; Supplementary Fig. 2).



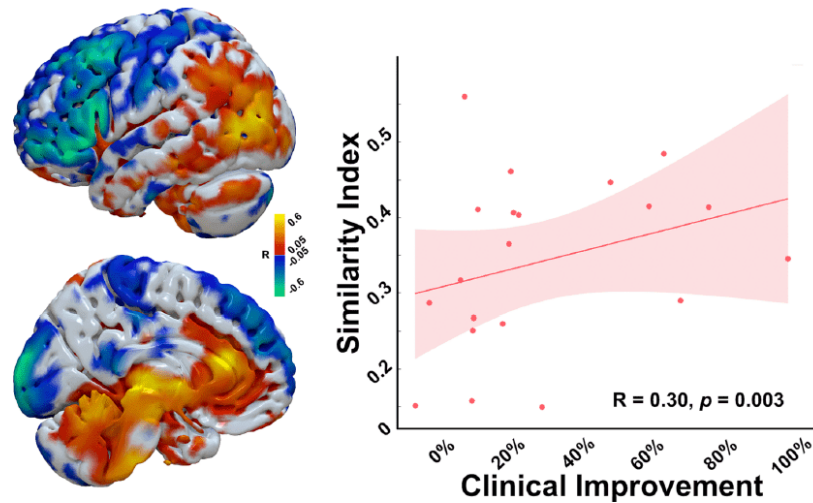


Fig. 5. Functional connectivity fingerprint of beneficial pallidal DBS. R-map DBS-network model projected on a surface mesh of pediatric MNI space showing different regions and their relevance to DBS outcome. Similarity of the DBS site-associated whole-brain connectivity correlated significantly with clinical improvement across patients in our cohort. DBS, deep brain stimulation.

#### 4. Discussion

Our study aimed to implement a pediatric neuroimaging dataset and showcase the local and remote network correlates of the therapeutic effects of DBS in children with dystonia included in a previous clinical trial (GEPESTIM) (Koy et al., 2017). This allowed us to describe a sweetspot statistical model representative of the clinical effects of DBS by inferring a relationship between stimulation location and clinical improvement in these patients. In addition, a functional-network correlate of effective DBS therapy was elucidated. Taken together, the current findings shed light into how local and remote information can be exploited to explore DBS outcomes in children using pediatric neuroimaging analysis tools.

##### 4.1. Towards a refined neuroimaging approach in pediatric DBS

The current understanding of neurological diseases and their therapies is highly dependent on group analysis of data. When neuroimaging data are considered, a common brain template is normally used to aggregate data and perform statistical inference (Treu et al., 2020). To this end, the use of an age-specific brain template will allow better estimation of developmental differences across age groups and account for any anatomical variance (Treu et al., 2020; Gogtay et al., 2004; Lenroot and Giedd, 2006). The use of the pediatric MNI template in our study is a good example. To the best of our knowledge, our study is the first to analyze DBS-related pediatric neuroimaging data using specifically pediatric imaging resources. The use of such a template also helps to minimize the amount of spatial deformation needed to warp the pediatric images to adult templates (Wilke et al., 2003; Molfese et al., 2021; Wilke et al., 2002). Additionally, we minimized the need for manual WarpDrive refinement and maximized structural alignment by using the pediatric MNI template when compared to the adult one as depicted in Supplementary Fig. 3. Although the WarpDrive tool has helped in mitigating minor local misalignments in the normalization, severe atrophied/degenerated structures could still be difficult to refine. However, we did not have such cases in our cohort.

The implementation of the pediatric MNI template has also enabled an atlas of subcortical structures (namely the DISTAL atlas) (Ewert et al., 2018) from the adult MNI space to be adjusted to the pediatric atlas. This atlas contained the main DBS target commonly used to treat childhood

dystonia, namely the GPi/GPe complex. These and further subcortical structures (STN and RN) worked as anchor points to refine spatial normalization using the Lead-DBS toolbox (Horn et al., 2019).

Given the current shift from location- to network-based understanding of neurological diseases and treatment options (Fox, 2018), the application of a normative pediatric functional connectome helps to advance an age-relevant connectomic approach in pediatric DBS studies. As structural and functional changes occur during development, connectivity patterns also change and reshape until the brain reaches maturity (Sussman et al., 2022; Solé-Padullés et al., 2016). While previous work relied on adult connectomes analyses (Coblentz et al., 2021; Tambirajoo et al., 2021), our pediatric connectome could facilitate future use of such a connectome in DBS and other pediatric research applications (for instance, mapping networks associated with specific lesions causing childhood neurological diseases) (Cohen et al., 2021). Furthermore, whole-brain mapping of the therapeutic effects of DBS allows a common network to be estimated that can also be targeted by other invasive and non-invasive neuromodulatory techniques (Fox et al., 2014).

Although we used a set of neuroimaging resources that covers the full age-range of our cohort (age at DBS implant – see Supplementary Table 2), future studies could benefit from an age-binned template/connectome to precisely suits the age-range of specific groups of patients. Furthermore, multi-templates (multi-atlases) approaches could also be useful in such scenarios although technically challenging due to difficulties in inter-templates images fusion (Phan et al., 2018). Taken together, the use of all three neuroimaging resources in our work (a template, an atlas, and a connectome) is a step closer toward personalized neuroimaging analysis in pediatric DBS research (Rajamani et al., 2022).

##### 4.2. A pallidal DBS sweetspot in children

Antidystonic pallidal sweetspots have previously been described in many adult DBS studies (Horn et al., 2022; Reich et al., 2019; Neumann et al., 2017; Schönecker et al., 2015; Okromelidze et al., 2020). Two recent studies reported an efficacious stimulation site in dystonic children implanted in the GPi using different methodologies (Coblentz et al., 2021; Lumsden et al., 2022). Of note, our sweetspot methodology has been recently used in an adult STN-DBS study (Tödt et al., 2022).

Crucially, overlap of the stimulation volume with the sweetspot “T-model” was significantly correlated with DBS-associated improvement across our cohort. This finding emphasizes the importance of treating the output of sweetspot methodology as a statistical model rather than a mere binary location (Reich et al., 2019). The anatomical distribution of the sweetspot in the posteroventral GPi indicated a lateral location in the interface between GPi and GPe. This could explain the importance of the role of the GPe and pallidal input fibers to the GPi in antidystonic DBS effects (Raghu et al., 2021). However, it is difficult to hypothesize the implication of fiber tracts, since our study did not use tractography as a method. Further experiments on how the effects of DBS can be relayed through fibers in the vicinity of the pallidum in children are needed, given the possible developmental differences compared to adults (Feldman et al., 2010). Nevertheless, the proper use of a normative structural connectome or atlas should be valuable, in addition to the well-acquired, native diffusion MRI of the patients. Another aspect is the ventral extension of the sweetspot to the subpallidal white matter. The latter could, to some degree, be regarded in line with the findings from a big adult cohort (Reich et al., 2019), especially when compared to the results of generalized dystonia in the study by Horn et al (Horn et al., 2022). Of note, previously published sweetspots were calculated using different statistical tests and were derived from different types of dystonia in adult populations. An example is the above-mentioned study by Horn et al where a voxel-wise correlation between e-field magnitude and percent improvement was used to estimate a sweetspot model.

#### 4.3. A functional connectivity correlate of antidystonic DBS effects in pediatric patients

As already mentioned, the use of network mapping of symptoms induced by brain lesions (Fox, 2018) – or in our case, mapping dystonia improvements induced by DBS – has gained increasing interest in recent years (Horn et al., 2022; Horn and Fox, 2020). Apart from understanding the link between network modulation and disease pathophysiology on a distributed brain topology, network mapping allows efficient translation between different invasive and non-invasive therapeutic strategies by targeting common connectivity substrates (Fox et al., 2014). Currently, there is limited applicability of non-invasive neuromodulation in children, and the concept of a common network target could be used in future trials in children. Our study highlighted a functional connectomic fingerprint that is partially in line with a relevant topology of previous work (Horn et al., 2022). Specifically, the negatively-correlated sensorimotor cortices were a central finding in multiple studies (Horn et al., 2022). Furthermore, the somatosensory cortex has repetitively been shown to have a major influence on the mechanism of dystonia, regardless of somatotopic distribution (focal or generalized) (Kojovic et al., 2013). Studies have demonstrated the role of cerebellar neuromodulation when mitigating dystonic symptoms with different therapies (Koch et al., 2014; Pizoli et al., 2002; Prudente et al., 2013). While the anterior cingulate cortex is not an obvious location associated with movement disorders, its contribution to motor control has been proved in primates and human behaviour (Paus, 2001). The connectomic fingerprint illustrated in our study overlaps partially with a recent one by Horn et al (Horn et al., 2022), which used an adult functional connectome to map the therapeutic effects of DBS in an adult dystonic cohort. However, some differences in the topology could be due to the inherent characteristics of the study cohort (heterogeneous types of dystonia). Another explanation could be that the DBS-related connectivity pattern is age dependent. This, however, should remain highly speculative until a proper systematic analysis between adult and pediatric DBS cohorts using respective imaging resources has been performed.

#### 4.4. Limitations

The small sample size of the dystonia cohort included in our study is

a limitation. However, dystonia is classified as a rare disease and its occurrence in childhood adds to the difficulties (Fernández-Alvarez and Nardocci, 2012). This aspect can be mitigated through collaboration with different clinical centers to overcome the problem of small cohorts. We strived to use all possible data from our cohort to maximize the number of participants included. Secondly, our cohort consisted of patients with different types of dystonia and different ages at surgery. These factors might have added to the heterogeneity of the data, especially when considering that the effects of DBS depend on the underlying pathophysiology (Kupsch et al., 2003; Ellis, 2011). We accounted for the possible influence of acquired dystonia by repeating the sweetspot and network analyses after excluding them. Further bigger cohorts should test the latter assumption using a more systematic approach. We did not analyze data from cases with acquired dystonia as a separate group in our sweetspot and network models due to lack of sufficient number of patients (N = 6). A forthcoming task would be to perform such analyses in larger groups of patients taken into consideration the heterogeneity of the causative factors. However, heterogeneity in the etiologies and body distribution of dystonic manifestations should always be taken into account especially in relation to functional therapeutic networks. An example is the study of Horn et al (Horn et al., 2022), where different networks were identified depending on the bases of the distribution of dystonia (cervical vs generalized).

Thirdly, the BFMDRS score was initially developed for adults with isolated dystonia (Burke et al., 1985). As patients with acquired dystonia often have a complex hyperkinetic movement disorder, encompassing choreoathetosis and ballism, the BFMDRS does not capture all aspects of the clinical picture. Even in patients with little or even absent observable changes in the BFMDRS, DBS can improve domains such as function and quality of life. Therefore, the sole use of the BFMDRS is insufficient to fully assess DBS effects in these patients (Gimeno et al., 2012). Accordingly, the use of multidisciplinary assessments of motor and non-motor domains should be aimed for in future studies in order to catch the full DBS effects in patients with acquired dystonia. Nevertheless, our data should be seen as a foundation to the technical approach in pediatric DBS patients, although associated results should also be interpreted with caution. A fourth limitation is the implementation of a normative connectome for DBS network mapping. Although the use of such connectomes has shown good performance in explaining the network effects of DBS in different studies (Horn et al., 2017; Al-Fatly et al., 2019; Horn et al., 2022; Ganos et al., 2022; Sobesky et al., 2022), a possible comparison to patient-specific connectivity data is of importance (Wang et al., 2021) as some patients have brain lesions that could impact the network. However, publicly-available data are usually collected for research purposes and are of higher resolution than clinically-collected data. Another specific limitation in children with movement disorders like dystonia is movement artefacts (Sussman et al., 2022). The latter could also favor the use of a more stable normative connectome. Additionally, average seed-based connectivity profiles derived from multiple subjects in a normative connectome can enhance the signal-to-noise ratio. Finally, the occurrence of other clinical features like epilepsy in GNAO1 cases (N = 2) could play additional roles defining the therapeutic networks. However, we focused on the improvement in BFMDRS as a clinical measurement for the severity of dystonia in our patients and used it as an independent variable to exclusively determine the “anti-dystonic” sweetspot and network. However, we focused on the percentage improvement in BFMDRS as a clinical measurement for the severity of dystonia in our patients and used it as an independent variable to exclusively determine the “anti-dystonic” sweetspot and network.

## 5. Conclusions

We used a set of pediatric resources to perform neuroimaging analyses on a group level in pediatric DBS patients. This enabled us to identify a sweetspot of beneficial pallidal DBS effects using a pediatric

template and atlas, as well as an optimal whole-brain functional connectomic network using a pediatric normative connectome. The latter corresponds to current knowledge about the pathophysiologic network model responsible for dystonia. Our findings confirm previous results and will facilitate future neuroimaging analyses in pediatric DBS research.

### Funding

AAK receives a grant by Dr. Rita and Dr. Hans Günther Herfort Stiftung, the institution of AAK receives a grant by Boston Scientific. AAK received travel grants and honoraria from Medtronic and Boston Scientific. LT received occasional payments as a consultant for Boston Scientific between September 2021–September 2022. LT received honoraria as a speaker on symposia sponsored by Boston Scientific, AbbVie, Novartis, Neuraxpharm, Teva, the Movement Disorders Society and DIAPLAN. VVV received payments from Boston Scientific for lectures and advisory boards. TAD was supported by the Cologne Clinician Scientist Program (CCSP)/Faculty of Medicine/University of Cologne, funded by the German Research Foundation (DFG, FI 773/15-1). AAK and BA-F are funded by the Deutsche Forschungsgemeinschaft (DFG, German Research Foundation) – Project-ID 390688087 – EXC-2049.

### CRedit authorship contribution statement

**Bassam Al-Fatly:** Conceptualization, Data curation, Formal analysis, Methodology, Software, Visualization, Writing – original draft. **Sabina J. Giesler:** Data curation, Investigation, Resources, Writing – review & editing. **Simon Oxenford:** Methodology, Software, Writing – review & editing. **Ningfei Li:** Methodology, Software, Writing – review & editing. **Till A. Dembek:** Project administration, Resources, Writing – review & editing. **Johannes Achtzehn:** Formal analysis, Resources, Writing – review & editing. **Patricia Krause:** Data curation, Investigation, Writing – review & editing. **Veerle Visser-Vandewalle:** Data curation, Investigation, Writing – review & editing. **Joachim K. Krauss:** Data curation, Investigation, Writing – review & editing. **Joachim Runge:** Data curation, Investigation, Writing – review & editing. **Vera Tadie:** Data curation, Investigation, Writing – review & editing. **Tobias Bäumer:** Data curation, Investigation, Writing – review & editing. **Alfons Schnitzler:** Data curation, Investigation, Writing – review & editing. **Jan Vesper:** Data curation, Investigation, Writing – review & editing. **Jochen Wirths:** Data curation, Investigation, Writing – review & editing. **Lars Timmermann:** Project administration, Writing – review & editing. **Andrea A. Kühn:** Conceptualization, Funding acquisition, Project administration, Supervision, Writing – review & editing. **Anne Key:** Conceptualization, Funding acquisition, Project administration, Supervision, Writing – review & editing.

### Declaration of Competing Interest

AAK received honoraria from Medtronic and Boston Scientific, not related to this work. AK is a principal investigator in the STIM-CP trial, partly sponsored by Boston Scientific. JKK is a consultant to Medtronic, Boston Scientific, aleva and Inomed. LT serves as the vice president of the German Neurological Society. TAD has received speaker honoraria from Medtronic & Boston Scientific.

The remaining authors declare that they have no known competing financial interests or personal relationships that could have appeared to influence the work reported in this paper.

### Data availability

Sensitive individual patients' data cannot be shared for data protection reasons. Neuroimaging resources collected and processed in this manuscript can be downloaded and queried from Lead-DBS GUI.

### Acknowledgments

We would like to thank Dr Andreas Horn for his kind advice during the data analysis and pediatric resources assembly. We would also like to extend our thanks to the patients and their families. AAK was supported by the Deutsche Forschungsgemeinschaft (DFG, German Research Foundation) – Project-ID 424778381 – TRR 295 and Project-ID 347325977 within the SPP 2041 Computational Connectomics. AK received a grant from Dr. Rita and Dr. Hans Günther Herfort Stiftung: 50069011-Rk.

### Appendix A. Supplementary data

Supplementary data to this article can be found online at <https://doi.org/10.1016/j.nicl.2023.103449>.

### References

- Albanese, A., Bhatia, K., Bressman, S.B., DeLong, M.R., Fahn, S., Fung, V.S.C., Hallett, M., Jankovic, J., Jinnah, H.A., Klein, C., Lang, A.E., Mink, J.W., Teller, J.K., 2013. Phenomenology and classification of dystonia: a consensus update. *Mov. Disord.* 28 (7), 863–873. <https://doi.org/10.1002/MDS.25475>.
- Al-Fatly, B., Ewert, S., Kübler, D., Kroneberg, D., Horn, A., Kühn, A.A., 2019. Connectivity profile of thalamic deep brain stimulation to effectively treat essential tremor. *Brain* 142 (10), 3086–3098. <https://doi.org/10.1093/BRAIN/AWZ236>.
- Åström, M., Diczfalusy, E., Martens, H., Wårdell, K., 2015. Relationship between neural activation and electric field distribution during deep brain stimulation. *IEEE Trans. Biomed. Eng.* 62 (2), 664–672. <https://doi.org/10.1109/TBME.2014.2363494>.
- Avants, B., Epstein, C., Grossman, M., Gee, J., 2008. Symmetric diffeomorphic image registration with cross-correlation: evaluating automated labeling of elderly and neurodegenerative brain. *Med. Image Anal.* 12 (1), 26–41. <https://doi.org/10.1016/j.media.2007.06.004>.
- Burke, R.E., Fahn, S., Marsden, C.D., Bressman, S.B., Moskowitz, C., Friedman, J., 1985. Validity and reliability of a rating scale for the primary torsion dystonias. *Neurology* 35 (1), 73. <https://doi.org/10.1212/WNL.35.1.73>.
- Caballero-Gaudes, C., Reynolds, R.C., 2017. Methods for cleaning the BOLD fMRI signal. *Neuroimage* 154, 128–149. <https://doi.org/10.1016/J.NEUROIMAGE.2016.12.018>.
- Coblentz, A., Elias, G.J.B., Boutet, A., Germann, J., Algarni, M., Oliveira, L.M., Neudorfer, C., Widjaja, E., Ibrahim, G.M., Kalia, S.K., Jain, M., Lozano, A.M., Fasano, A., 2021. Mapping efficacious deep brain stimulation for pediatric dystonia. *J. Neurosurg. Pediatr.* 27 (3), 346–356. <https://doi.org/10.3171/2020.7.PEDS20322>.
- Cohen, A.L., Mulder, B.P.F., Prohl, A.K., Soussand, L., Davis, P., Kroeck, M.R., McManus, P., Gholipour, A., Scherrer, B., Bebin, E.M., Wu, J.Y., Northrup, H., Krueger, D.A., Sahin, M., Warfield, S.K., Fox, M.D., Peters, J.M., 2021. Tuber locations associated with infantile spasms map to a common brain network. *Ann. Neurol.* 89 (4), 726–739. <https://doi.org/10.1002/ANA.26015>.
- Dembek, T.A., Roediger, J., Horn, A., Reker, P., Oehrn, C., Dafsari, H.S., Li, N., Kühn, A.A., Fink, G.R., Visser-Vandewalle, V., Barbe, M.T., Timmermann, L., 2019. Probabilistic sweet spots predict motor outcome for deep brain stimulation in Parkinson disease. *Ann. Neurol.* 86 (4), 527–538. <https://doi.org/10.1002/ANA.25567>.
- Dembek, T.A., Baldernann, J.C., Petry-Schmelzer, J.-N., Jergas, H., Treuer, H., Visser-Vandewalle, V., Dafsari, H.S., Barbe, M.T., 2022. Sweetspot mapping in deep brain stimulation: strengths and limitations of current approaches. *Neuromodulation* 25 (6), 877–887. <https://doi.org/10.1111/ner.13356>.
- Ellis, T.L., 2011. Dystonia and the role of deep brain stimulation. *ISRN Surg.* 2011, 1–5. <https://doi.org/10.5402/2011/193718>.
- Ewert, S., Plettig, P., Li, N., Chakravarty, M.M., Collins, D.L., Herrington, T.M., Kühn, A.A., Horn, A., 2018. Toward defining deep brain stimulation targets in MNI space: a subcortical atlas based on multimodal MRI, histology and structural connectivity. *Neuroimage* 170, 271–282. <https://doi.org/10.1016/J.NEUROIMAGE.2017.05.015>.
- Feldman, H.M., Yeatman, J.D., Lee, E.S., Barde, L.H.F., Gaman-Bean, S., 2010. Diffusion tensor imaging: a review for pediatric researchers and clinicians. *J. Dev. Behav. Pediatr.* 31 (4), 346. <https://doi.org/10.1097/DBP.0B013E3181DCAA8B>.
- Fernández-Alvarez, E., Nardocci, N., 2012. Update on pediatric dystonias: etiology, epidemiology, and management. *Degener. Neurol. Neuromuscul. Dis.* 2, 29. <https://doi.org/10.2147/DNND.S16082>.
- Fonov, V., Evans, A.C., Botteron, K., Almli, C.R., McKinstry, R.C., Collins, D.L., 2011. Unbiased average age-appropriate atlases for pediatric studies. *Neuroimage* 54 (1), 313. <https://doi.org/10.1016/J.NEUROIMAGE.2010.07.033>.
- Fox, M.D., 2018. Mapping symptoms to brain networks with the human connectome. *N. Engl. J. Med.* 379 (23), 2237–2245. [https://doi.org/10.1056/NEJMRA1706158/SUPPL\\_FILE/NEJMRA1706158\\_DISCLOSURES.PDF](https://doi.org/10.1056/NEJMRA1706158/SUPPL_FILE/NEJMRA1706158_DISCLOSURES.PDF).
- Fox, M.D., Snyder, A.Z., Vincent, J.L., Corbetta, M., van Essen, D.C., Raichle, M.E., 2005. The human brain is intrinsically organized into dynamic, anticorrelated functional networks. *Proc. Natl. Acad. Sci. USA* 102 (27), 9673–9678. [https://doi.org/10.1073/PNAS.0504136102/SUPPL\\_FILE/04136FIG5.PDF](https://doi.org/10.1073/PNAS.0504136102/SUPPL_FILE/04136FIG5.PDF).
- Fox, M.D., Zhang, D., Snyder, A.Z., Raichle, M.E., 2009. The global signal and observed anticorrelated resting state brain networks. *J. Neurophysiol.* 101 (6), 3270–3283.

- <https://doi.org/10.1152/JN.90777.2008/ASSET/IMAGES/LARGE/Z9K0060994950007.JPEG>.
- Fox, M.D., Buckner, R.L., Liu, H., Mallar Chakravarty, M., Lozano, A.M., Pascual-Leone, A., 2014. Resting-state networks link invasive and noninvasive brain stimulation across diverse psychiatric and neurological diseases. *Proc. Natl. Acad. Sci. USA* 111 (41), E4367–E4375. [https://doi.org/10.1073/PNAS.1405003111/SUPPL\\_FILE/PNAS.201405003SL.PDF](https://doi.org/10.1073/PNAS.1405003111/SUPPL_FILE/PNAS.201405003SL.PDF).
- Friston, K.J., Holmes, A.P., Worsley, K.J., Poline, J.-P., Frith, C.D., Frackowiak, R.S.J., 1994. Statistical parametric maps in functional imaging: a general linear approach. *Hum. Brain Mapp.* 2 (4), 189–210. <https://doi.org/10.1002/HBM.460020402>.
- Ganos, C., Al-Fatly, B., Fischer, J.F., et al., 2022. A neural network for tics: insights from causal brain lesions and deep brain stimulation. *Brain* 145 (12), 4385–4397. <https://doi.org/10.1093/brain/awac009>.
- Ghosh, P.S., MacHado, A.G., Deogaonkar, M., Ghosh, D., 2013. Deep brain stimulation in children with dystonia: experience from a tertiary care center. *Pediatr. Neurosurg.* 48 (3), 146–151. <https://doi.org/10.1159/000345830>.
- Gimeno, H., Tustin, K., Selway, R., Lin, J.P., 2012. Beyond the Burke-Fahn-Marsden Dystonia rating scale: deep brain stimulation in childhood secondary dystonia. *Eur. J. Paediatr. Neurol.* 16 (5), 501–508. <https://doi.org/10.1016/j.ejpn.2011.12.014>.
- Gogtay, N., Giedd, J.N., Lusk, L., et al., 2004. Dynamic mapping of human cortical development during childhood through early adulthood. *Proc. Natl. Acad. Sci. USA* 101 (21), 8174–8179. [https://doi.org/10.1073/PNAS.0402680101/SUPPL\\_FILE/02680MOVIE4.MPG](https://doi.org/10.1073/PNAS.0402680101/SUPPL_FILE/02680MOVIE4.MPG).
- Horn, A., Al-Fatly, B., Neumann, W.J., Neudorfer, C., 2022. Connectomic DBS: An introduction. *Connectomic Deep Brain Stimulation*. Published online January 1:3–23. doi:10.1016/B978-0-12-821861-7.00020-8.
- Horn, A., Fox, M.D., 2020. Opportunities of connectomic neuromodulation. *Neuroimage* 221, 117180. <https://doi.org/10.1016/J.NEUROIMAGE.2020.117180>.
- Horn, A., Reich, M., Vorwerk, J., Li, N., Wenzel, G., Fang, Q., Schmitz-Hübisch, T., Nickl, R., Kupsch, A., Volkmann, J., Kühn, A.A., Fox, M.D., 2017. Connectivity Predicts deep brain stimulation outcome in Parkinson disease. *Ann. Neurol.* 82 (1), 67–78. <https://doi.org/10.1002/ANA.24974>.
- Horn, A., Li, N., Dembek, T.A., Kappel, A., Boulay, C., Ewert, S., Tietze, A., Husch, A., Perera, T., Neumann, W.-J., Reiser, M., Si, H., Oostenveld, R., Rorden, C., Yeh, F.-C., Fang, Q., Herrington, T.M., Vorwerk, J., Kühn, A.A., 2019. Lead-DBS v2: towards a comprehensive pipeline for deep brain stimulation imaging. *Neuroimage* 184, 293–316. <https://doi.org/10.1016/J.NEUROIMAGE.2018.08.068>.
- Horn, A., Reich, M.M., Ewert, S., Li, N., Al-Fatly, B., Lange, F., Roothaus, J., Oxenford, S., Horn, I., Paschen, S., Runge, J., Wodarg, F., Witt, K., Nickl, R.C., Wittstock, M., Schneider, G.-H., Mahlknecht, P., Poewe, W., Eisner, W., Helmers, A.-K., Matthies, C., Krauss, J.K., Deuschl, G., Volkmann, J., Kühn, A.A., 2022. Optimal deep brain stimulation sites and networks for cervical vs. generalized dystonia. *Proc. Natl. Acad. Sci. USA* 119 (14). <https://doi.org/10.1073/PNAS.2114985119>.
- Husch, A., Petersen, M.V., Gemmar, P., Goncalves, J., Hertel, F., 2018. A fully automated method for electrode trajectory and contact reconstruction in deep brain stimulation. *Neuroimage Clin.* 17, 80–89. <https://doi.org/10.1016/J.NICL.2017.10.004>.
- Jenkinson, M., Beckmann, C.F., Behrens, T.E.J., Woolrich, M.W., Smith, S.M., 2012. FSL. *Neuroimage* 62 (2), 782–790. <https://doi.org/10.1016/J.NEUROIMAGE.2011.09.015>.
- Koch, G., Porcacchia, P., Ponzio, V., Carrillo, F., Cáceres-Redondo, M.T., Brusa, L., Desiato, M.T., Arciprete, F., Di Lorenzo, F., Pisani, A., Caltagirone, C., Palomar, F.J., Mir, P., 2014. Effects of two weeks of cerebellar theta burst stimulation in cervical dystonia patients. *Brain Stimul.* 7 (4), 564–572. <https://doi.org/10.1016/J.BRS.2014.05.002>.
- Kojovic, M., Pareés, L., Kassavitis, P., et al., 2013. Secondary and primary dystonia: pathophysiological differences. *Brain* 136 (Pt 7), 2038–2049. <https://doi.org/10.1093/BRAIN/AWT150>.
- Koy, A., Lin, J.-P., Sanger, T.D., Marks, W.A., Mink, J.W., Timmermann, L., 2016. Advances in management of movement disorders in children. *Lancet Neurol.* 15 (7), 719–735. [https://doi.org/10.1016/S1474-4422\(16\)00132-0](https://doi.org/10.1016/S1474-4422(16)00132-0).
- Koy, A., Weinsheimer, M., Pauls, K.A.M., Kühn, A.A., Krause, P., Huebl, J., Schneider, G.-H., Deuschl, G., Erasmi, R., Falk, D., Krauss, J.K., Lütjens, G., Schnitzler, A., Wojtecki, L., Vesper, J., Korinthenberg, R., Coenen, V.A., Visser-Vandewalle, V., Hellmich, M., Timmermann, L., 2017. German registry of paediatric deep brain stimulation in patients with childhood-onset dystonia (GEPESTIM). *Eur. J. Paediatr. Neurol.* 21 (1), 136–146. <https://doi.org/10.1016/j.ejpn.2016.05.023>.
- Koy, A., Kühn, A.A., Huebl, J., et al., 2022. Quality of life after deep brain stimulation of pediatric patients with dyskinetic cerebral palsy: a prospective, single-arm, multicenter study with a subsequent randomized double-blind crossover (STIM-CP). *Mov. Disord.* 37 (4), 799–811. <https://doi.org/10.1002/MDS.26898>.
- Krause, P., Lauritsch, K., Lipp, A., Horn, A., Weschke, B., Kupsch, A., Kiening, K.L., Schneider, G.-H., Kühn, A.A., 2016. Long-term results of deep brain stimulation in a cohort of eight children with isolated dystonia. *J. Neurol.* 263 (11), 2319–2326. <https://doi.org/10.1007/S00415-016-8253-6>.
- Kupsch, A., Kuehn, A., Klaffke, S., Meissner, W., Harnack, D., Winter, C., Haelbig, T.D., Kivi, A., Arnold, G., Einhäupl, K.-M., Schneider, G.-H., Trottenberg, T., 2003. Deep brain stimulation in dystonia. *J. Neurol.* 250 (S1), i47–i52. <https://doi.org/10.1007/S00415-003-1110-2>.
- Lenroot, R.K., Giedd, J.N., 2006. Brain development in children and adolescents: insights from anatomical magnetic resonance imaging. *Neurosci. Biobehav. Rev.* 30 (6), 718–729. <https://doi.org/10.1016/J.NEUBIOREV.2006.06.001>.
- Li, N., Baldermann, J.C., Kibleur, A., et al., 2020. A unified connectomic target for deep brain stimulation in obsessive-compulsive disorder. *Nat. Commun.* 11 (1), 1–12. <https://doi.org/10.1038/s41467-020-16734-3>.
- Lumsden, D.E., Kaminska, M., Tomlin, S., Lin, J.-P., 2016. Medication use in childhood dystonia. *Eur. J. Paediatr. Neurol.* 20 (4), 625–629. <https://doi.org/10.1016/j.ejpn.2016.02.003>.
- Lumsden, D.E., Tambirajoo, K., Hasegawa, H., Gimeno, H., Kaminska, M., Ashkan, K., Selway, R., Lin, J.-P., 2022. Probabilistic mapping of deep brain stimulation in childhood dystonia. *Parkinsonism Relat. Disord.* 105, 103–110. <https://doi.org/10.1016/J.PARKRELDIS.2022.11.006>.
- Molfese, P.J., Glen, D., Mesite, L., et al., 2021. The Haskins pediatric atlas: a magnetic-resonance-imaging-based pediatric template and atlas. *Pediatr. Radiol.* 51 (4), 628–639. <https://doi.org/10.1007/S00247-020-04875-Y/TABLES/3>.
- Neudorfer, C., Butenko, K., Oxenford, S., Rajamani, N., Achtzehn, J., Goede, L., Hollunder, B., Rios, A.S., Hart, L., Tasserie, J., Fernando, K.B., Nguyen, T.A.K., Al-Fatly, B., Vissani, M., Fox, M., Richardson, R.M., van Rienen, U., Kühn, A.A., Husch, A.D., Opri, E., Dembek, T., Li, N., Horn, A., 2023. Lead-DBS v3.0: mapping deep brain stimulation effects to local anatomy and global networks. *Neuroimage* 268, 119862. <https://doi.org/10.1016/J.NEUROIMAGE.2023.119862>.
- Neumann, W.-J., Horn, A., Ewert, S., Huebl, J., Brücke, C., Slentz, C., Schneider, G.-H., Kühn, A.A., 2017. A localized pallidal physiologic marker in cervical dystonia. *Ann. Neurol.* 82 (6), 912–924. <https://doi.org/10.1002/ana.25095>.
- Kromelidze, L., Tsuboi, T., Eisinger, R.S., Burns, M.R., Charbel, M., Rana, M., Grewal, S., Lu, C.-Q., Almeida, L., Foote, K.D., Okun, M.S., Middlebrooks, E.H., 2020. Functional and structural connectivity patterns associated with clinical outcomes in deep brain stimulation of the globus pallidus internus for generalized dystonia. *Am. J. Neuroradiol.* 41 (3), 508–514. <https://doi.org/10.3174/AJNR.A6429>.
- Olaya, J.E., Christian, E., Ferman, D., Luc, Q., Krieger, M.D., Sanger, T.D., Liker, M.A., 2013. Deep brain stimulation in children and young adults with secondary dystonia: the children's hospital Los Angeles experience. *Neurosurg. Focus.* 35 (5), E7. <https://doi.org/10.3171/2013.8.FOCUSI3300>.
- Oxenford, S., Roediger, J., Neudorfer, C., et al., 2022. Lead-OR: a multimodal platform for deep brain stimulation surgery. *Elife* 11. <https://doi.org/10.7554/eLife.72929>.
- Paus, T., 2001. Primate anterior cingulate cortex: where motor control, drive and cognition interface. *Nat. Rev. Neurosci.* 2 (6), 417–424. <https://doi.org/10.1038/35077500>.
- Permutation, Parametric and Bootstrap Tests of Hypotheses. *Permutation and Bootstrap Tests of Hypotheses*. Published online 2005. doi:10.1007/B138696.
- Phan, T.V., Smeets, D., Talcott, J.B., Vandermosten, M., 2018. Processing of structural neuroimaging data in young children: bridging the gap between current practice and state-of-the-art methods. *Dev. Cogn. Neurosci.* 33, 206–223. <https://doi.org/10.1016/J.DCN.2017.08.009>.
- Pizoli, C.E., Jinnah, H.A., Billingsley, M.L., Hess, E.J., 2002. Abnormal cerebellar signaling induces dystonia in mice. *J. Neurosci.* 22 (17), 7825. <https://doi.org/10.1523/JNEUROSCI.22-17-07825.2002>.
- Power, J.D., Mitra, A., Laumann, T.O., Snyder, A.Z., Schlaggar, B.L., Petersen, S.E., 2014. Methods to detect, characterize, and remove motion artifact in resting state fMRI. *Neuroimage* 84, 320–341. <https://doi.org/10.1016/J.NEUROIMAGE.2013.08.048>.
- Prudente, C.N., Pardo, C.A., Xiao, J., Hanfelt, J., Hess, E.J., Ledoux, M.S., Jinnah, H.A., 2013. Neuropathology of cervical dystonia. *Exp. Neurol.* 241, 95–104. <https://doi.org/10.1016/J.JEXPNEURO.2012.11.019>.
- Raghu, A.L.B., Eraifej, J., Sarangmat, N., et al., 2021. Pallido-putaminal connectivity predicts outcomes of deep brain stimulation for cervical dystonia. *Brain* 144 (12), 3589–3596. <https://doi.org/10.1093/BRAIN/AWAB280>.
- Rajamani, N., Horn, A., Hollunder, B., 2022. Outlook: towards personalized connectomic deep brain stimulation. *Connect. Deep Brain Stimul.* 527–542. <https://doi.org/10.1016/B978-0-12-821861-7.00009-9>.
- Reich, M.M., Horn, A., Lange, F., et al., 2019. Probabilistic mapping of the antidystonic effect of pallidal neurostimulation: a multicenter imaging study. *Brain* 142 (5), 1386–1398. <https://doi.org/10.1093/BRAIN/AWZ046>.
- Sanger, T.D., Chen, D., Fehlings, D.L., Hallett, M., Lang, A.E., Mink, J.W., Singer, H.S., Alter, K., Ben-Pazi, H., Butler, E.E., Chen, R., Collins, A., Dayanidhi, S., Forssberg, H., Fowler, E., Gilbert, D.L., Gorman, S.L., Gormley, M.E., Jinnah, H.A., Kornblau, B., Krosschell, K.J., Lehman, R.K., MacKinnon, C., Malanga, C.J., Mesterman, R., Michaels, M.B., Pearson, T.S., Rose, J., Russman, B.S., Sternad, D., Swoboda, K.J., Valero-Cuevas, F., 2010. Definition and classification of hyperkinetic movements in childhood. *Mov. Disord.* 25 (11), 1538–1549. <https://doi.org/10.1002/MDS.23088>.
- Schönecker, T., Gruber, D., Kivi, A., Müller, B., Lobsien, E., Schneider, G.-H., Kühn, A.A., Hoffmann, K.-T., Kupsch, A.R., 2015. Postoperative MRI localisation of electrodes and clinical efficacy of pallidal deep brain stimulation in cervical dystonia. *J. Neurol. Neurosurg. Psychiatry.* 86 (8), 833–839. <https://doi.org/10.1136/JNNP-2014-308159>.
- Sobesky, L., Goede, L., Odekerken, V.J.J., et al., 2022. Subthalamic and pallidal deep brain stimulation: are we modulating the same network? *Brain* 145 (1), 251–262. <https://doi.org/10.1093/BRAIN/AWAB258>.
- Solé-Padullés, C., Castro-Fornieles, J., de la Serna, E., Calvo, R., Baeza, I., Moya, J., Lázaro, L., Rosa, M., Bargallo, N., Sugranyes, G., 2016. Intrinsic connectivity networks from childhood to late adolescence: effects of age and sex. *Dev. Cogn. Neurosci.* 17, 35–44. <https://doi.org/10.1016/J.DCN.2015.11.004>.
- Sussman, B.L., Wyckoff, S.N., Heim, J., et al., 2022. Is resting state functional MRI effective connectivity in movement disorders helpful? A focused review across lifespan and disease. *Front. Neurol.* 13, 734. <https://doi.org/10.3389/FNEUR.2022.847834/BIBTEX>.
- Tambirajoo, K., Furlanetti, L., Hasegawa, H., Raslan, A., Gimeno, H., Lin, J.-P., Selway, R., Ashkan, K., 2021. Deep brain stimulation of the internal pallidum in Lesch-Nyhan syndrome: clinical outcomes and connectivity analysis. *Neuromodulation* 24 (2), 380–391. <https://doi.org/10.1111/NER.13217>.
- Thompson, P.M., Giedd, J.N., Woods, R.P., MacDonald, D., Evans, A.C., Toga, A.W., 2000. Growth patterns in the developing brain detected by using continuum

- mechanical tensor maps. *Nature* 404 (6774), 190–193. <https://doi.org/10.1038/35004593>.
- Tödt, I., Al-Fatly, B., Granert, O., Kühn, A.A., Krack, P., Rau, J., Timmermann, L., Schnitzler, A., Paschen, S., Helmers, A.-K., Hartmann, A., Bardin, E., Schuepbach, M., Barbe, M.T., Dembek, T.A., Fraix, V., Kübler, D., Brefel-Courbon, C., Gharabaghi, A., Wojtecki, L., Pinsker, M.O., Thobois, S., Damier, P., Witjas, T., Houeto, J.-L., Schade-Brittinger, C., Vidailhet, M., Horn, A., Deuschl, G., 2022. The contribution of subthalamic nucleus deep brain stimulation to the improvement in motor functions and quality of life. *Mov. Disord.* 37 (2), 291–301. <https://doi.org/10.1002/MDS.28952>.
- Treu, S., Strange, B., Oxenford, S., et al., 2020. Deep brain stimulation: Imaging on a group level. *Neuroimage* 219, 117018. <https://doi.org/10.1016/j.neuroimage.2020.117018>.
- van Egmond, M.E., Kuiper, A., Eggink, H., Sinke, R.J., Brouwer, O.F., Verschuuren-Bemelmans, C.C., Sival, D.A., Tijssen, M.A.J., de Koning, T.J., 2015. Dystonia in children and adolescents: a systematic review and a new diagnostic algorithm. *J. Neurol. Neurosurg. Psychiatry* 86 (7), 774–781. <https://doi.org/10.1136/jnnp-2014-309106>.
- Volkman, J., Wolters, A., Kupsch, A., Müller, J., Kühn, A.A., Schneider, G.-H., Poewe, W., Hering, S., Eisner, W., Müller, J.-U., Deuschl, G., Pinsker, M.O., Skogseid, I.-M., Roeste, G.K., Krause, M., Tronnier, V., Schnitzler, A., Voges, J., Nikkha, G., Vesper, J., Classen, J., Naumann, M., Benecke, R., 2012. Pallidal deep brain stimulation in patients with primary generalised or segmental dystonia: 5-year follow-up of a randomised trial. *Lancet Neurol.* 11 (12), 1029–1038. [https://doi.org/10.1016/S1474-4422\(12\)70257-0](https://doi.org/10.1016/S1474-4422(12)70257-0).
- Wang, Q., Akram, H., Muthuraman, M., Gonzalez-Escamilla, G., Sheth, S.A., Oxenford, S., Yeh, F.-C., Groppa, S., Vanegas-Arroyave, N., Zrinzo, L., Li, N., Kühn, A., Horn, A., 2021. Normative vs. patient-specific brain connectivity in deep brain stimulation. *Neuroimage* 224, 117307. <https://doi.org/10.1016/j.neuroimage.2020.117307>.
- Wilke, M., Schmithorst, V.J., Holland, S.K., 2002. Assessment of spatial normalization of whole-brain magnetic resonance images in children. *Hum. Brain Mapp.* 17 (1), 48. <https://doi.org/10.1002/HBM.10053>.
- Wilke, M., Schmithorst, V.J., Holland, S.K., 2003. Normative pediatric brain data for spatial normalization and segmentation differs from standard adult data. *Magn. Reson. Med.* 50 (4), 749–757. <https://doi.org/10.1002/MRM.10606>.
- Zuo, X.N., Anderson, J.S., Bellec, P., et al., 2014. An open science resource for establishing reliability and reproducibility in functional connectomics. *Sci. Data* 1 (1), 1–13. <https://doi.org/10.1038/sdata.2014.49>.

**Curriculum Vitae**

My curriculum vitae does not appear in the electronic version of my paper for reasons of data protection.

## Publication list

1. Migraine-like headache caused by rheumatic heart disease: The second case of 'Mahler's migraine'? Iodice F, Della Marca G, **Alfalty B**, Barbato F, Vollono C. *Cephalalgia* 37 (14), 1398-1399. **IF: 4.9**
2. Acute Motor Axonal Neuropathy in Association with Hepatitis E. Al-Saffar A, **Al-Fatly B**. *Front Neurol*. 2018 Feb 9;9:62. doi: 10.3389/fneur.2018.00062. eCollection 2018. **IF: 3.4**
3. Coherence: a unifying mechanism of deep brain stimulation. **Al-Fatly B**. *J Neurophysiol*. 2019 Jan 1;121(1):1-3. doi: 10.1152/jn.00563.2018. Epub 2018 Sep 26. **IF: 2.5**
4. Connectivity profile of thalamic deep brain stimulation to effectively treat essential tremor. **Al-Fatly B**, Ewert S, Kübler D, Kroneberg D, Horn A\*, Kühn AA\*. *Brain*. 2019 Oct 1;142(10):3086-3098. doi: 10.1093/brain/awz236.
5. A unified connectomic target for deep brain stimulation in obsessive-compulsive disorder. Li N, Baldermann JC, Kibleur A, Treu S, Akram H, Elias GJB, Boutet A, Lozano AM, **Al-Fatly B**, Strange B, Barcia JA, Zrinzo L, Joyce E, Chabardes S, Visser-Vandewalle V, Polosan M, Kuhn J, Kühn AA, Horn A. *Nat Commun*. 2020 Jul 3;11(1):3364. doi: 10.1038/s41467-020-16734-3. **IF: 16.6**
6. Impact of deep brain stimulation of the subthalamic nucleus on natural language in patients with Parkinson's disease. Ehlen F, **Al-Fatly B**, Kühn AA, Klostermann F. *PLoS One*. 2020 Dec 29;15(12):e0244148. doi: 10.1371/journal.pone.0244148. eCollection 2020. **IF: 3.7**
7. Waveform changes with the evolution of beta bursts in the human subthalamic nucleus. Yeh CH, **Al-Fatly B**, Kühn AA, Meidahl AC, Tinkhauser G, Tan H, Brown P. *Clin Neurophysiol*. 2020 Sep;131(9):2086-2099. doi: 10.1016/j.clinph.2020.05.035. Epub 2020 Jun 29. **IF: 4.7**
8. A Unified Functional Network Target for Deep Brain Stimulation in Obsessive-Compulsive Disorder. Li N, Hollunder B, Baldermann JC, Kibleur A, Treu S, Akram H, **Al-Fatly B**, Strange BA, Barcia JA, Zrinzo L, Joyce EM, Chabardes S, Visser-Vandewalle V, Polosan M, Kuhn J, Kühn AA, Horn A. *Biol Psychiatry*. 2021 Nov 15;90(10):701-713. doi: 10.1016/j.biopsych.2021.04.006. Epub 2021 Apr 20. **IF: 10.6**
9. Determining an efficient deep brain stimulation target in essential tremor - Cohort study and review of the literature. Kübler D\*, Kroneberg D\*, **Al-Fatly B**, Schneider GH, Ewert S, van Riesen C, Gruber D, Ebersbach G, Kühn AA. *Parkinsonism Relat Disord*. 2021 Aug;89:54-62. doi: 10.1016/j.parkreldis.2021.06.019. Epub 2021 Jun 29. **IF: 4.1**
10. Subthalamic and pallidal deep brain stimulation: are we modulating the same network?. Sobesky L, Goede L, Odekerken VJJ, Wang Q, Li N, Neudorfer C, Rajamani N, **Al-Fatly B**, Reich M, Volkmann J, de Bie RMA, Kühn AA, Horn A. *Brain*. 2022 Mar 29;145(1):251-262. doi: 10.1093/brain/awab258. **IF: 14.5**
11. A neural network for tics: insights from causal brain lesions and deep brain stimulation. Ganos C\*, **Al-Fatly B\***, Fischer JF, Baldermann JC, Hennen C, Visser-Vandewalle V, Neudorfer C, Martino D, Li J, Bouwens T, Ackermanns L, Leentjens AFG, Pyatigorskaya N, Worbe Y, Fox MD, Kühn AA\*, Horn A\*. *Brain*. 2022 Dec 19;145(12):4385-4397. doi: 10.1093/brain/awac009.
12. The Contribution of Subthalamic Nucleus Deep Brain Stimulation to the Improvement in Motor Functions and Quality of Life. Tödt I\*, **Al-Fatly B\***, Granert O, Kühn

- AA, Krack P, Rau J, Timmermann L, Schnitzler A, Paschen S, Helmers AK, Hartmann A, Bardinet E, Schuepbach M, Barbe MT, Dembek TA, Fraix V, Kübler D, Brefel-Courbon C, Gharabaghi A, Wojtecki L, Pinski MO, Thobois S, Damier P, Witjas T, Houeto JL, Schade-Brittinger C, Vidailhet M, Horn A, Deuschl G. *Mov Disord.* 2022 Feb;37(2):291-301. doi: 10.1002/mds.28952. Epub 2022 Feb 3. **IF: 8.6**
13. Probabilistic Mapping Reveals Optimal Stimulation Site in Essential Tremor. Nowacki\* A, Barlatey S\*, **Al-Fatly B**, Dembek T, Bot M, Green AL, Kübler D, Lachenmayer ML, Debove I, Segura-Amil A, Horn A, Visser-Vandewalle V, Schuurman R, Barbe M, Aziz TZ, Kühn AA, Nguyen TAK, Pollo C. *Ann Neurol.* 2022 May;91(5):602-612. doi: 10.1002/ana.26324. Epub 2022 Mar 3. **IF: 11.2**
  14. Personalizing Deep Brain Stimulation Using Advanced Imaging Sequences. Neudorfer C, Kroneberg D, **Al-Fatly B**, Goede L, Kübler D, Faust K, van Rienen U, Tietze A, Picht T, Herrington TM, Middlebrooks EH, Kühn A, Schneider GH, Horn A. *Ann Neurol.* 2022 May;91(5):613-628. doi: 10.1002/ana.26326. Epub 2022 Mar 7. **IF: 11.2**
  15. Optimal deep brain stimulation sites and networks for cervical vs. generalized dystonia. Horn A, Reich MM, Ewert S, Li N, **Al-Fatly B**, Lange F, Roothans J, Oxenford S, Horn I, Paschen S, Runge J, Wodarg F, Witt K, Nickl RC, Wittstock M, Schneider GH, Mahlknecht P, Poewe W, Eisner W, Helmers AK, Matthies C, Krauss JK, Deuschl G, Volkmann J, Kühn AA. *Proc Natl Acad Sci U S A.* 2022 Apr 5;119(14):e2114985119. doi: 10.1073/pnas.2114985119. Epub 2022 Mar 31. **IF: 11.1**
  16. Toward therapeutic electrophysiology: beta-band suppression as a biomarker in chronic local field potential recordings. Feldmann LK, Lofredi R, Neumann WJ, **Al-Fatly B**, Roediger J, Bahners BH, Nikolov P, Denison T, Saryyeva A, Krauss JK, Faust K, Florin E, Schnitzler A, Schneider GH, Kühn AA. *NPJ Parkinsons Dis.* 2022 Apr 19;8(1):44. doi: 10.1038/s41531-022-00301-2. **IF: 8.7**
  17. Reply to "Deep Brain Stimulation for Tremor: Direct Targeting of a Novel Imaging Biomarker". Neudorfer C, Kroneberg D, **Al-Fatly B**, Goede LL, Kübler D, Faust K, van Rienen U, Tietze A, Picht T, Herrington TM, Middlebrooks EH, Kühn A, Schneider GH, Horn A. *Ann Neurol.* 2022 Aug;92(2):343-344. doi: 10.1002/ana.26420. Epub 2022 Jun 6. **IF: 11.1**
  18. Overnight unilateral withdrawal of thalamic deep brain stimulation to identify reversibility of gait disturbances. Kroneberg D, **Al-Fatly B**, Schmitz-Hübsch T, Gandor F, Gruber D, Ebersbach G, Horn A, Kühn AA. *Exp Neurol.* 2022 Sep;355:114135. doi: 10.1016/j.expneurol.2022.114135. Epub 2022 Jun 6. **IF: 5.3**
  19. Spectral and spatial distribution of subthalamic beta peak activity in Parkinson's disease patients. Darcy N, Lofredi R, Al-Fatly B, Neumann WJ, Hübl J, Brücke C, Krause P, Schneider GH, Kühn A. *Exp Neurol.* 2022 Oct;356:114150. doi: 10.1016/j.expneurol.2022.114150. Epub 2022 Jun 19. **IF: 5.3**
  20. A Functional Connectome of Parkinson's Disease Patients Prior to Deep Brain Stimulation: A Tool for Disease-Specific Connectivity Analyses. Loh A, Boutet A, Germann J, **Al-Fatly B**, Elias GJB, Neudorfer C, Krotz J, Wong EHY, Parmar R, Gramer R, Paff M, Horn A, Chen JJ, Azevedo P, Fasano A, Munhoz RP, Hodaie M, Kalia SK, Kucharczyk W, Lozano AM. *Front Neurosci.* 2022 Jun 24;16:804125. doi: 10.3389/fnins.2022.804125. eCollection 2022. **IF: 4.3**
  21. Lead-DBS v3.0: Mapping deep brain stimulation effects to local anatomy and global networks. Neudorfer C, Butenko K, Oxenford S, Rajamani N, Achtzehn J, Goede L, Hollunder B, Ríos AS, Hart L, Tasserie J, Fernando KB, Nguyen TAK,



- AI-Fatly B**, Vissani M, Fox M, Richardson RM, van Rienen U, Kühn AA, Husch AD, Opri E, Dembek T, Li N, Horn A. *Neuroimage*. 2023 Mar;268:119862. doi: 10.1016/j.neuroimage.2023.119862. Epub 2023 Jan 5. **IF: 5.7**
22. Christmas-Related Reduction in Beta Activity in Parkinson's Disease. Feldmann LK, Lofredi R, **AI-Fatly B**, Busch JL, Mathiopoulou V, Roediger J, Krause P, Schneider GH, Faust K, Horn A, Kühn AA, Neumann WJ. *Mov Disord*. 2023 Apr;38(4):692-697. doi: 10.1002/mds.29334. Epub 2023 Jan 31. **IF: 8.6**
23. Pallidal neuromodulation of the explore/exploit trade-off in decision-making. de A Marcelino AL, Gray O, **AI-Fatly B**, Gilmour W, Douglas Steele J, Kühn AA, Gilbertson T. *Elife*. 2023 Feb 2;12:e79642. doi: 10.7554/eLife.79642.
24. Structural and metabolic correlates of neuropsychological profiles in multiple system atrophy and Parkinson's disease. Kübler D, Kobylecki C, McDonald KR, Anton-Rodriguez JM, Herholz K, Carter SF, Hinz R, Thompson JC, **AI-Fatly B**, Gerhard A. *Parkinsonism Relat Disord*. 2023 Feb;107:105277. doi: 10.1016/j.parkreldis.2022.105277. Epub 2023 Jan 2. **IF: 4.1**
25. Mapping a network for tics in Tourette syndrome using causal lesions and structural alterations. Zouki JJ, Ellis EG, Morrison-Ham J, Thomson P, Jesuthasan A, **AI-Fatly B**, Joutsa J, Silk TJ, Corp DT. *Brain Commun*. 2023 Apr 4;5(3):fcad105. doi: 10.1093/braincomms/fcad105. eCollection 2023. **IF: 4.8**
26. Neuroimaging-based analysis of DBS outcomes in pediatric dystonia: Insights from the GEPESTIM registry. **AI-Fatly B**, Giesler SJ, Oxenford S, Li N, Dembek TA, Achtzehn J, Krause P, Visser-Vandewalle V, Krauss JK, Runge J, Tadic V, Bäumer T, Schnitzler A, Vesper J, Wirths J, Timmermann L, Kühn AA, Koy A; GEPESTIM consortium. *Neuroimage Clin*. 2023 Jun 10;39:103449. doi: 10.1016/j.nicl.2023.103449. Online ahead of print.

## **Acknowledgments**

I would like to express my heartfelt gratitude to my supervisors for their unwavering guidance, support, and invaluable insights throughout my thesis journey. Their mentorship has been instrumental in shaping the outcome of this work. To my loving family, who stood by me with endless patience and encouragement, I owe a debt of gratitude that words cannot fully capture. My heartfelt thanks also extend to my dear friends who provided moral support, cheered me on during the challenging times, and celebrated with me in moments of success. Your friendship has been a source of inspiration. I am profoundly grateful to my exceptional lab colleagues for their immeasurable contributions to my academic and personal growth.